

NONLINEAR DYNAMICS AND SYSTEMS THEORY

An International Journal of Research and Surveys

Volume 20

Number 1

2020

CONTENTS

PERSONAGE IN SCIENCE

- Professor V.M. Starzhinskii. To the 100th Birthday Anniversary.....1
A.A. Martynyuk, N.A. Izobov, A.G. Mazko and V.I. Zhukovskii

- Generalized Monotone Method for Nonlinear Caputo Fractional Impulsive Differential Equations.....3
Y.Bai and A.S. Vatsala

- Control Design for Non-Linear Uncertain Systems via Coefficient Diagram Method: Application to Solar Thermal Cylindrical Parabolic Trough Concentrators 21
Z. Fenchouche, M. Chakir, O. Benzineb, M.S. Boucherit and M. Tadjine

- Adaptive Sliding Mode Control Synchronization of a Novel, Highly Chaotic 3-D System with Two Exponential Nonlinearities..... 38
F. Hannachi

- Motion Control Design of UNUSAITS AUV Using Sliding PID 51
T. Herlambang, S. Subchan, H. Nurhadi and D. Adzkiya

- Alternative Legendre Functions for Solving Nonlinear Fractional Fredholm Integro-Differential Equation 61
Khawlah H. Hussain

- On the Boundedness of a Novel Four-Dimensional Hyperchaotic System.... 72
S. Rezzag

- Periodic Solutions in Non-Homogeneous Hill Equation 78
A. Rodriguez and J. Collado

- Estimates of Accuracy for Asymptotic Soliton-Like Solutions to the Singularly Perturbed Benjamin-Bona-Mahony Equation..... 92
V. H. Samoilenko, Yu. I. Samoilenko and L. V. Vovk

- Oscillation Criteria for Delay Equations with Several Non-Monotone Arguments..... 107
I. P. Stavroulakis, Zh. Kh. Zhunussova, L. Kh. Zhunussova and K. Dosmagulova

NONLINEAR DYNAMICS & SYSTEMS THEORY

Volume 20, No. 1, 2020

Nonlinear Dynamics and Systems Theory

An International Journal of Research and Surveys

EDITOR-IN-CHIEF A.A.MARTYNYUK

*S.P.Timoshenko Institute of Mechanics
National Academy of Sciences of Ukraine, Kiev, Ukraine*

REGIONAL EDITORS

P.BORNE, Lille, France
 M.FABRIZIO, Bologna, Italy
Europe

M.BOHNER, Rolla, USA
 HAO WANG, Edmonton, Canada
USA and Canada

T.A.BURTON, Port Angeles, USA
 C.CRUZ-HERNANDEZ, Ensenada, Mexico
USA and Latin America

M.ALQURAN, Irbid, Jordan
Jordan and Middle East

K.L.TEO, Perth, Australia
Australia and New Zealand

Nonlinear Dynamics and Systems Theory

An International Journal of Research and Surveys

EDITOR-IN-CHIEF A.A.MARTYNYUK

The S.P.Timoshenko Institute of Mechanics, National Academy of Sciences of Ukraine,
Nesterov Str. 3, 03680 MSP, Kiev-57, UKRAINE / e-mail: journalndst@gmail.com

MANAGING EDITOR I.P.STAVROULAKIS

Department of Mathematics, University of Ioannina
451 10 Ioannina, HELLAS (GREECE) / e-mail: ipstav@cc.uoi.gr

ADVISORY EDITOR A.G.MAZKO

Institute of Mathematics of NAS of Ukraine, Kiev (Ukraine)
e-mail: mazko@imath.kiev.ua

REGIONAL EDITORS

M.ALQURAN (Jordan), e-mail: marwan04@just.edu.jo
P.BORNE (France), e-mail: Pierre.Borne@ec-lille.fr
M.BOHNER (USA), e-mail: bohner@mst.edu
T.A.BURTON (USA), e-mail: taburton@olympen.com
C.CRUZ-HERNANDEZ (Mexico), e-mail: ccruz@cicese.mx
M.FABRIZIO (Italy), e-mail: mauro.fabrizio@unibo.it
HAO WANG (Canada), e-mail: hao8@ualberta.ca
K.L.TEO (Australia), e-mail: K.L.Teo@curtin.edu.au

EDITORIAL BOARD

Aleksandrov, A.Yu. (Russia)	Jafari, H. (South African Republic)
Artstein, Z. (Israel)	Khusainov, D.Ya. (Ukraine)
Awrejcewicz, J. (Poland)	Kloeden, P. (Germany)
Benrejeb, M. (Tunisia)	Kokologiannaki, C. (Greece)
Braiek, N.B. (Tunisia)	Krishnan, E.V. (Oman)
Chen Ye-Hwa (USA)	Limarchenko, O.S. (Ukraine)
D'Anna, A. (Italy)	Nguang Sing Kiong (New Zealand)
De Angelis, M. (Italy)	Okninski, A. (Poland)
Denton, Z. (USA)	Peterson, A. (USA)
Vasundhara Devi, J. (India)	Radziszewski, B. (Poland)
Djemai, M. (France)	Shi Yan (Japan)
Dshalalow, J.H. (USA)	Sivasundaram, S. (USA)
Eke, F.O. (USA)	Sree Hari Rao, V. (India)
Gajic Z. (USA)	Staicu V. (Portugal)
Georgiou, G. (Cyprus)	Stavrakakis, N.M. (Greece)
Herlambang T. (Indonesia)	Vatsala, A. (USA)
Honglei Xu (Australia)	Zuyev, A.L. (Germany)
Izobov, N.A. (Belarus)	

ADVISORY COMPUTER SCIENCE EDITORS

A.N.CHERNIENKO and A.S.KHOROSHUN, Kiev, Ukraine

ADVISORY LINGUISTIC EDITOR

S.N.RASSHYVALOVA, Kiev, Ukraine

© 2020, InforMath Publishing Group, ISSN 1562-8353 print, ISSN 1813-7385 online, Printed in Ukraine
No part of this Journal may be reproduced or transmitted in any form or by any means without
permission from InforMath Publishing Group.

INSTRUCTIONS FOR CONTRIBUTORS

(1) General. Nonlinear Dynamics and Systems Theory (ND&ST) is an international journal devoted to publishing peer-refereed, high quality, original papers, brief notes and review articles focusing on nonlinear dynamics and systems theory and their practical applications in engineering, physical and life sciences. Submission of a manuscript is a representation that the submission has been approved by all of the authors and by the institution where the work was carried out. It also represents that the manuscript has not been previously published, has not been copyrighted, is not being submitted for publication elsewhere, and that the authors have agreed that the copyright in the article shall be assigned exclusively to InforMath Publishing Group by signing a transfer of copyright form. Before submission, the authors should visit the website:

<http://www.e-ndst.kiev.ua>

for information on the preparation of accepted manuscripts. Please download the archive Sample_NDST.zip containing example of article file (you can edit only the file Samplefilename.tex).

(2) Manuscript and Correspondence. Manuscripts should be in English and must meet common standards of usage and grammar. To submit a paper, send by e-mail a file in PDF format directly to

Professor A.A. Martynyuk, Institute of Mechanics,
Nesterov str.3, 03057, MSP 680, Kiev-57, Ukraine
e-mail: journalndst@gmail.com

or to one of the Regional Editors or to a member of the Editorial Board. Final version of the manuscript must typeset using LaTex program which is prepared in accordance with the style file of the Journal. Manuscript texts should contain the title of the article, name(s) of the author(s) and complete affiliations. Each article requires an abstract not exceeding 150 words. Formulas and citations should not be included in the abstract. AMS subject classifications and key words must be included in all accepted papers. Each article requires a running head (abbreviated form of the title) of no more than 30 characters. The sizes for regular papers, survey articles, brief notes, letters to editors and book reviews are: (i) 10-14 pages for regular papers, (ii) up to 24 pages for survey articles, and (iii) 2-3 pages for brief notes, letters to the editor and book reviews.

(3) Tables, Graphs and Illustrations. Each figure must be of a quality suitable for direct reproduction and must include a caption. Drawings should include all relevant details and should be drawn professionally in black ink on plain white drawing paper. In addition to a hard copy of the artwork, it is necessary to attach the electronic file of the artwork (preferably in PCX format).

(4) References. Each entry must be cited in the text by author(s) and number or by number alone. All references should be listed in their alphabetic order. Use please the following style:

Journal: [1] H. Poincare, Title of the article. *Title of the Journal volume*
(issue) (year) pages. [Language]

Book: [2] A.M. Lyapunov, *Title of the Book*. Name of the Publishers, Town, year.

Proceeding: [3] R. Bellman, Title of the article. In: *Title of the Book*. (Eds.).
Name of the Publishers, Town, year, pages. [Language]

(5) Proofs and Sample Copy. Proofs sent to authors should be returned to the Editorial Office with corrections within three days after receipt. The corresponding author will receive a sample copy of the issue of the Journal for which his/her paper is published.

(6) Editorial Policy. Every submission will undergo a stringent peer review process. An editor will be assigned to handle the review process of the paper. He/she will secure at least two reviewers' reports. The decision on acceptance, rejection or acceptance subject to revision will be made based on these reviewers' reports and the editor's own reading of the paper.

NONLINEAR DYNAMICS AND SYSTEMS THEORY

An International Journal of Research and Surveys

Published by InforMath Publishing Group since 2001

Volume 20

Number 1

2020

CONTENTS

PERSONAGE IN SCIENCE

- Professor V.M. Starzhinskii. To the 100th Birthday Anniversary 1
A.A. Martynyuk, N.A. Izobov, A.G. Mazko and V.I. Zhukovskii

- Generalized Monotone Method for Nonlinear Caputo Fractional
Impulsive Differential Equations 3
Y.Bai and A.S. Vatsala

- Control Design for Non-Linear Uncertain Systems via Coefficient
Diagram Method: Application to Solar Thermal Cylindrical
Parabolic Trough Concentrators 21
*Z. Fenchouche, M. Chakir, O. Benzineb, M.S. Boucherit
and M. Tadjine*

- Adaptive Sliding Mode Control Synchronization of a Novel, Highly
Chaotic 3-D System with Two Exponential Nonlinearities 38
F. Hannachi

- Motion Control Design of UNUSAITS AUV Using Sliding PID 51
T. Herlambang, S. Subchan, H. Nurhadi and D. Adzkiya

- Alternative Legendre Functions for Solving Nonlinear Fractional
Fredholm Integro-Differential Equations 61
Khawlah H. Hussain

- On the Boundedness of a Novel Four-Dimensional Hyperchaotic System 72
S. Rezzag

- Periodic Solutions in Non-Homogeneous Hill Equation 78
A. Rodriguez and J. Collado

- Estimates of Accuracy for Asymptotic Soliton-Like Solutions to the
Singularly Perturbed Benjamin-Bona-Mahony Equation 92
V. H. Samoilenko, Yu. I. Samoilenko and L. V. Vovk

- Oscillation Criteria for Delay Equations with Several Non-Monotone
Arguments 107
*I. P. Stavroulakis, Zh. Kh. Zhunussova, L. Kh. Zhunussova
and K. Dosmagulova*

Founded by A.A. Martynyuk in 2001.

Registered in Ukraine Number: KB 5267 / 04.07.2001.

NONLINEAR DYNAMICS AND SYSTEMS THEORY

An International Journal of Research and Surveys

Impact Factor from SCOPUS for 2018: 0.870, SJR – 0.292, and h-index – 15.

Nonlinear Dynamics and Systems Theory (ISSN 1562–8353 (Print), ISSN 1813–7385 (Online)) is an international journal published under the auspices of the S.P. Timoshenko Institute of Mechanics of National Academy of Sciences of Ukraine and Curtin University of Technology (Perth, Australia). It aims to publish high quality original scientific papers and surveys in areas of nonlinear dynamics and systems theory and their real world applications.

AIMS AND SCOPE

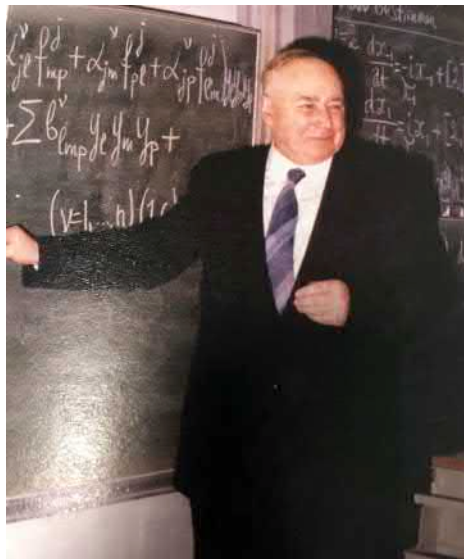
Nonlinear Dynamics and Systems Theory is a multidisciplinary journal. It publishes papers focusing on proofs of important theorems as well as papers presenting new ideas and new theory, conjectures, numerical algorithms and physical experiments in areas related to nonlinear dynamics and systems theory. Papers that deal with theoretical aspects of nonlinear dynamics and/or systems theory should contain significant mathematical results with an indication of their possible applications. Papers that emphasize applications should contain new mathematical models of real world phenomena and/or description of engineering problems. They should include rigorous analysis of data used and results obtained. Papers that integrate and interrelate ideas and methods of nonlinear dynamics and systems theory will be particularly welcomed. This journal and the individual contributions published therein are protected under the copyright by International InforMath Publishing Group.

PUBLICATION AND SUBSCRIPTION INFORMATION

Nonlinear Dynamics and Systems Theory will have 4 issues in 2020, printed in hard copy (ISSN 1562–8353) and available online (ISSN 1813–7385), by InforMath Publishing Group, Nesterov str., 3, Institute of Mechanics, Kiev, MSP 680, Ukraine, 03057. Subscription prices are available upon request from the Publisher, EBSCO Information Services (<mailto:journals@ebsco.com>), or website of the Journal: <http://e-ndst.kiev.ua>. Subscriptions are accepted on a calendar year basis. Issues are sent by airmail to all countries of the world. Claims for missing issues should be made within six months of the date of dispatch.

ABSTRACTING AND INDEXING SERVICES

Papers published in this journal are indexed or abstracted in: Mathematical Reviews / MathSciNet, Zentralblatt MATH / Mathematics Abstracts, PASCAL database (INIST–CNRS) and SCOPUS.



Professor V.M. Starzhinskii

To the 100th Birthday Anniversary

On March 10, 2018, the renowned Russian scientist in the area of mathematics and mechanics, Viacheslav Mikhaylovich Starzhinskii, would have turned 100 years old. To commemorate Professor Starzhinskii's valuable contribution to nonlinear dynamics, the Editorial Board of the Journal presents a short biographical sketch of his life and academic activities. A detailed review of his scientific and pedagogical activities is presented in the Section "Personage in Science" in the article "Professor V.M. Starzhinskii" by A.A. Martynyuk, J.H. Dshalalow, and V.I. Zhukovskii, Nonlinear Dynamics and Systems Theory, 8(1) (2008) 1–6.

Viacheslav Mikhaylovich Starzhinskii was born on March 10, 1918, in the village of Lemeshevichi of the Pinsky district, part of the Pinsky region (now the Brest region in Belarus). In 1935, he was admitted to the Department of Mechanics and Mathematics of Moscow State University to study mechanics. His graduation from Moscow State University coincided with the beginning of the Second World War. As a result, from 1941 to 1944, he worked as a constructor engineer at the military plants in Stupino town of the Moscow region and Verkhnyaya Salda town of the Sverdlov region. Then, from August 17, 1944 till September 9, 1945, he taught at the Verkhne-Salda Avia-Metallurgical Technical School of Narkomaviaprom (The Ministry of Aircraft Industry).

In October, 1945, Viacheslav Mikhaylovich was accepted to a full-time post-graduate school at the Scientific Research Institute of Mechanics of Moscow State University. At that time he got interested in automatic control systems. This influenced the topic of his upcoming PhD thesis "Some problems in the theory of tracking systems", which he successfully defended in June, 1948. That same year (on February 2, 1948) he was

appointed as a senior researcher in one of the scientific research institutes of the Ministry of Industry of Communications.

From September 1, 1950, he became an associate Professor of Mathematics in Calculus Program at the All-Union Correspondent Institute of Textil and Light Industry (A-UCITLI). On August 1, 1957, Viacheslav Mikhailovich became an associate Professor of Theoretical Mechanics Program at the A-UCITLI. In March, 1958, after defending his habilitation thesis, he became a Professor and then the Chair of the Program of Theoretical Mechanics.

Forty three years of his work at the A-UCITLI proved to be the most fruitful ones in the life of Viacheslav Mikhailovich. In 1952, he published his first paper "Sufficient stability conditions for a mechanical system with one degree of freedom". For the period of 1952–1957, he published seven more papers on the problems of stability of periodic motions. At that time, Viacheslav Mikhailovich entered a post-doctoral program for his habilitation degree at the Institute of Problems of Mechanics of the Academy of Sciences (his supervisor was the Corresponding Member of the Ac. of Sci. of the USSR, Professor N.G. Chetayev), and in 1957, he defended his habilitation thesis.

V.M. Starzhinskii published more than 150 papers and books (including 27 monographs and textbooks). His work covers the following areas:

- 1) The second Lyapunov method: first, second, third and fourth order equations;
- 2) Stability of periodic motions: estimations of characteristic constants in the second and n -th order systems; the theory of parametric resonance Mathieu and Hill equations;
- 3) Oscillations of substantially nonlinear systems, combination of the Lyapunov and Poincare methods, oscillating chains, energy jump, damped oscillating systems, computation of normal modes; normal modes for third, fourth and sixth order systems;
- 4) Application of parametric resonance theory to acoustic and electromagnetic waveguides;
- 5) Dynamics of a solid body: dimensionless form of the Euler-Poisson equations, oscillations of a heavy body with a fixed point, exclusive cases of Kovalevskaya gyroscope motion, QP -procedure for Kovalevskaya's case;
- 6) Applied problems: calculation of thread tension, elastic shaft, dynamical stability of rods, problem of three bodies, torsion oscillations of crank-shafts, pendulum on spring, thread mechanics, servo systems, cyclical accelerators.

Viacheslav Mikhailovich was a skillful lecturer. He conveyed a very complex material to his students in a clear fashion, without a compromise to the depth. His long-term teaching experience has also eventuated in the publication of many textbooks on theoretical mechanics.

During 1980 to 1988, Professor Starzhinskii delivered a series of lectures on nonlinear oscillations and parametric resonance for post-graduate students of the Mechanical and Mathematical Department of Moscow State University. His lectures have always been a success as they attracted many listeners who were inspired by his teaching. He worked actively with post-graduates and supervised four doctoral and five habilitation theses.

Professor Starzhinskii was a member of the Scientific-Methodical Council of Theoretical Mechanics of the Ministry of Education, the USSR, and a member of the Editorial Board of the Publishing House "Mir". He was among the active contributors to the Mathematical Encyclopedia.

V.M. Starzhinskii was rewarded with three medals of honor. In 1985, he received the reward "For Successes in the Field of Higher Education".

A.A. Martynyuk, N.A. Izobov, A.G. Mazko, V.I. Zhukovskii



Generalized Monotone Method for Nonlinear Caputo Fractional Impulsive Differential Equations

Y. Bai and A. S. Vatsala*

Department of Mathematics, University of Louisiana at Lafayette, Louisiana – 70504.

Received: September 22, 2019; Revised: January 8, 2020

Abstract: Generalized monotone method is a useful technique to prove the existence of coupled minimal and maximal solutions when the nonlinear function is the sum of an increasing and decreasing functions. In this work, we develop generalized monotone method for Caputo fractional impulsive differential equations with initial conditions, using coupled lower and upper solutions of Type 1. For that purpose we develop comparison results for Caputo fractional impulsive differential equation. Further, under uniqueness assumption, we prove the existence of the unique solution of the nonlinear Caputo fractional impulsive differential equation with initial conditions.

Keywords: *nonlinear Caputo fractional differential equations; impulsive differential equations; generalized monotone method.*

Mathematics Subject Classification (2010): 34A08, 34A37.

1 Introduction

In the past few decades, the impulsive equations have exhibited more advantages in the mathematical models of physical and biological models. See [2, 3, 6–8, 14, 23] for details. These equations can describe more naturally and more closed to the real world problems. See [9, 12, 15]. In the past four decades, the study of fractional differential equations has gained lots of importance due to its applications. See [1, 4, 5, 10, 11, 13, 25, 26]. In fact, the dynamic equations with fractional derivative have represented as better and economical models in various branches of science and engineering. See [12, 13, 15–17].

In this work, we develop generalized monotone method combined with coupled lower and upper solutions for nonlinear Caputo fractional impulsive differential equations with initial conditions. In general, explicit solution for nonlinear problems is rarely possible.

* Corresponding author: <mailto:vatsala@louisiana.edu>

In addition, explicit solution even for linear Caputo fractional differential equations with variable coefficients with or without impulses and initial conditions is not trivial either. However, explicit solution of the solution and/or representation form of the solution of linear Caputo fractional impulsive differential equation with initial condition is possible. See [22] for more details. In addition, in [22], the uniqueness of the solution of the linear Caputo fractional impulsive differential equation has been proved by developing a comparison result.

We apply generalized monotone method, Laplace transform and some properties in the main result. See [6, 18–21, 24, 27, 28] for more details. In [22], we have obtained explicit solutions for the linear Caputo fractional impulsive differential equations with initial condition. In addition, we have also developed a comparison result in [22] relative to coupled lower and upper solutions.

In the present work, we have also developed linear comparison results as an auxiliary result which is useful in our main result. We have developed monotone sequences $\{v_n\}$ and $\{w_n\}$ which are piece-wise left continuous using the coupled lower and upper solutions, when the nonlinear function is the sum of non-decreasing and non-increasing functions. We have established the monotone sequences which converge uniformly and monotonically to coupled minimal and maximal solutions of the nonlinear problem. Furthermore, under uniqueness assumptions on the nonlinear terms, we prove that the coupled minimal and maximal solutions reduce to the unique solutions of the nonlinear problem.

2 Preliminary Results

In this section, we introduce some known definitions and results, which are needed for the main results. First, we recall some basic definitions.

Definition 2.1 The Riemann-Liouville fractional integral of $u(t)$ of order q is defined by

$$D_t^{-q}u = \frac{1}{\Gamma(q)} \int_0^t (t-s)^{q-1}u(s)ds, \quad (1)$$

where $0 < q \leq 1$.

Definition 2.2 The Caputo (left) fractional derivative of $u(t)$ of order q , when $0 < q < 1$, is defined as:

$${}^c D_t^q u(t) = \frac{1}{\Gamma(1-q)} \int_0^t (t-s)^{-q}u'(s)ds. \quad (2)$$

Definition 2.3 The Riemann-Liouville (left-sided) fractional derivative of $u(t)$ of order q , when $0 < q < 1$, is defined as

$$D^q u(t) = \frac{1}{\Gamma(1-q)} \frac{d}{dt} \int_0^t (t-s)^{-q}u(s)ds, \quad t > 0. \quad (3)$$

The relation between Caputo derivative and Riemann-Liouville derivative of a function $f(t)$ is given by

$${}^c D^q u(t) = D^q(u(t) - u(0)).$$

This relation will be useful for results relative to differential inequalities.

Next we define the Mittag-Leffler function which is useful in computing the solution of the linear fractional differential equations.

Definition 2.4 The two parameter Mittag-Leffler function is defined as

$$E_{q,r}(\lambda t^q) = \sum_{k=0}^{\infty} \frac{(\lambda t^q)^k}{\Gamma(qk+r)}. \quad (4)$$

If $r = q$, the relation (4) reduces to

$$E_{q,q}(\lambda t^q) = \sum_{k=0}^{\infty} \frac{(\lambda t^q)^k}{\Gamma q(k+1)}. \quad (5)$$

If $r = 1$, the Mittag-leffler function is defined as

$$E_{q,1}(\lambda t^q) = \sum_{k=0}^{\infty} \frac{(\lambda t^q)^k}{\Gamma q(k+1)}. \quad (6)$$

See [5, 10, 13, 16] for more details.

In our next definition we assume $p = 1 - q$, when $0 < q < 1$, $J = (0, T]$ and $J_0 = [0, T]$.

Definition 2.5 A function $\phi(t) \in C(J, \mathbb{R})$ is a C_p continuous function on J if $t^{1-q}\phi(t) \in C(J_0, \mathbb{R})$. The set of C_p continuous functions is denoted by $C_p(J, \mathbb{R})$. Further, given a function $\phi(t) \in C_p(J, \mathbb{R})$, we call the function $t^{1-q}\phi(t)$ the continuous extension of $\phi(t)$.

Next, we introduce some theorems and lemmas which are useful to our main results.

Lemma 2.1 Let $J = [0, T]$, $m \in C_p(J, \mathbb{R})$ be such that for some $t^0 \in J$, we have $m(t^0) = 0$ and $m(t) \leq 0$ for $t \in [0, t^0]$, then (Riemann-Liouville fractional derivative) $D^q m(t^0) \geq 0$.

See [4, 5] for the details of the proof.

Lemma 2.2 Let $J = [0, T]$, such that $0 < t_1 < t_2 < \dots < t_{N-1} < t_N = T$, and m be piece-wise left continuous on each $(t_i, t_{i+1}]$. Suppose there exists a $t^0 \in J$, such that $m(t^0) = 0$ and $m(t) \leq 0$ for $t \in [0, t^0]$, then $D^q m(t^0) \geq 0$.

See [4, 21] for the details of the proof.

Remark: The above result is also true with Caputo derivative in place of Riemann-Liouville derivative. The proof can be easily obtained by applying the relation between the Caputo derivative and the Riemann-Liouville derivative, which is ${}^C D^q m(t) = D^q(m(t) - m(0))$.

Consider the linear Caputo fractional differential equation

$${}^C D^q u = \lambda u + f(t), \quad u(0) = u_0. \quad (7)$$

Then the solution of (7) is given by

$$u(t) = u_0 E_{q,1}(\lambda t^q) + \int_0^t (t-s)^{q-1} E_{q,q}(\lambda(t-s)^q) f(s) ds. \quad (8)$$

Consider the nonlinear Caputo fractional impulsive differential equations with initial condition

$$\begin{cases} {}^cD^q u(t) = \lambda u(t) + \sum_{i=1}^N c_i \chi(t - t_i) s_i(t - t_i) u(t_i) \\ \quad + \sum_{i=1}^N b_i \chi(t - t_i) r_i(t - t_i) u(t_i) + f(t, u(t)) + g(t, u(t)), \\ u(0) = u_0, \end{cases} \quad (9)$$

where $t \in [0, T]$, and $0 < t_1 < t_2 < \dots < t_N = T$. Also, $\chi(t - t_i)$ is the Heaviside unit step function which is left continuous,

$$\chi(t - t_i) = \begin{cases} 1, & \text{if } t > t_i, \\ 0, & \text{if } t \leq t_i. \end{cases} \quad (10)$$

Furthermore, we assume that $\lambda \neq 0$, and for each $1 \leq i \leq N$, $c_i \chi(t - t_i) s_i(t - t_i) \geq 0$ and $b_i \chi(t - t_i) r_i(t - t_i) \leq 0$. The function $f(t, u)$ is nondecreasing in u and $g(t, u)$ is nonincreasing in u . In addition, $s_i(t - t_i)$ and $r_i(t - t_i)$ are continuous on each interval $[t_i, t_{i+1}]$ for $i = 1, \dots, N - 1$. Therefore, they are bounded on each interval.

Next we define the coupled lower and upper solutions of natural type as well of Type 1. See [9] for other types of coupled lower and upper solutions.

Definition 2.6 If $u : C[0, T] \rightarrow \mathbb{R}$ which is piecewise left continuous at t_i , $i = 1, 2, \dots, N$, such that $0 < t_1 \leq t_2 \leq \dots \leq t_N = T$, and whose Caputo derivative of order q exists on $[0, T]$. Then we denote $f \in PC^q[[0, T], \mathbb{R}]$.

Definition 2.7 We say that v, w are $PC^q[[0, T], \mathbb{R}]$ piecewise left continuous on (t_i, t_{i+1}) for $i = 1, \dots, N - 1$. Then we say v and w are coupled lower and upper solutions of natural type of (9) if they satisfy the inequalities:

$$\begin{aligned} {}^cD^q v(t) &\leq \lambda v(t) + \sum_{i=1}^N a_i \chi(t - t_i) s_i(t - t_i) v(t_i) + \sum_{i=1}^N b_i \chi(t - t_i) r_i(t - t_i) v(t_i) \\ &\quad + f(t, v) + g(t, v), \\ v(0) &\leq u_0, \end{aligned} \quad (11)$$

$$\begin{aligned} {}^cD^q w(t) &\geq \lambda w(t) + \sum_{i=1}^N a_i \chi(t - t_i) s_i(t - t_i) w(t_i) + \sum_{i=1}^N b_i \chi(t - t_i) r_i(t - t_i) w(t_i) \\ &\quad + f(t, w) + g(t, w), \\ w(0) &\geq u_0. \end{aligned} \quad (12)$$

Definition 2.8 We say that v, w are $PC^q[[0, T], \mathbb{R}]$ piecewise left continuous on (t_i, t_{i+1}) for $i = 1, \dots, N - 1$. Then we say v and w are coupled lower and upper solutions of type 1 if they satisfy the inequalities:

$$\begin{aligned} {}^cD^q v(t) &\leq \lambda v(t) + \sum_{i=1}^N a_i \chi(t - t_i) s_i(t - t_i) v(t_i) + \sum_{i=1}^N b_i \chi(t - t_i) r_i(t - t_i) w(t_i) \\ &\quad + f(t, v) + g(t, w) \\ v(0) &\leq u_0, \end{aligned} \quad (13)$$

$$\begin{aligned} {}^cD^q w(t) &\geq \lambda w(t) + \sum_{i=1}^N a_i \chi(t - t_i) s_i(t - t_i) w(t_i) + \sum_{i=1}^N b_i \chi(t - t_i) r_i(t - t_i) v(t_i) \\ &\quad + f(t, w) + g(t, v), \\ w(0) &\geq u_0. \end{aligned} \tag{14}$$

Theorem 2.1 If $\lambda \neq 0$, $v(t)$ and $w(t)$ are coupled lower and upper solutions of type 1 of the nonlinear Caputo impulsive fractional differential equation (9), where $f(t, u)$ and $g(t, u)$ satisfy the one-sided Lipschitz condition in u , of the following form with $u_1 \geq u_2$

$$f(t, u_1) - f(t, u_2) \leq L_1(u_1 - u_2), \tag{15}$$

$$g(t, u_1) - g(t, u_2) \geq -L_2(u_1 - u_2), \tag{16}$$

where $L_1 \geq 0$ and $L_2 \geq 0$. Then $v(0) \leq w(0)$ implies that $v(t) \leq w(t)$, $\forall t \geq J = [0, T]$.

See [22] for the details of the proof.

3 Auxiliary Results

In this section, we prove a comparison theorem which will be used to prove the generalized monotone method in the main result.

Theorem 3.1 If the functions $P(t)$ and $Q(t)$ are $PC^q[[0, T], \mathbb{R}]$ such that satisfy the following inequalities:

$${}^cD^q P \leq \lambda P + \sum_{i=1}^N c_i \chi(t - t_i) s_i(t - t_i) P(t_i) + \sum_{i=1}^N b_i \chi(t - t_i) r_i(t - t_i) Q(t_i), \tag{17}$$

$${}^cD^q Q \geq \lambda Q + \sum_{i=1}^N c_i \chi(t - t_i) s_i(t - t_i) Q(t_i) + \sum_{i=1}^N b_i \chi(t - t_i) r_i(t - t_i) P(t_i), \tag{18}$$

where $\lambda \geq 0$, and for each $1 \leq i \leq N$, $c_i \chi(t - t_i) s_i(t - t_i) \geq 0$ and $b_i \chi(t - t_i) r_i(t - t_i) \leq 0$, then the initial condition $P(0) \leq 0$ and $Q(0) \geq 0$ implies $P(t) \leq 0$ and $Q(t) \geq 0$ for all $t \in [0, T]$.

Proof. We prove by the method of mathematical induction. For $t \in [0, t_1)$

$${}^cD^q P(t) \leq \lambda P(t), \quad {}^cD^q Q(t) \geq \lambda Q(t). \tag{19}$$

Then we can get

$$P(t) \leq P(0) E_{q,1}(\lambda t^q) \leq 0, \quad Q(t) \geq Q(0) E_{q,1}(\lambda t^q) \geq 0. \tag{20}$$

For $t = t_1$, we have

$$P(t_1) \leq P(0) E_{q,1}(\lambda t_1^q) \leq 0, \quad Q(t_1) \geq Q(0) E_{q,1}(\lambda t_1^q) \geq 0. \tag{21}$$

Assume the result is true for $t \in [t_{k-1}, t_k]$, for $0 \leq k \leq N-1$, which yields $P(t_k) \leq 0$ and $Q(t_k) \geq 0$ for all $0 \leq k \leq N-1$. Then, for $t \in [t_k, t_{k+1})$,

$${}^cD^q P(t) \leq \lambda P(t) + \sum_{i=1}^k c_i \chi(t - t_i) s_i(t_{k+1} - t_i) P(t_i) + \sum_{i=1}^k b_i \chi(t - t_i) r_i(t_{k+1} - t_i) Q(t_i). \tag{22}$$

With the result of $P(t_k) \leq 0$ and $Q(t_k) \geq 0$ for all $0 \leq k \leq N-1$, we can get ${}^cD^q P \leq \lambda P$. Therefore we have $P(t) \leq P(0)E_{q,1}(\lambda t^q) \leq 0$ on $[0, t_{k+1}]$. Then for $t = t_{k+1}$, we have $P(t_{k+1}) \leq 0$. Similarly, we have the results for $Q(t)$,

$$Q(t) \geq Q(0)E_{q,1}(\lambda t^q) \geq 0.$$

Then $Q(t_{k+1}) \geq 0$. Since it is true for $i = 1$, therefore, by induction, for all t_i , $0 \leq i \leq N$, $P(t_i) \leq 0$ and $Q(t_i) \geq 0$. Then we have $P(t) \leq 0$ and $Q(t) \geq 0$ for all $0 \leq t \leq t_N$, which completes the proof.

Lemma 3.1 *If the functions $P(t)$ and $Q(t)$ are $PC^q[[0, T], \mathbb{R}]$ such that to satisfy the following inequalities:*

$${}^cD^q P \leq \lambda P + \sum_{i=1}^N c_i \chi(t - t_i) s_i(t - t_i) P(t_i), \quad (23)$$

$${}^cD^q Q \geq \lambda Q + \sum_{i=1}^N c_i \chi(t - t_i) s_i(t - t_i) Q(t_i). \quad (24)$$

where $\lambda \neq 0$, $\sum_{i=1}^N c_i \chi(t - t_i) s_i(t - t_i) \geq 0$, then the initial condition $P(0) \leq 0$ and $Q(0) \geq 0$ implies $P(t) \leq 0$ and $Q(t) \geq 0$ for all $t \in [0, T]$.

Proof. This is a special case of Theorem 3.1 with $b_i = 0$ for all $i = 1, 2, \dots, N$. Therefore the proof is almost the same as the one in Theorem 3.1.

4 Main Result

In this section, we consider the nonlinear Caputo impulsive differential equation of the form (9), which has application in science and biology. Since it is rarely possible to compute the solution of the nonlinear problem with or without impulses and with integer derivatives or fractional derivatives, hence we develop generalized monotone method together with coupled lower and upper solution. See [9, 18] for more details.

The method yields monotone sequences which converge uniformly and monotonically to coupled minimal and maximal solutions of (9) on the sector defined by coupled lower and upper solutions. Furthermore, if the nonlinear functions satisfy uniqueness condition, then the coupled minimal and maximal solutions coincide to be the unique solution of (9).

Note that the generalized monotone method is a more appropriate method to prove the existence of the nonlinear Caputo fractional impulsive differential equations when the nonlinear function is the sum of nondecreasing and nonincreasing functions.

In order to prove our main results, we need the existence and uniqueness of solution of two linear systems of Caputo fractional impulsive differential equations with initial condition. This is precisely the next result.

Theorem 4.1 *Let v_0, w_0 be coupled lower and upper solutions of (9) of type 1, such that $v_0(t) \leq w_0(t)$ on $t \in [0, T]$. Suppose η and μ are any two functions such that*

$v_0 \leq \eta \leq \mu \leq w_0$ on $[0, T]$, then the solution of the following linear Caputo fractional impulsive differential equations:

$$\begin{cases} {}^cD^q p = \lambda p + f(t, \eta) + g(t, \mu) + \sum_{i=1}^N c_i \chi(t-t_i) s_i(t-t_i) p(t_i) + \sum_{i=1}^N b_i \chi(t-t_i) r_i(t-t_i) q(t_i), \\ p(0) = u_0, \end{cases} \quad (25)$$

$$\begin{cases} {}^cD^q q = \lambda q + f(t, \mu) + g(t, \eta) + \sum_{i=1}^N c_i \chi(t-t_i) s_i(t-t_i) q(t_i) + \sum_{i=1}^N b_i \chi(t-t_i) r_i(t-t_i) p(t_i), \\ q(0) = u_0, \end{cases} \quad (26)$$

exists and it is unique.

Proof. Since $\mu(t)$ and $\eta(t)$ are known functions of t , it is easy to see that $f(t, \mu)$, $f(t, \eta)$, $g(t, \mu)$ and $g(t, \eta)$ become functions of t and let us denote

$$f(t, \eta) + g(t, \mu) = F(t), \quad f(t, \mu) + g(t, \eta) = G(t). \quad (27)$$

Then the equations (25) and (26) become linear system of Caputo fractional impulsive differential equations, namely

$$\begin{cases} {}^cD^q p = \lambda p + F(t) + \sum_{i=1}^N c_i \chi(t-t_i) s_i(t-t_i) p(t_i) + \sum_{i=1}^N b_i \chi(t-t_i) r_i(t-t_i) q(t_i), \\ p(0) = u_0, \end{cases} \quad (28)$$

$$\begin{cases} {}^cD^q q = \lambda q + G(t) + \sum_{i=1}^N c_i \chi(t-t_i) s_i(t-t_i) q(t_i) + \sum_{i=1}^N b_i \chi(t-t_i) r_i(t-t_i) p(t_i), \\ q(0) = 0. \end{cases} \quad (29)$$

Applying the Laplace transformation, the solution of the $p(t)$ and $q(t)$ are given by

$$\begin{cases} p = u_0 E_{q,1}(\lambda t^q) + \int_0^t (t-s)^{q-1} E_{q,q}(\lambda(t-s)^q) F(s) ds \\ \quad + \sum_{i=1}^N c_i \chi(t-t_i) S_i(t-t_i) p(t_i) + \sum_{i=1}^N b_i \chi(t-t_i) R_i(t-t_i) q(t_i), \\ q = u_0 E_{q,1}(\lambda t^q) + \int_0^t (t-s)^{q-1} E_{q,q}(\lambda(t-s)^q) G(s) ds \\ \quad + \sum_{i=1}^N c_i \chi(t-t_i) S_i(t-t_i) q(t_i) + \sum_{i=1}^N b_i \chi(t-t_i) R_i(t-t_i) p(t_i), \end{cases} \quad (30)$$

where $S_i(t-t_i) = \mathcal{L}^{-1}\left(\frac{\mathcal{L}(s_i)}{s^q - \lambda}\right)$ and $R_i(t-t_i) = \mathcal{L}^{-1}\left(\frac{\mathcal{L}(r_i)}{s^q - \lambda}\right)$, for $i = 1, 2, \dots, N$. \mathcal{L} and \mathcal{L}^{-1} are the Laplace transformation and the inverse Laplace transformation, respectively. Then for $t \in [0, t_1]$, the equations (28) and (29) reduce to

$${}^cD^q p = \lambda p + F(t), \quad {}^cD^q q = \lambda q + G(t). \quad (31)$$

Use the result of (8). The solution $p(t)$ and $q(t)$ can be given by

$$\begin{cases} p = u_0 E_{q,1}(\lambda t^q) + \int_0^t (t-s)^{q-1} E_{q,q}(\lambda(t-s)^q) F(s) ds, \\ q = u_0 E_{q,1}(\lambda t^q) + \int_0^t (t-s)^{q-1} E_{q,q}(\lambda(t-s)^q) G(s) ds. \end{cases} \quad (32)$$

For $t = t_1$, we get

$$\begin{cases} p(t_1) = u_0 E_{q,1}(\lambda t_1^q) + \int_0^{t_1} (t_1 - s)^{q-1} E_{q,q}(\lambda(t_1 - s)^q) F(s) ds, \\ q(t_1) = u_0 E_{q,1}(\lambda t_1^q) + \int_0^{t_1} (t_1 - s)^{q-1} E_{q,q}(\lambda(t_1 - s)^q) G(s) ds. \end{cases} \quad (33)$$

For $t \in [t_1, t_2]$, the equations (28) and (29) reduce to

$${}^c D^q p = \lambda p + F(t) + c_1 s_1(t - t_1) p(t_1) + b_1 r_1(t - t_1) q(t_1), \quad (34)$$

$${}^c D^q q = \lambda q + G(t) + c_1 s_1(t - t_1) q(t_1) + b_1 r_1(t - t_1) p(t_1). \quad (35)$$

The solution can be given as

$$\begin{cases} p = u_0 E_{q,1}(\lambda t^q) + \int_0^t (t - s)^{q-1} E_{q,q}(\lambda(t - s)^q) F(s) ds \\ \quad + c_1 S_1(t - t_1) p(t_1) + b_1 R_1(t - t_1) q(t_1), \\ q = u_0 E_{q,1}(\lambda t^q) + \int_0^t (t - s)^{q-1} E_{q,q}(\lambda(t - s)^q) G(s) ds \\ \quad + c_1 S_1(t - t_1) q(t_1) + b_1 R_1(t - t_1) p(t_1). \end{cases} \quad (36)$$

After substituting $p(t_1)$ and $q(t_1)$, the equation (36) reduces to

$$\begin{cases} p = u_0 E_{q,1}(\lambda t^q) + \int_0^t (t - s)^{q-1} E_{q,q}(\lambda(t - s)^q) F(s) ds \\ \quad + c_1 S_1(t - t_1) \left(u_0 E_{q,1}(\lambda t_1^q) + \int_0^{t_1} (t_1 - s)^{q-1} E_{q,q}(\lambda(t_1 - s)^q) F(s) ds \right) \\ \quad + b_1 R_1(t - t_1) \left(u_0 E_{q,1}(\lambda t_1^q) + \int_0^{t_1} (t_1 - s)^{q-1} E_{q,q}(\lambda(t_1 - s)^q) G(s) ds \right), \\ q = u_0 E_{q,1}(\lambda t^q) + \int_0^t (t - s)^{q-1} E_{q,q}(\lambda(t - s)^q) G(s) ds \\ \quad + c_1 S_1(t - t_1) \left(u_0 E_{q,1}(\lambda t_1^q) + \int_0^{t_1} (t_1 - s)^{q-1} E_{q,q}(\lambda(t_1 - s)^q) G(s) ds \right) \\ \quad + b_1 R_1(t - t_1) \left(u_0 E_{q,1}(\lambda t_1^q) + \int_0^{t_1} (t_1 - s)^{q-1} E_{q,q}(\lambda(t_1 - s)^q) F(s) ds \right), \end{cases} \quad (37)$$

where $S_1(t - t_1) = \mathfrak{L}^{-1} \left(\frac{\mathfrak{L}(s_1)}{s^q - \lambda} \right)$ and $R_1(t - t_1) = \mathfrak{L}^{-1} \left(\frac{\mathfrak{L}(r_1)}{s^q - \lambda} \right)$. Then we can find the value of $p(t_2)$ and $q(t_2)$ by substituting t_2 into the equation (37). Then after another iteration, we can get the solution for $t \in [t_2, t_3]$. If we continue the above process, we can obtain a closed form of solution of (25)-(26) for all $t \in [0, T]$.

In order to prove the uniqueness of the solution of the equations (25) and (26), let (p_1, q_1) and (p_2, q_2) be two solutions. Then let $m = p_1 - p_2$ and $n = q_1 - q_2$. Then,

$${}^c D^q m = \lambda m + \sum_{i=1}^N c_i \chi(t - t_i) s_i(t - t_i) m(t_i) + \sum_{i=1}^N b_i \chi(t - t_i) r_i(t - t_i) n(t_i), \quad (38)$$

$$m(0) = 0,$$

$${}^c D^q n = \lambda n + \sum_{i=1}^N c_i \chi(t - t_i) s_i(t - t_i) n(t_i) + \sum_{i=1}^N b_i \chi(t - t_i) r_i(t - t_i) m(t_i), \quad (39)$$

$$n(0) = 0.$$

Then by applying Theorem 3.1, we can get that $m \equiv 0$ and $n \equiv 0$ for all $t \in [0, T]$, which means $p_1 \equiv p_2$ and $q_1 \equiv q_2$ for all $t \in [0, T]$. Hence the solution of the system (25)-(26) is unique. This concludes the proof.

In the next result, we construct the sequences v_n and w_n , which are monotonically increasing and decreasing sequences. The sequences v_n and w_n are the solution of the following linear system of Caputo fractional impulsive differential equation. They are defined as

$$\begin{aligned} {}^cD^q v_n &= \lambda v_n + f(t, v_{n-1}) + g(t, w_{n-1}) \\ &\quad + \sum_{i=1}^N c_i \chi(t - t_i) s_i(t - t_i) v_n(t_i) + \sum_{i=1}^N b_i \chi(t - t_i) r_i(t - t_i) w_n(t_i), \end{aligned} \quad (40)$$

$$v_n(0) = u_0,$$

$$\begin{aligned} {}^cD^q w_n &= \lambda w_n + f(t, w_{n-1}) + g(t, v_{n-1}) \\ &\quad + \sum_{i=1}^N c_i \chi(t - t_i) s_i(t - t_i) w_n(t_i) + \sum_{i=1}^N b_i \chi(t - t_i) r_i(t - t_i) v_n(t_i), \end{aligned} \quad (41)$$

$$w_n(0) = u_0.$$

Here v_0 and w_0 are coupled lower and upper solutions of Type 1 of the problem (9).

In order to prove our first next main result, we need the following sector Ω , defined as

$$\Omega = [(t, u) : v_0(t) \leq u \leq w_0(t), t \in [0, T]], \quad (42)$$

where v_0 and w_0 are coupled lower and upper solution of suitable type of equation (9)

Theorem 4.2 *Assume*

(A₁). v_0 and w_0 are coupled lower and upper solutions of type 1 of the equation (9), such that $v_0 \leq w_0$ on $[0, T]$;

(A₂). $f(t, u)$ and $g(t, u)$ are nondecreasing and nonincreasing, respectively, on Ω .

Then the sequences $\{v_n\}$ and $\{w_n\}$ defined by (40)-(41) are well defined and satisfy the following results:

(i). $\{v_n\}$ and $\{w_n\}$ satisfy the inequality

$$v_0 \leq v_1 \leq v_2 \leq \cdots \leq v_n \leq w_n \leq w_{n-1} \leq \cdots \leq w_1 \leq w_0, \quad \forall t \in [0, T]. \quad (43)$$

(ii). If u is any solution of equation (9) such that $v_0 \leq u \leq w_0$, then the sequences $\{v_n\}$ and $\{w_n\}$ converge uniformly and monotonically to the coupled minimal and maximal solutions $v(t)$ and $w(t)$, respectively, such that $v(t) \leq u \leq w(t)$.

(iii). Furthermore, if $f(t, u)$ and $g(t, u)$ satisfy the one-sided Lipschitz condition of the form

$$f(t, u_1) - f(t, u_2) \leq L_1(u_1 - u_2), \quad g(t, u_1) - g(t, u_2) \geq L_2(u_1 - u_2), \quad (44)$$

where $u_1 \geq u_2$, $L_1 \geq 0$ and $L_2 \geq 0$, $\forall t \in [0, T]$, then we have $v(t) = w(t) = u(t)$ being the unique solution of (9) on $[0, T]$.

Proof. We know that $v_0 \leq w_0$. Then from Theorem 4.1, it is easy to see that $v_1(t)$ and $w_1(t)$ exist and are unique as well as $v_n(t)$ and $w_n(t)$ for each $n \geq 1$. In order to prove that v_n and w_n are monotonically non-decreasing and non-increasing respectively and $v_n \leq w_n$ for all $n \geq 1$, we use the method of mathematical induction. Initially, we prove $v_0 \leq v_1$ and $w_1 \leq w_0$. Assume $P(t) = v_0(t) - v_1(t)$ and $Q(t) = w_0(t) - w_1(t)$. Then we have

$$P(0) \leq u_0 - u_0 = 0 \quad Q(0) \geq u_0 - u_0 = 0, \quad (45)$$

and

$$\begin{aligned}
 {}^cD^q P &= {}^cD^q(v_0 - v_1) = {}^cD^q v_0 - {}^cD^q v_1 \\
 &\leq \lambda P + \sum_{i=1}^N c_i \chi(t - t_i) s_i(t - t_i) P(t_i) + \sum_{i=1}^N b_i \chi(t - t_i) r_i(t - t_i) Q(t_i), \\
 {}^cD^q Q &= {}^cD^q(w_0 - w_1) = {}^cD^q w_0 - {}^cD^q w_1 \\
 &\geq \lambda Q + \sum_{i=1}^N c_i \chi(t - t_i) s_i(t - t_i) Q(t_i) + \sum_{i=1}^N b_i \chi(t - t_i) r_i(t - t_i) P(t_i).
 \end{aligned} \tag{46}$$

Using Theorem 3.1, we have $P(t) \leq 0$ and $Q(t) \geq 0$. This proves $v_0 \leq v_1$ and $w_1 \leq w_0$ for all $t \in [0, T]$.

Assume that $v_n \leq v_{n+1}$ and $w_{n+1} \leq w_n$ are true for $n = k$, $k \geq 0$. Therefore, $v_k \leq v_{k+1}$ and $w_{k+1} \leq w_k$ for all $t \in [0, T]$. Then let $n = k + 1$, let $P(t) = v_{k+1} - v_{k+2}$ and $Q(t) = w_{k+1} - w_{k+2}$. Therefore $P(0) = Q(0) = 0$.

With the assumption (A_2) on f and g , we can get

$$\begin{aligned}
 {}^cD^q P &= \lambda P + f(t, v_k) - f(t, v_{k+1}) + g(t, w_k) - g(t, w_{k+1}) \\
 &\quad + \sum_{i=1}^N c_i \chi(t - t_i) s_i(t - t_i) P(t_i) + \sum_{i=1}^N b_i \chi(t - t_i) r_i(t - t_i) Q(t_i) \\
 &\leq \lambda P + \sum_{i=1}^N c_i \chi(t - t_i) s_i(t - t_i) P(t_i) + \sum_{i=1}^N b_i \chi(t - t_i) r_i(t - t_i) Q(t_i).
 \end{aligned} \tag{47}$$

Similarly, for $Q(t)$ we can get

$$\begin{aligned}
 {}^cD^q Q &= \lambda Q + f(t, w_k) - f(t, w_{k+1}) + g(t, v_k) - g(t, v_{k+1}) \\
 &\quad + \sum_{i=1}^N c_i \chi(t - t_i) s_i(t - t_i) Q(t_i) + \sum_{i=1}^N b_i \chi(t - t_i) r_i(t - t_i) P(t_i) \\
 &\geq \lambda Q + \sum_{i=1}^N c_i \chi(t - t_i) s_i(t - t_i) Q(t_i) + \sum_{i=1}^N b_i \chi(t - t_i) r_i(t - t_i) P(t_i).
 \end{aligned} \tag{48}$$

Using Theorem 3.1, we have $P(t) \leq 0$ and $Q(t) \geq 0$. This proves $v_{k+1} \leq v_{k+2}$ and $w_{k+2} \leq w_{k+1}$ for all $0 \leq t \leq t_N$. Certainly, it is true for $k = 1$, hence, by induction, we have the result

$$v_0 \leq v_1 \leq \cdots \leq v_{n-1} \leq v_n, \quad w_n \leq w_{n-1} \leq \cdots \leq w_1 \leq w_0. \tag{49}$$

Next we prove that $v_n \leq w_n$ on $t \in [0, T]$ for all $n \geq 1$. We prove it using the method of mathematical induction.

Let $p(t) = v_1(t) - w_1(t)$, then $p(0) = v_1(0) - w_1(0) = u_0 - u_0 = 0$. Using the

assumption (A_2) on f and g , we can get

$$\begin{aligned} {}^cD^q p &= \lambda p + f(t, v_0) - f(t, w_0) + g(t, w_0) - g(t, v_0) \\ &\quad + \sum_{i=1}^N c_i \chi(t - t_i) s_i(t - t_i) p(t_i) + \sum_{i=1}^N b_i \chi(t - t_i) r_i(t - t_i) (-p(t_i)) \\ &\leq \lambda p + \sum_{i=1}^N c_i \chi(t - t_i) s_i(t - t_i) p(t_i) + \sum_{i=1}^N b_i \chi(t - t_i) r_i(t - t_i) (-p(t_i)) \\ &\leq \lambda p + \sum_{i=1}^N (c_i \chi(t - t_i) s_i(t - t_i) - b_i \chi(t - t_i) r_i(t - t_i)) p(t_i). \end{aligned} \quad (50)$$

By Lemma 3.1, we have $p(t) \leq 0$. Therefore, $v_1 \leq w_1$ for all $t \in [0, T]$.

Assume the result $v_n \leq w_n$ is true for $n = k$, which is $v_k \leq w_k$ for all $t \in [0, T]$. For $n = k + 1$, we let $p(t) = v_{k+1}(t) - w_{k+1}(t)$, then $p(0) = u_0 - u_0 = 0$. With the assumption (A_2) , we have

$$\begin{aligned} {}^cD^q p &= \lambda p + f(t, v_k) - f(t, w_k) + g(t, w_k) - g(t, v_k) \\ &\quad + \sum_{i=1}^N c_i \chi(t - t_i) s_i(t - t_i) p(t_i) + \sum_{i=1}^N b_i \chi(t - t_i) r_i(t - t_i) (-p(t_i)) \\ &\leq \lambda p + \sum_{i=1}^N c_i \chi(t - t_i) s_i(t - t_i) p(t_i) + \sum_{i=1}^N b_i \chi(t - t_i) r_i(t - t_i) (-p(t_i)) \\ &\leq \lambda p + \sum_{i=1}^N (c_i \chi(t - t_i) s_i(t - t_i) - b_i \chi(t - t_i) r_i(t - t_i)) p(t_i). \end{aligned} \quad (51)$$

Using the result of Lemma 3.1, we have $p(t) \leq 0$. Therefore, $v_{k+1} \leq w_{k+1}$ for all $t \in [0, T]$. Since it is true for $k = 1$, therefore, by induction, we have the conclusion $v_n \leq w_n$ is true for every $n \geq 1$. Since we have already assumed that $v_0 \leq w_0$, we can obtain the inequality

$$v_0 \leq v_1 \leq \cdots \leq v_{n-1} \leq v_n \leq w_n \leq w_{n-1} \leq \cdots \leq w_1 \leq w_0. \quad (52)$$

In the next result, we will show that $v_0 \leq u \leq w_0$ implies $v_n \leq u \leq w_n$ for all $n \geq 1$. We prove by the method of mathematical induction. For $n = 1$, let

$$P(t) = v_1(t) - u(t), \quad Q(t) = u(t) - w_1(t). \quad (53)$$

The initial condition is $P(0) = Q(0) = u_0 - u_0 = 0$.

Then with the assumption (A_2) , we have

$$\begin{aligned} {}^cD^q P &= \lambda P + f(t, v_0) - f(t, u) + g(t, w_0) - g(t, u) \\ &\quad + \sum_{i=1}^N c_i \chi(t - t_i) s_i(t - t_i) P(t_i) + \sum_{i=1}^N b_i \chi(t - t_i) r_i(t - t_i) Q(t_i) \\ &\leq \lambda P + \sum_{i=1}^N c_i \chi(t - t_i) s_i(t - t_i) P(t_i) + \sum_{i=1}^N b_i \chi(t - t_i) r_i(t - t_i) Q(t_i). \end{aligned} \quad (54)$$

Similarly, for $Q(t)$ we have

$$\begin{aligned} {}^cD^q Q &= \lambda Q + f(t, u) - f(t, w_0) + g(t, u) - g(t, v_0) \\ &\quad + \sum_{i=1}^N c_i \chi(t - t_i) s_i(t - t_i) Q(t_i) + \sum_{i=1}^N b_i \chi(t - t_i) r_i(t - t_i) P(t_i) \\ &\leq \lambda Q + \sum_{i=1}^N c_i \chi(t - t_i) s_i(t - t_i) Q(t_i) + \sum_{i=1}^N b_i \chi(t - t_i) r_i(t - t_i) P(t_i). \end{aligned} \quad (55)$$

Then, by Theorem 3.1, we can get $P(t) \leq 0$ and $Q(t) \leq 0$. Therefore, $v_1 \leq u \leq w_1$ for all $t \in [0, T]$.

Assume the result $v_n \leq w_n$ is true for $n = k$, then we have $v_k \leq u \leq w_k$. Then for $n = k + 1$, let

$$P(t) = v_{k+1}(t) - u(t), \quad Q(t) = u(t) - w_{k+1}(t). \quad (56)$$

The initial condition is $P(0) = Q(0) = u_0 - u_0 = 0$.

Using the assumption (A_2) , we can get

$$\begin{aligned} {}^cD^q P &= \lambda P + f(t, v_k) - f(t, u) + g(t, w_k) - g(t, u) \\ &\quad + \sum_{i=1}^N c_i \chi(t - t_i) s_i(t - t_i) P(t_i) + \sum_{i=1}^N b_i \chi(t - t_i) r_i(t - t_i) Q(t_i) \\ &\leq \lambda P + \sum_{i=1}^N c_i \chi(t - t_i) s_i(t - t_i) P(t_i) + \sum_{i=1}^N b_i \chi(t - t_i) r_i(t - t_i) Q(t_i). \end{aligned} \quad (57)$$

Similarly, for $Q(t)$ we have

$$\begin{aligned} {}^cD^q Q &= \lambda Q + f(t, u) - f(t, w_k) + g(t, u) - g(t, v_k) \\ &\quad + \sum_{i=1}^N c_i \chi(t - t_i) s_i(t - t_i) Q(t_i) + \sum_{i=1}^N b_i \chi(t - t_i) r_i(t - t_i) P(t_i) \\ &\leq \lambda Q + \sum_{i=1}^N c_i \chi(t - t_i) s_i(t - t_i) Q(t_i) + \sum_{i=1}^N b_i \chi(t - t_i) r_i(t - t_i) P(t_i). \end{aligned} \quad (58)$$

Then, by Theorem 3.1, we can get $P(t) \leq 0$ and $Q(t) \leq 0$. Therefore, $v_{k+1} \leq u \leq w_{k+1}$ for all $t \in [0, T]$. Since the result is true for $k = 1$, then by induction, we have $v_n(t) \leq u(t) \leq w_n(t)$ for all $n \geq 0$ and $t \in [0, T]$,

If we consider the result above and the result (i) we proved, we can have

$$v_0 \leq v_1 \leq \cdots \leq v_n \leq u \leq w_n \leq w_{n-1} \leq \cdots \leq w_1 \leq w_0. \quad (59)$$

For the next result, we will prove that the sequences $\{v_n\}$ and $\{w_n\}$ are uniformly bounded and equicontinuous.

Since $v_0(t)$ and $w_0(t)$ are continuous on each interval $[t_k, t_{k+1}]$, we can get they are bounded on the whole interval $[0, T]$. Then assume $|v_0(t)| \leq M_v$ and $|w_0(t)| \leq M_w$. Then for every n and $t \in [0, T]$, by monotonicity we have

$$0 \leq v_n - v_0 \leq w_0 - v_0. \quad (60)$$

We take the absolute value to obtain

$$|v_n| \leq |v_n - v_0| + |v_0| \leq |w_0 - v_0| + |v_0| \leq |w_0| + |v_0| + |v_0| \leq M_w + 2M_v. \quad (61)$$

Therefore, there exists some positive constant M which is independent of t or N , such that $|v_n| \leq M$.

Similarly,

$$|v_n| \leq |w_n - w_0| + |w_0| \leq |v_0 - w_0| + |w_0| \leq |v_0| + |w_0| + |w_0| \leq M_v + 2M_w. \quad (62)$$

Therefore, there exists some positive constant M' which is independent of t or N such that $|w_n| \leq M'$. Furthermore, M and M' do not depend on n or t . Then the sequences $\{v_n(t)\}$ and $\{w_n(t)\}$ are uniformly bounded on the interval $[0, T]$.

In order to prove the equicontinuity, we use the integral representation of $v_n(t)$,

$$\begin{aligned} v_n(t) = u_0 &+ \frac{1}{\Gamma(q)} \int_0^t (t-s)^{q-1} \left(f(s, v_{n-1}(s)) + g(s, w_{n-1}(s)) + \lambda v_n(s) \right. \\ &\left. + \sum_{i=1}^k c_i s_i (t-t_i) v_n(t_i) + \sum_{i=1}^k b_i r_i (t-t_i) w_n(t_i) \right) ds. \end{aligned} \quad (63)$$

Then for any $k = 0, 1, \dots, N-1$, let $t^1 \in [t_k, t_{k+1}]$, $t^2 \in [t_k, t_{k+1}]$. Without losing the generalization, we assume that $t^1 > t^2$ and $|t^1 - t^2| < \delta$, where M is some positive constant. Since $s_i(t-t_i)$, $r_i(t-t_i)$ and $f(t, u(t))$, $g(t, u(t))$ are continuous in t on the interval $[t_i, t_{i+1}]$, we can let $|c_i s_i(t-t_i)| \leq C_s$, $|b_i r_i(t-t_i)| \leq C_r$ and $|f(t, u(t))| \leq M_f$, $|g(t, u(t))| \leq M_g$. Based on the uniformly boundedness, we have $|v_n| \leq M_v$ and $|w_n| \leq M_w$, then we have

$$\begin{aligned} |v_n(t^1) - v_n(t^2)| &= \left| \frac{1}{\Gamma(q)} \int_0^{t^1} (t^1 - s)^{q-1} \left(f(s, v_{n-1}(s)) + g(s, w_{n-1}(s)) + \lambda v_n(s) \right. \right. \\ &\quad \left. \left. + \sum_{i=1}^k c_i s_i (t^1 - t_i) v_n(t_i) + \sum_{i=1}^k b_i r_i (t^1 - t_i) w_n(t_i) \right) ds \right. \\ &\quad \left. - \frac{1}{\Gamma(q)} \int_0^{t^2} (t^2 - s)^{q-1} \left(f(s, v_{n-1}(s)) + g(s, w_{n-1}(s)) + \lambda v_n(s) \right. \right. \\ &\quad \left. \left. + \sum_{i=1}^k c_i s_i (t^2 - t_i) v_n(t_i) + \sum_{i=1}^k b_i r_i (t^2 - t_i) w_n(t_i) \right) ds \right|. \end{aligned} \quad (64)$$

For any $t \in [t_k, t_{k+1}]$ we have

$$\begin{aligned} &\left| f(t, v_{n-1}(t)) + g(t, w_{n-1}(t)) + \lambda v_n(t) + \sum_{i=1}^k c_i s_i (t - t_i) v_n(t_i) + \sum_{i=1}^k b_i r_i (t - t_i) w_n(t_i) \right| \\ &\leq M_f + M_g + \sum_{i=1}^k C_s M_v + \sum_{i=1}^k b_i M_w. \end{aligned} \quad (65)$$

We let $M = M_f + M_g + \sum_{i=1}^k C_s M_v + \sum_{i=1}^k b_i M_w$, then for any $t \in [t_k, t_{k+1}]$,

$$\left| f(t, v_{n-1}(t)) + g(t, w_{n-1}(t)) + \lambda v_n(t) + \sum_{i=1}^k c_i s_i(t - t_i) v_n(t_i) + \sum_{i=1}^k b_i r_i(t - t_i) w_n(t_i) \right| \leq M. \quad (66)$$

Therefore, we have

$$\begin{aligned} |v_n(t^1) - v_n(t^2)| &\leq \frac{M}{\Gamma(q)} \int_0^{t^2} |(t^1 - s)^{q-1} - (t^2 - s)^{q-1}| ds + \frac{M}{\Gamma(q)} \int_{t^2}^{t^1} |(t^1 - s)^{q-1}| ds \\ &\leq \frac{M}{\Gamma(q+1)} (t^1 - t^2)^q + \frac{M}{\Gamma(q+1)} (t^1 - t^2)^q = \frac{2M}{\Gamma(q+1)} |t^1 - t^2|^q < \epsilon. \end{aligned} \quad (67)$$

Providing $|t^1 - t^2| \leq \delta = \left(\frac{\epsilon \Gamma(q+1)}{2M}\right)^{\frac{1}{q}}$, we can have that v_n is equicontinuous.

Similarly, for w_n we have

$$\begin{aligned} &\left| f(t, w_{n-1}(t)) + g(t, v_{n-1}(t)) + \lambda w_n(t) + \sum_{i=1}^k c_i s_i(t - t_i) w_n(t_i) + \sum_{i=1}^k b_i r_i(t - t_i) v_n(t_i) \right| \\ &\leq M_f + M_g + \sum_{i=1}^k C_s M_w + \sum_{i=1}^k b_i M_v. \end{aligned} \quad (68)$$

Let $M' = M_f + M_g + \sum_{i=1}^k C_s M_w + \sum_{i=1}^k b_i M_v$, then for any $t \in [t_k, t_{k+1}]$,

$$\left| f(t, w_{n-1}(t)) + g(t, v_{n-1}(t)) + \lambda w_n(t) + \sum_{i=1}^k c_i s_i(t - t_i) w_n(t_i) + \sum_{i=1}^k b_i r_i(t - t_i) v_n(t_i) \right| \leq M'. \quad (69)$$

Therefore, we have

$$\begin{aligned} |w_n(t^1) - w_n(t^2)| &\leq \frac{M'}{\Gamma(q)} \int_0^{t^2} |(t^1 - s)^{q-1} - (t^2 - s)^{q-1}| ds + \frac{M'}{\Gamma(q)} \int_{t^2}^{t^1} |(t^1 - s)^{q-1}| ds \\ &\leq \frac{M'}{\Gamma(q+1)} (t^1 - t^2)^q + \frac{M'}{\Gamma(q+1)} (t^1 - t^2)^q = \frac{2M'}{\Gamma(q+1)} |t^1 - t^2|^q < \epsilon. \end{aligned} \quad (70)$$

We provide $|t^1 - t^2| \leq \delta = \left(\frac{\epsilon \Gamma(q+1)}{2M'}\right)^{\frac{1}{q}}$, then w_n is equicontinuous. Therefore, if we take the minimum of these two, $\delta = \min\left(\left(\frac{\epsilon \Gamma(q+1)}{2M}\right)^{\frac{1}{q}}, \left(\frac{\epsilon \Gamma(q+1)}{2M'}\right)^{\frac{1}{q}}\right)$, then can obtain that $\{v_n(t)\}$ and $\{w_n(t)\}$ are equicontinuous on the interval $[t_k, t_{k+1}]$. Since $k = 0, 1, \dots, N-1$ was arbitrary, we proved that $\{v_n(t)\}$ and $\{w_n(t)\}$ are equicontinuous on the interval $[0, t_N = T]$.

Since we have proved that $\{v_n(t)\}$ and $\{w_n(t)\}$ are equicontinuous and uniformly

bounded on the interval $[0, T]$, by Ascoli-Arzela's theorem, there exist subsequences $\{v_{n_k}(t)\}$ and $\{w_{n_k}(t)\}$, which converge uniformly to $v(t)$ and $w(t)$, respectively, on $[0, T]$. Because of the monotonicity of the sequences $\{v_n(t)\}$ and $\{w_n(t)\}$ we have shown, we can get that the entire sequences $\{v_n(t)\}$ and $\{w_n(t)\}$ converge uniformly and monotonically to $v(t)$ and $w(t)$, respectively.

For the next step, we will prove that $v(t)$ and $w(t)$ we have above are the minimal and maximal solutions of the problem (9). Furthermore, we want to show that they are equivalent to the solution of the equation (9).

We use the integral representation.

$$\begin{aligned} v_n(t) = u_0 + \frac{1}{\Gamma(q)} \int_0^t (t-s)^{q-1} & \left(f(s, v_{n-1}(s)) + g(s, w_{n-1}(s)) + \lambda v_n(s) \right. \\ & \left. + \sum_{i=1}^k c_i s_i (t-t_i) v_n(t_i) + \sum_{i=1}^k b_i r_i (t-t_i) w_n(t_i) \right) ds. \end{aligned} \quad (71)$$

Then, we take the limit of n on both sides. Since $\{v_n\}$ converges uniformly, we have

$$\begin{aligned} \lim_{n \rightarrow \infty} v_n = \lim_{n \rightarrow \infty} & \left(u_0 + \frac{1}{\Gamma(q)} \int_0^t (t-s)^{q-1} \left(f(s, v_{n-1}(s)) + g(s, w_{n-1}(s)) + \lambda v_n(s) \right. \right. \\ & \left. \left. + \sum_{i=1}^k c_i s_i (t-t_i) v_n(t_i) + \sum_{i=1}^k b_i r_i (t-t_i) w_n(t_i) \right) ds. \right) \end{aligned} \quad (72)$$

Then,

$$\begin{aligned} v(t) = u_0 + \frac{1}{\Gamma(q)} \int_0^t (t-s)^{q-1} & \left(f(s, v(s)) + g(s, w(s)) + \lambda v(s) \right. \\ & \left. + \sum_{i=1}^k c_i s_i (t-t_i) v(t_i) + \sum_{i=1}^k b_i r_i (t-t_i) w(t_i) \right) ds. \end{aligned} \quad (73)$$

Similarly, for w_n we have

$$\begin{aligned} w_n(t) = u_0 + \frac{1}{\Gamma(q)} \int_0^t (t-s)^{q-1} & \left(f(s, w_{n-1}(s)) + g(s, v_{n-1}(s)) + \lambda w_n(s) \right. \\ & \left. + \sum_{i=1}^k c_i s_i (t-t_i) w_n(t_i) + \sum_{i=1}^k b_i r_i (t-t_i) v_n(t_i) \right) ds. \end{aligned} \quad (74)$$

After taking the limits of n on both sides, we can get

$$\begin{aligned} \lim_{n \rightarrow \infty} w_n = \lim_{n \rightarrow \infty} & \left(u_0 + \frac{1}{\Gamma(q)} \int_0^t (t-s)^{q-1} \left(f(s, w_{n-1}(s)) + g(s, v_{n-1}(s)) + \lambda w_n(s) \right. \right. \\ & \left. \left. + \sum_{i=1}^k c_i s_i (t-t_i) w_n(t_i) + \sum_{i=1}^k b_i r_i (t-t_i) v_n(t_i) \right) ds \right). \end{aligned} \quad (75)$$

Then,

$$\begin{aligned} w(t) = u_0 + \frac{1}{\Gamma(q)} \int_0^t (t-s)^{q-1} & \left(f(s, w(s)) + g(s, v(s)) + \lambda w(s) \right. \\ & \left. + \sum_{i=1}^k c_i s_i (t-t_i) w(t_i) + \sum_{i=1}^k b_i r_i (t-t_i) v(t_i) \right) ds. \end{aligned} \quad (76)$$

Now we can get that $v(t)$ and $w(t)$ satisfy the equation (9). Therefore, $v(t)$ and $w(t)$ are coupled minimal and maximal solutions of equation (9). Thus, we have already shown that $v_n \leq u \leq w_n$. Taking the limits of n we can get $\lim_{n \rightarrow \infty} v_n \leq \lim_{n \rightarrow \infty} u \leq \lim_{n \rightarrow \infty} w_n$. Then we can obtain $v \leq u \leq w$.

In the last result, we will show that if f and g satisfy the one-sided Lipschitz condition, then the coupled minimal and maximal solutions are equivalent to the solution u of the equation (9).

Let $m(t) = w(t) - v(t)$, then $m(0) = w(0) - v(0) = u_0 - u_0 = 0$, and we can get

$$\begin{aligned} {}^cD^q m(t) &= {}^cD^q(w(t) - v(t)) = {}^cD^q w(t) - {}^cD^q v(t) \\ &= \lambda(w(t) - v(t)) + [f(t, w(t)) - f(t, v(t))] + [g(t, v(t)) - g(t, w(t))] \\ &\quad + \sum_{i=1}^N c_i \chi(t - t_i) s_i(t - t_i)(w(t_i) - v(t_i)) + \sum_{i=1}^N b_i \chi(t - t_i) r_i(t - t_i)(v(t_i) - w(t_i)). \end{aligned} \quad (77)$$

Let $\Lambda = \lambda + L_1 + L_2$, we can get

$${}^cD^q m(t) \leq \Lambda m(t) + \sum_{i=1}^N c_i \chi(t - t_i) s_i(t - t_i)m(t_i) - \sum_{i=1}^N b_i \chi(t - t_i) r_i(t - t_i)m(t_i). \quad (78)$$

Then, by using the Laplace transformation, we can get

$$m(t) \leq m(0) E_{q,1}(\Lambda t^q) + \sum_{i=1}^{N-1} c_i S_i(t - t_i) m(t_i) - \sum_{i=1}^{N-1} b_i R_i(t - t_i) m(t_i). \quad (79)$$

We know that $m(0) = 0$, then according to the result of Theorem 3.1, we have $m(t) \leq 0$, $\forall t \in [0, t_N]$. By definition of $m(t)$ we can get $\forall t \in [0, T]$, $w(t) \leq v(t)$. Since we have proved the monotonicity $v(t) \leq u(t) \leq w(t)$, we can get that $\forall t \in [0, T]$, $v(t) = u(t) = w(t)$, which concludes the proof.

Theorem 4.3 Assume

(A₁). v_0 and w_0 are coupled lower and upper solutions of natural type of the equation (9), such that $v_0 \leq u \leq w_0$ on $[0, T]$;

(A₂). $f(t, u)$ and $g(t, u)$ are nondecreasing and nonincreasing, respectively, on Ω .

Then the sequences v_n and w_n defined by (40)-(41) are well defined and satisfy the following results:

(i). For all $n \geq 1$, on $[0, T]$ we have

$$v_0 \leq v_1 \leq v_2 \leq \cdots \leq v_n \leq w_n \leq w_{n-1} \leq \cdots \leq w_1 \leq w_0, \quad (80)$$

provided $v_0 \leq v_1$ and $w_1 \leq w_0$.

(ii). The sequences v_n and w_n converge uniformly and monotonically to the coupled minimal and maximal solutions $v(t)$ and $w(t)$, respectively. Furthermore, if u is any solution of equation (9), then $v(t) \leq u \leq w(t)$.

(iii). Furthermore, if $f(t, u)$ and $g(t, u)$ satisfy the one-sided Lipschitz condition, which is for any $u_1 \geq u_2$, we have

$$f(t, u_1) - f(t, u_2) \leq L_1(u_1 - u_2), \quad g(t, u_1) - g(t, u_2) \geq L_2(u_1 - u_2), \quad (81)$$

where $L_1 \geq 0$ and $L_2 \geq 0$, then $\forall t \in [0, T]$, we have $v(t) = u(t) = w(t)$, the uniqueness of (9) holds on $[0, T]$.

Proof. The proof follows the same lines as the proof of Theorem 4.2 except in the first part, instead of proving $v_0 \leq v_1$ and $w_1 \leq w_0$, we have this result provided. The rest of the proof is the same.

5 Conclusion

We generalized the monotone method and use the method to prove that for the nonlinear Caputo fractional impulsive differential equation (9), under certain conditions, the coupled lower and upper solutions of both the natural type and type 1 converge to the exact solution of the problem. Therefore, in the future work, the monotone method will be significantly useful to approximate the solution of the problem. In the numerical results, we will discuss another method which converges faster than this method.

Acknowledgment

This research is partially supported by Louisiana Board of Regents Support Fund LEQSF(2016-17)-C-17.

References

- [1] D. Baleanu and Z. B. Güvenc. *New Trends in Nanotechnology and Fractional Calculus Applications*. Springer, New York, 2010.
- [2] M. Benchohra and B. A. Slimani. Existence and uniqueness of solutions to impulsive fractional differential equations. *Electronic Journal of Differential Equations* **2009** 10 (2009) 1–11.
- [3] J. Cao and H. Chen. Impulsive fractional differential equations with nonlinear boundary conditions. *Mathematical and Computer Modelling* **55** (2012) 303–311.
- [4] Z. Denton and A. S. Vatsala. Monotone iterative technique for finite systems of nonlinear Riemann-Liouville fractional differential equations. *Opuscula Mathematica* **31** (3) (2011).
- [5] Z. Denton, P. W. Ng and A. S. Vatsala. Quasilinearization method via lower and upper solutions for Riemann-Liouville fractional differential equation. *Nonlinear Dynamics and Systems Theory* **11** (3) (2011) 239–251
- [6] R. Gorenflo, A. A. Kilbas, F. Rogosin and S. V. *Mittag-Leffler functions, Related topic and applications*. Springer Monographs in Mathematics, 2014.
- [7] W. M. Haddad, V. Chellaboina and S. G. Nersessov. *Impulsive and Hybrid Dynamical Systems, Stability Dissipativity and Control*. Princeton Series in Applied Mathematics, 2006.
- [8] S. Heidarkhani, M. Ferrara, G. Caristi and A. Salari. Existence of Three Solutions for Impulsive Nonlinear Fractional Boundary Value Problems. *Opuscula Math.* **37** (2) (2017) 281–301.
- [9] TH. T. Pham, J. D. Ramirez and A. S. Vatsala. Generalized monotone method for Caputo fractional differential equation with applications to population models. *Neural, Parallel and Scientific Computations* **20** (2012) 119–132.
- [10] A. A. Kilbas, H. M. Srivastava and J. J. Trujillo. *Theory and Applications of Fractional Differential Equations*. North Holland, 2006.
- [11] V. Kiryakova. Generalized fractional calculus and applications. *Pitman Res. Notes Math. Ser.* Vol. 301, New York: Longman-Wiley, 1994.
- [12] V. Lakshmikantham, D. D. Bainov and P.S. Simeonov. *Theory of Impulsive Differential Equations*. World Scientific Publishing Co. Pvt Ltd.: Singapore, 1989.

- [13] V. Lakshmikantham, S. Leela and D. Vasundhara. *Theory of Fractional Dynamic Systems*. Cambridge Scientific Publishers: Cambridge, UK, 2009.
- [14] I. Matychyn and V. Onyshchenko. Impulsive differential equations with fractional derivatives. *International Journal of Difference Equations* **9** (1) (2014) 101-109.
- [15] B. Oldham and J. Spanier. *The Fractional Calculus*. Academic Press, New-York-London, 1974.
- [16] I. Podlubny. *Fractional Differential Equations*. San Diego: Academic Press, 1999.
- [17] S. Poseh, H. S. Rodrigues, and D. F. Torres. Fractional derivatives in Dengue epidemics. *AIP Conf. M. Proc.* **1389** (2011) 739–742.
- [18] D. Stutson, and A. S. Vatsala. Generalized monotone method for Caputo fractional differential systems via coupled lower and upper solutions. *Dynamic Systems and Applications* **20** (2011) 495–504.
- [19] A. S. Vatsala and M. Sowmya. Laplace transform method for linear sequential Riemann-Liouville and Caputo fractional differential equations. *AIP Conference Proceedings* **1798** (020171) (2017).
- [20] A. S. Vatsala, M. Sowmya and D. S. Stutson. Generalized monotone method for ordinary Caputo fractional differential equations. *Dynamic Systems and Applications* **24** (2015) 429–438.
- [21] A. S. Vatsala, and B. Sambandham. Laplace transform method for sequential Caputo fractional differential equations. In: *Mathematics, Engineering, Science and Aerospace MESA* **7** (2) (2016) 339–347.
- [22] A. S. Vatsala, and Y. Bai. Nonlinear Caputo fractional impulsive differential equations and generalized comparison results. *AIP Conference Proceedings* **2046** (020105) (2018).
- [23] A. A. Kilbas, A. A. Koroleva, and S. V. Rogosin. Multi-parametric Mittag-Leffler functions and their extension. *Fractional Calculus & Applied Analysis* **16** (2) (2018).
- [24] R. Gorenflo, J. Loutchko and Y. Luchko. Computation of the Mittag-Leffler function $E_{\alpha,\beta}(z)$ and its derivative. *Fractional Calculus & Applied Analysis* (2002).
- [25] F. Mainardi. On the distinguished role of the Mittag-Leffler and Wright functions in fractional calculus. *Special Functions in the 21st Century: Theory & Applications*. Washington DC, 6-8 April 2011. [USA]
- [26] F. Mainardi. On some properties of the Mittag-Leffler function $E_\alpha(-t^\alpha)$, completely monotone for $t > 0$ with $0 < \alpha < 1$. *Discrete and Continuous Dynamical Systems – Series B (DCDS-B)* **19** (17) (2014).
- [27] H. J. Haubold, A. M. Mathai, and R. K. Saxena. Mittag-Leffler functions and their applications. *Journal of Applied Mathematics* **2001**, Article ID 298628.
- [28] S. Rogosin. The role of the Mittag-Leffler function in fractional modeling. *Mathematics* **3** (2015) 368–381.



Control Design for Non-Linear Uncertain Systems via Coefficient Diagram Method: Application to Solar Thermal Cylindrical Parabolic Trough Concentrators

Z. Fenchouche^{1*}, M. Chakir¹, O. Benzineb², M.S. Boucherit¹
and M. Tadjine¹

¹ Automatic Control Department, LCP, National Polytechnic School, Algeria

² Electronics Department, University of Blida, Blida, Algeria

Received: June 21, 2019; Revised: December 30, 2019

Abstract: In this paper, we propose a new application of the coefficient diagram method (CDM) to design a robust controller of non-linear uncertain system, the control is applied to a distributed collector field of a solar power plant based on cylindrical parabolic trough concentrators. The non-linear uncertain system is represented by two PDEs of both the fluid and the metal. To design the control, a linearization of the non-linear system is made around an equilibrium point to have a transfer function, this point represents the simulation's steady state of the real system, then the controller is obtained using the form of Manabe for the CDM. Comparing the results of this method with those of the PID controller, it is shown that the CDM design is an easy and robust control for a non-linear system, that gives enhanced stability with good settling time with respect to the large rise time.

Keywords: coefficient diagram method (CDM); partial differential equation (PDE); cylindrical parabolic trough concentrator; nonlinear uncertain system.

Mathematics Subject Classification (2010): 93C10, 93D09.

* Corresponding author: <mailto:zakaria.fenchouche@g.enp.edu.dz>

1 Introduction

In the last decade, renewable energies have received more and more attention in order to meet the exponential growth of energy demand. Among renewable energies, the interest in solar energy has increased, many solar electricity systems were developed, such as concentrated solar thermal, and more precisely, cylindrical-parabolic trough collectors (Fig. 1), which are the most used technologies for concentrating solar energy. Today, some plants are under construction, while others are already operating, such as the Platform Solar of Almeria (ACUREX) [1].

The main problem in solar energy sources is the independency of the solar radiation variations, in addition, it can not be adjusted to suit demands that we desire. We note, for example, cloud cover, humidity and air transparency as atmospheric conditions that may affect the solar radiation by unpredictable variations [2].

From the perspective of research, many works have been proposed to either model, control or observe the system [1]. The authors in [3–7] have given different models of the solar system with different levels of complexity and accuracy, like the bilinear reduced or the non-linear distributed system [1].

On the other side, many automatic control strategies have been implemented, that is to make the plant work close to the nominal operating point. In what follows, we cite well known tests experimented at the plant ACUREX: with a self-tuning PID controller in [2], in [8] the authors have designed a fuzzy logic controller, the model predictive control (RMPCT) has been implemented in [9], etc. Additionally, other controller's strategies are based on the predictors and the estimators of variables like effective solar radiation or the system's temperature as in [10].

It is well known that even with a development in the control side, the PID remains a very important controller in the industry with a percentage of 95 % among the controllers used in the practice [11]. However, many constraints are imposed in the practical applications as noted in the previous reference, such as the upper limit of magnitude of the control signal, the unexpected non-linear effects occurred by the saturation or others. For these reasons, it is necessary to develop a robust control application to obtain better control performances of double integrating unstable systems, where the stability is not ensured by the PID controller which is developed for stable systems [12].

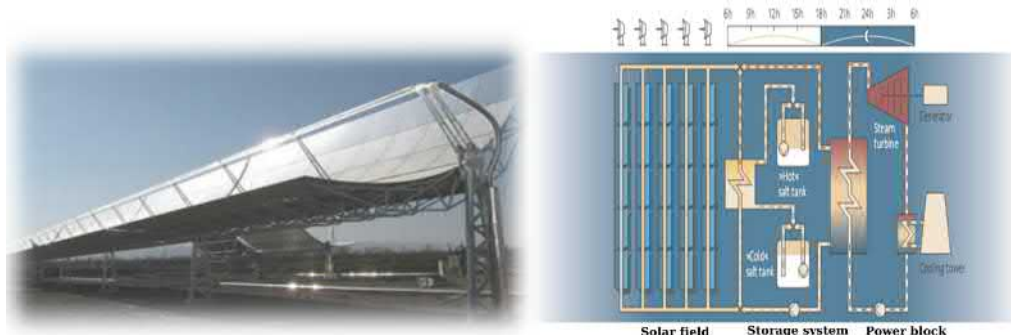


Figure 1: Parabolic distributed solar collector with the schematic diagram of solar thermal hydraulic circuit.

Hence, in this work we propose the use of an algebraic approach that has proved its

robustness in several works. It is a new robust controller known as a Coefficient Diagram Method (CDM), developed for uncertain systems and introduced by many researchers such as Manabe, see [13], [14] and [15] (it is important to note that we will not talk about the advanced controls applied in other works, because we are interested in controls to apply in practical and in industrial systems such as PID and RQG).

The CDM is based on a spatial diagram called a coefficient diagram, which is used as a vehicle to carry the necessary design information and as a criteria of good design. The method is recently used because of the simplest and robust controller that can be found for any plant under practical limitations, in addition, this simplicity makes it very powerful for systems with various uncertainties. In other words, the CDM can give a controller design which is both stable and robust, and has the desired system response speed, and also is less sensitive to disturbances and parameter variations, without overshoots and is obtained for specified settling time [16].

This paper is organized as follows. First, the solar plant is described in Section 2 with the system modelling, approximations, discretization and linearization. Subsequently, the CDM structure and its design are presented in Section 3 followed by its application on the plant in Section 4. Then, numerical tests and simulations to assess the robustness and stability of the controller are also shown in this section. Finally, Section 5 summarizes the obtained results.

2 Solar Power Plant Description and Modeling

2.1 Plant description

Most of the thermo-plants in the world use the cylindrical-parabolic collectors because of their significant energy productivity, and the simplicity of the method. It consists of linear parabolic mirrors that reflect and concentrate solar energy (irradiations) on a metal tube which represents the receiver that is positioned along a focal line. This allows to heat oil, used as a heat-transfer fluid (HTF), to reach temperatures that ensure evaporation on the level of the turbine (Fig. 1).

Moreover, the Platform ACUREX of ALMERIA is a well-known station in the field of research. It consists of 10 loops, each one is made up of two lines of 12 modules, and the length of each loop is 172 m, it also consists of a pump with a limited operation between the maximum capacity 12 L/s and the safety threshold 2 L/s.

2.2 Plant modeling

The distributed solar collector field can be described by a distributed parameter model of the temperature while considering general assumptions and hypotheses. The model is represented by the following system of partial differential equations (PDE) which describes the energy balance [17]:

$$\frac{\partial T_f}{\partial t} = \frac{\delta_p H_t}{\rho_f C_f A_f} (T_m - T_f) - \frac{q}{A_f} \frac{\partial T_f}{\partial l}, \quad (1)$$

$$\frac{\partial T_m}{\partial t} = \frac{K_{opt} \eta_0 G}{\rho_m C_m A_m} I - \frac{G H_l}{\rho_m C_m A_m} (T_m - T_a) - \frac{\delta_p H_t}{\rho_m C_m A_m} (T_m - T_f), \quad (2)$$

where the subindex m refers to the metal and that of f to the fluid. The parameters of the system and their values are given in Table 1, where

$$H_v = 2.17 \times 10^6 - 5.01 \times 10^4 T_f + 4.53 \times 10 T_f^2 - 1.64 T_f^3 + 2.1 \times 10^{-3} T_f^4, \quad (3)$$

T_{in} , T_{out} and T_a are the inlet temperature, the outlet temperature and the ambient temperature, respectively.

Parameter	Description	Value	Unit
δ_p	Wet perimeter	0.1257	m
ρ_f	Density of f	$903 - 0.672 \cdot T_f$	$\text{kg} \cdot \text{m}^{-3}$
C_f	S.H.C of f	$1820 + 3.478 \cdot T_f$	$\text{J} \cdot \text{kg}^{-1} \cdot {}^\circ\text{C}^{-1}$
D_f & D_m	Diameters	0.04 & 0.07	m
A_f & A_m	Sections	0.0013 & 0.0038	m^2
H_t	C.H.T.C	$q^{0.8} H_v$	$\text{W} \cdot {}^\circ\text{C}^{-1} \cdot \text{m}^{-2}$
H_l	C.H.T.C	$0.00249 \Delta \bar{T} - 0.06133$	$\text{W} \cdot {}^\circ\text{C}^{-1} \cdot \text{m}^{-2}$
I	Irradiation	variable	$\text{W} \cdot \text{m}^{-2}$
q	Fluid flow	to control	$\text{m}^3 \cdot \text{s}^{-1}$
K_{opt}	Optical efficiency	$\eta_{opt} = \eta_0 \cdot K_{opt} = 0.7$	—
η_0	Collector efficiency	—	—
G	Collector aperture	$= \delta_p \cdot \pi = 1.83$	—
ρ_m	density of m	1100	$\text{Kg} \cdot \text{m}^{-3}$
C_m	S.H.C of m	840	$\text{J} \cdot \text{Kg}^{-1} \cdot {}^\circ\text{C}^{-1}$
$\Delta \bar{T}$	—	$= \left(\frac{T_{in} + T_{out}}{2} - T_a \right)$	${}^\circ\text{C}$

Table 1: Parameters description.

Many authors used different simplified models, based on simplified energy balances, such as neglecting heat losses, or controlling the system using just one equation which corresponds to the variation of the fluid temperatures. However, the system should be used under a non-simplified model, as described in equations (1) and (2), to have an accurate control. Hence, that is the first contribution of this paper.

The aim of our work is to control the outlet temperature of the tube denoted $T_{out}(t) = T_f(t, L)$ around a set-point. The incoming energy depends on several parameters such as the efficiency of the collectors, the mirror reflectivity and on the effective reflecting surface.

We used this model for control synthesis and simulation. The parameters and the properties of the fluid used may be considered constant or variable depending on the variations of the temperature. We also remind that the flow of the fluid is comprised between

$$2 \text{ L} \cdot \text{s}^{-1} \leq q \leq 12 \text{ L} \cdot \text{s}^{-1}, \quad (4)$$

and the difference between T_{out} and T_{in} must be less than $80 \text{ } {}^\circ\text{C}$:

$$T_{out} - T_{in} \leq 80 \text{ } {}^\circ\text{C}. \quad (5)$$

The first equation of the PDEs obtained from the energy balance, contains two differentials depending on space (x) and time (t). For simplification reasons, the first differential will be eliminated using a discretization on the space as mentioned in Fig. 2, so we discretize the system on $\frac{n}{2}$ segments ($\frac{n}{2}$ is just a token, to have a dimension of the system equal n which will be explained in Section 2.3, and it represents the number of segments of the tube). In this case, we may introduce a truncation error

$$\frac{\partial T_f}{\partial l} = \frac{T_f(l_i) - T_f(l_{i-1})}{\Delta l} + \Theta(\Delta l). \quad (6)$$

But, as long as this approximation of the derivative may not be very accurate for the control synthesis, the truncation error will be added to the general perturbation terms.

Hence, we rewrite the first system as follows :

$$\frac{\partial T_f(l_i)}{\partial t} = \frac{\delta_p H_t}{\rho_f C_f A_f} (T_m(l_i) - T_f(l_i)) - \frac{q}{A_f \cdot \Delta l} (T_f(l_i) - T_f(l_{i-1})), \quad (7)$$

$$\frac{\partial T_m(l_i)}{\partial t} = \frac{K_{opt} \eta_0 G}{\rho_m C_m A_m} I - \frac{G H_l}{\rho_m C_m A_m} (T_m(l_i) - T_a) - \frac{\delta_p H_t}{\rho_m C_m A_m} (T_m(l_i) - T_f(l_i)), \quad (8)$$

where the state vector is as follows:

$$\begin{aligned} X &= [T_f(l_1) \ T_f(l_2) \ \cdots \ T_f(l_{\frac{n}{2}}) \ T_m(l_1) \ T_m(l_2) \ T_m(l_3) \ \cdots \ T_m(l_{\frac{n}{2}})]^T \\ &= [x_1 \ x_2 \ \cdots \ x_{\frac{n}{2}-1} \ x_{\frac{n}{2}} \ x_{\frac{n}{2}+1} \ x_{\frac{n}{2}+2} \ \cdots \ x_{n-1} \ x_n]^T, \end{aligned} \quad (9)$$

and

$$\begin{cases} x_1 &= T_{out}, \\ x_{\frac{n}{2}} &= T_{in}. \end{cases} \quad (10)$$

Also, we write the system equations in the following state form:

$$\begin{cases} \dot{X} &= F(X, u), \\ Y &= h(X) = x_1, \end{cases} \quad (11)$$

where

$$u = q(t), \quad (12)$$

and

$$\dim(\dot{X}) = \dim(X) = n \times 1. \quad (13)$$

\dot{X} is given by

$$\dot{X} = F(X, u) = \left[\begin{array}{l} \frac{\delta_p \cdot H_t(1)}{\rho_f(1) \cdot C_f(1) \cdot A_f} (x_{\frac{n}{2}+1} - x_1) - \frac{u}{A_f \cdot \Delta l} (x_1 - x_2) \\ \frac{\delta_p \cdot H_t(2)}{\rho_f(2) \cdot C_f(2) \cdot A_f} (x_{\frac{n}{2}+2} - x_2) - \frac{u}{A_f \cdot \Delta l} (x_2 - x_3) \\ \vdots \\ \frac{\delta_p \cdot H_t(\frac{n}{2}-1)}{\rho_f(\frac{n}{2}-1) \cdot C_f(\frac{n}{2}-1) \cdot A_f} (x_{n-1} - x_{\frac{n}{2}-1}) - \frac{u}{A_f \cdot \Delta l} (x_{\frac{n}{2}-1} - x_{\frac{n}{2}}) \\ \frac{\delta_p \cdot H_t(\frac{n}{2})}{\rho_f(\frac{n}{2}) \cdot C_f(\frac{n}{2}) \cdot A_f} (x_n - x_{\frac{n}{2}}) - \frac{u}{A_f \cdot \Delta l} (x_{\frac{n}{2}} - T_{in}) \\ \frac{K_{opt} \eta_0 G}{\rho_m C_m A_m} I - \frac{G H_l}{\rho_m C_m A_m} (x_{\frac{n}{2}+1} - T_a) - \frac{\delta_p H_t(1)}{\rho_m C_m A_m} (x_{\frac{n}{2}+1} - x_1) \\ \frac{K_{opt} \eta_0 G}{\rho_m C_m A_m} I - \frac{G H_l}{\rho_m C_m A_m} (x_{\frac{n}{2}+2} - T_a) - \frac{\delta_p H_t(2)}{\rho_m C_m A_m} (x_{\frac{n}{2}+2} - x_2) \\ \vdots \\ \frac{K_{opt} \eta_0 G}{\rho_m C_m A_m} I - \frac{G H_l}{\rho_m C_m A_m} (x_n - T_a) - \frac{\delta_p H_t(n)}{\rho_m C_m A_m} (x_n - x_{\frac{n}{2}}) \end{array} \right]$$

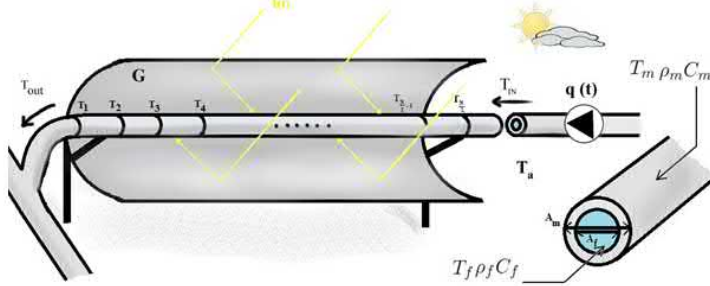


Figure 2: Diagram of the collector showing parameters and spatial discretization.

2.3 Operating point and control model

In this work we use the three blocks structure of Fig. 3 based on the CDM. This method requires the transfer function of the system, but knowing that the model is non-linear, we must have a linearization around an operating point $P_0(x_0, u_0)$.

Besides, to have $\dot{X} = 0$, this point must be an equilibrium point where the state is steady, we propose to use the results of real simulations of controls applied on the ACUREX in some works such as [18]. For the linearization we will use Taylor's series.

Using Taylor's series we get the system

$$\begin{cases} \dot{X} \simeq \dot{X}_0 + \frac{\partial F}{\partial X} |_{(X_0, u_0)} (X - X_0) + \frac{\partial F}{\partial u} |_{(X_0, u_0)} (u - u_0) + \zeta(X, u), \\ Y \simeq \frac{\partial h}{\partial X} |_{(X_0, u_0)}, \end{cases} \quad (14)$$

where

$$\begin{cases} u - u_0 &= \Delta u, \\ X - X_0 &= \Delta X, \\ Y - Y_0 &= \Delta Y, \end{cases} \quad (15)$$

and

$$(X - X_0) = \dot{X} - \dot{X}_0 = \dot{X} \quad (\dot{X}_0 = 0). \quad (16)$$

Thus

$$\dot{\Delta X} = \dot{X}. \quad (17)$$

We take

$$\begin{cases} A_F &= \frac{\partial F}{\partial X} |_{(X_0, u_0)}, \\ B &= \frac{\partial F}{\partial u} |_{(X_0, u_0)}, \\ C &= \frac{\partial h}{\partial X} |_{(X_0, u_0)}. \end{cases} \quad (18)$$

Finally, the system may be written on state space eliminating the error of second order as follows :

$$\begin{cases} \dot{\Delta X} &= A_F \cdot \Delta X + B \cdot \Delta u, \\ \Delta Y &= C \cdot \Delta X. \end{cases} \quad (19)$$

After the deduction of system matrices in state space, we conclude the transfer function $G(s)$:

$$G(s) = \frac{\Delta Y(s)}{\Delta U(s)} = C \cdot (sI - A_F)^{-1} \cdot B. \quad (20)$$

For the simulation, the number of the discretization segments is taken as desired, for example, 15. If so doing, the denominator of the transfer function calculated has, in general, $\dim = n = 30$.

3 Recall on CDM Control Design

The CDM is a novel robust controller which uses an algebraic approach and is developed for uncertain non-linear systems. It is based on a spatial diagram called a coefficient diagram [14, 19].

The design of the CDM controller is composed of three blocks (Fig. 3), $A(s)$ is the forward denominator polynomial, $F(s)$ and $B(s)$ are two numerators polynomials, the first for the reference and the second for feedback. These polynomials in this structure are designed to have better performance on tracking the desired reference signal and rejection disturbances, in addition to that, it helps to avoid the cancellation of unstable pole-zero. [14]

For the controller synthesis, we must have a transfer function, let it be $G(s)$, formed by the numerator $N(s)$ and the denominator $D(s)$.

The characteristic polynomial of the closed loop $P(s)$ is as follows [20] :

$$P(s) = D(s)A(s) + N(s)B(s) = \sum_{i=0}^n a_i s^i. \quad (21)$$

To make the design of the CDM, we must also know three parameters on which the design is based, the equivalent time constant (τ), the stability indices (γ_i) and the stability limits (γ_i^*), they are defined in function of the coefficients of the characteristic polynomial [20, 21]:

$$\gamma_i = \frac{a_i^2}{a_{i+1}a_{i-1}}, \quad i = 1, \dots, n-1, \quad (22)$$

$$\gamma_0 = \gamma_n = \infty, \quad (23)$$

$$\tau = \frac{a_1}{a_0}, \quad (24)$$

$$\gamma_i^* = \frac{1}{\gamma_{i-1}} + \frac{1}{\gamma_{i+1}}. \quad (25)$$

Using these relations between the parameters and the coefficients, the characteristic polynomial $P(s)$ (also called the target characteristic polynomial) can be formulated in terms of (τ) and (γ_i) as follows [15]:

$$P(s) = a_0 \left[\left\{ \sum_{i=2}^n \left(\prod_{j=1}^{i-1} \frac{1}{\gamma_{i-j}^i} \right) (\tau s)^i \right\} + \tau s + 1 \right]. \quad (26)$$

Note that we can give the expression of the equivalent time function of the settling time t_s as follows [15]:

$$\tau = \alpha \cdot t_s, \quad \alpha \in [0.33, 0.4]. \quad (27)$$

Many authors recommend the standard Manabe form to be used for the CDM design [14]. This form has been found after many studies, and stability indices have been chosen as [22]

$$\gamma_i = \{2.5, 2, 2, \dots, 2\} \text{ for } i = 1 \sim (n-1). \quad (28)$$

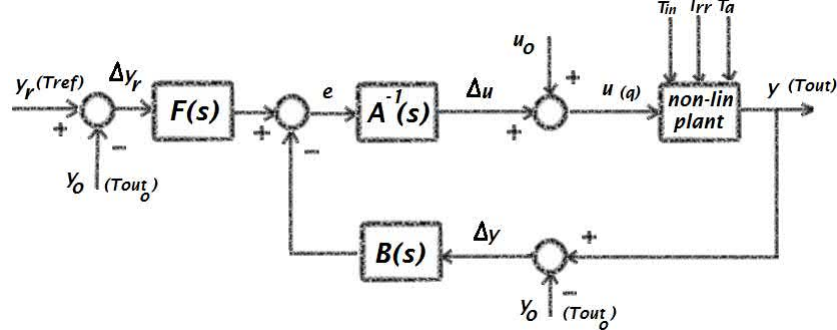


Figure 3: The block diagram of the CDM applied on the non-linear plant.

The procedure to design a controller using the CDM is given in [13]. Following this procedure step by step, we apply the method on our system.

Thus, the transfer function in polynomial form is given by

$$\frac{N(s)}{D(s)} = \frac{b_m s^m + b_{m-1} s^{m-1} + \dots + b_1 s + b_0}{d_n s^n + d_{n-1} s^{n-1} + \dots + d_1 s + d_0}, \quad (29)$$

where $N(s)$ and $D(s)$ are the numerator polynomial of degree m and the denominator polynomial of degree n , respectively, with $m \leq n$.

The controller structure shown in Fig. 3 is based on two polynomials, namely, $A(s)$ and $B(s)$, that are given by

$$A(s) = \sum_{i=0}^p l_i s^i, \quad B(s) = \sum_{i=0}^q k_i s^i. \quad (30)$$

Many criteria are considered to choose the degree of the controller polynomials, where the perturbations are one of these criteria.

To define the degrees for the different cases of the disturbances, a table is given by [14], where n is given as a degree of the denominator's polynomial of the transfer function $G(s)$, and the pre-controller defined by the polynomial $F(s)$ is chosen to be

$$F(s) = \left(\frac{P(s)}{N(s)} \right)_{|s=0}. \quad (31)$$

The coefficients of the controller polynomials are computed using the Diophantine equation given by

$$A(s)D(s) + B(s)N(s) = P(s). \quad (32)$$

We note that $P(s)$ is determined by substituting values of the parameters γ_i , a_0 and τ in the equation (26). γ_i , $i \sim (n-1)$ are chosen from the Manabe form. a_0 and τ are replaced by different values until we obtain the desired results.

$D(s)$ and $N(s)$ are given from the polynomial form of the transfer function of the system. It remains to find l_i and k_i being the parameters of $A(s)$ and $B(s)$, respectively, using the linear relation of coefficients [19].

For instance, with $m = 2, n = 3$ and taking the model of step disturbances, we have $\deg(P(s)) = 6$, $\deg(B(s)) = 3$ and $\deg(A(s)) = 3$ with $l_0 = 0$. We can write

$$\begin{pmatrix} d_3 & 0 & 0 & 0 & 0 & 0 & 0 \\ d_2 & d_3 & 0 & b_2 & 0 & 0 & 0 \\ d_1 & d_2 & d_3 & b_1 & b_2 & 0 & 0 \\ d_0 & d_1 & d_2 & b_0 & b_1 & b_2 & 0 \\ 0 & d_0 & d_1 & 0 & b_0 & b_1 & b_2 \\ 0 & 0 & d_0 & 0 & 0 & b_0 & b_1 \\ 0 & 0 & 0 & 0 & 0 & 0 & b_0 \end{pmatrix} \begin{pmatrix} l_3 \\ l_2 \\ l_1 \\ k_3 \\ k_2 \\ k_1 \\ k_0 \end{pmatrix} = \begin{pmatrix} a_6 \\ a_5 \\ a_4 \\ a_3 \\ a_2 \\ a_1 \\ a_0 \end{pmatrix}, \quad (33)$$

which is also called the Sylvester form that can be shortened as follows:

$$[C]_{7 \times 7} \begin{bmatrix} l_i \\ k_i \end{bmatrix}_{7 \times 1} = [a_i]_{7 \times 1}. \quad (34)$$

Parameters are simply calculated by solving the linear equation, then $F(s)$ can be computed by the equation (31):

$$\begin{bmatrix} l_i \\ k_i \end{bmatrix} = [C]^{-1}[a_i]. \quad (35)$$

Generally, after using the standard Manabe form, no adjustments in the parameters are needed, except when dealing with systems that require accurate control. In this case, we may need some adjustments after doing the first design of the controller, modifying the design parameters and repeating the process until getting the best response and desired results.

For instance, if the system reaches saturation, we may increase τ sufficiently and repeat the process. While decreasing τ can accelerate the response as desired.

4 Solar Plant Controller with CDM

The block diagram of CDM applied on the solar plant is shown on Fig. 3.

First, we choose an equilibrium point, and we linearize the system around this point. Taking $P_0(T_{out} = 250^\circ\text{C}, T_{in} = 180^\circ\text{C}, I = 750 \text{ W/m}^2, u = 7.3 \text{ L/s (0.0073 m}^3.\text{s}^{-1}\text{)})$, the linear system around P_0 is represented by the following transfer function :

$$G(s) = \frac{-54.03s^{29} - 157.9s^{28} - \dots - 1.945 \times 10^{-31}s}{s^{30} + 2.764s^{29} + \dots + 3.868 \times 10^{-36}s} \frac{-3.27 \times 10^{-34}}{+3.846 \times 10^{-39}}, \quad (36)$$

where $G(s)$ is obtained from the formula in (20).

Model reduction: As we see, the denominator of $G(s)$ has $\dim = n = 30$. Hence, the synthesis of the regulator is difficult because of the high order of the transfer function. In this case, we must reduce the order of our system, using a Matlab function that calculates the Gramians, it reduces the order from $\dim = n$ to 2 or 3 as desired (*modred* function with *balreal*) to obtain a reduced function denoted $G_r(s)$.

The transfer function $G_r(s)$ will be used only in synthesizing the regulator. Then, this regulator will be applied on the non-linear system.

Using the model reduction function we obtain

$$G_r(s) = \frac{N(s)}{D(s)} = \frac{-3610s^2 - 41.55s - 1.287}{s^2 + 0.00667s + 1.513 \times 10^{-5}}. \quad (37)$$

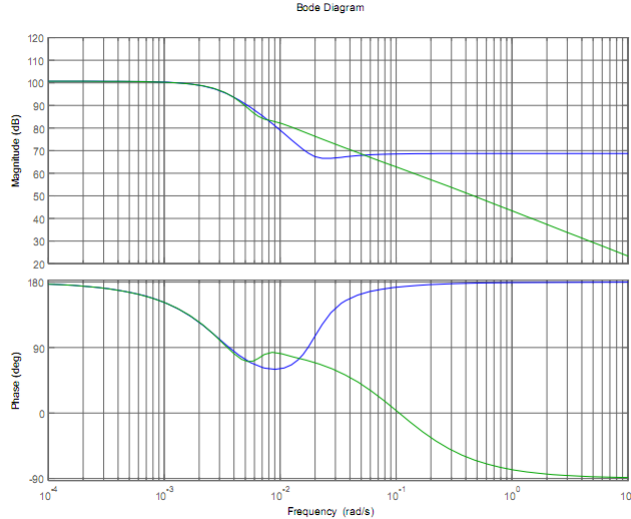


Figure 4: Comparison of the Bode diagram of $G(s)$ model (in green) versus its approximated second-order model $G_r(s)$ (in blue).

The comparison of the Bode diagram of $G(s)$ model versus its approximated second-order model $G_r(s)$ is given in Fig. 4.

It is seen that the reduced system magnitude and phase are the same as those of the original system in frequency less than $10^{-2} Hz$, for our case it does not impose a problem, because the study will be made in low frequencies.

Simulation will be done using Matlab and Simulink programs, where in Simulink we control the non-linear system with CDM and PID controllers in the structure shown before, this system is represented by two partial differential equations written in file of Matlab (file.m) and introduced to Simulink by s-function.

In this simulation, we will consider models related to step disturbances taking the $A(s)$ and $B(s)$ degrees according to the rules mentioned in the table given in [14] to get the correct polynomials.

For the CDM controller synthesis, we give values of τ and a_0 to find the polynomials using the Sylvester form. As mentioned in the method description in Section 3, we vary the value of τ until obtaining the best response.

In this case, we have

$$\tau = 278.5 [s], \quad a_0 = 0.4. \quad (38)$$

Thus, the controller polynomials are found as follows:

$$A(s) = 5836s^2 + 201900s, \quad (39)$$

$$B(s) = -5331s^2 - 74.17s - 0.3109, \quad (40)$$

and the pre-controller is given by

$$F(s) = \left(\frac{P(s)}{N(s)} \right)_{|_{(s=0)}} = \frac{0.4}{-1.287} = -0.3109. \quad (41)$$

Controller	Response time	IAE	ISE	ITAE	Rise time	Settling time	Peak overshoot	Disturbance's peak
CDM	278.5 s	2472	15640	$2.525 \cdot 10^7$	432 s	612 s	0 (0 %)	0 (0 %)
PID	270 s	5828	8156	$5.441 \cdot 10^7$	108 s	1260 s	0.5 (5 %)	2.5 (25 %)

Table 2: Performance of CDM and PID controllers applied on the solar plant A.

Parameters of PID controller have been chosen using the block of PID controller in Simulink containing the PID tuning tool, knowing that a transfer function of a conventional PID controller is written as

$$G_c(s) = K_p \left(1 + \frac{K_i}{s} + sK_d \right), \quad (42)$$

where K_p is the proportional gain, K_I is the integral constant and K_D is the derivative constant.

We took PID parameters that ensure the best system's response according to stability, robustness and response time. These parameters correspond to the PID controller, where

$$K_p = -8.274 \cdot 10^{-3}, \quad K_I = -6.412 \cdot 10^{-4}, \quad K_D = 8.913 \cdot 10^{-3} \quad (43)$$

(small values because the output of the controller is Δu with the unit $m^3 \cdot s^{-1}$).

4.1 Performances tests

The comparison between the two controllers is based on the following performance criteria. These criteria are based on the integral error, they are used as a good measure for evaluating the precision of the set point tracking and disturbances rejection [23].

IAE is the integral of the absolute tracking error which penalizes small errors [24]:

$$IAE = \int_0^\infty |e(t)| dt. \quad (44)$$

ITAE is the integral of the time-weighted absolute error which penalizes the errors that persist for a long time:

$$ITAE = \int_0^\infty te(t) dt, \quad (45)$$

and ISE is the integral of the tracking error squared which penalizes large errors:

$$ISE = \int_0^\infty e^2(t) dt. \quad (46)$$

For simulation, we propose a profile of variant inlet temperature, ambient temperature and solar irradiance that are shown in Fig. 5, Fig. 6 and Fig. 7, respectively (the profiles have been taken approximately to real values as used in other papers).

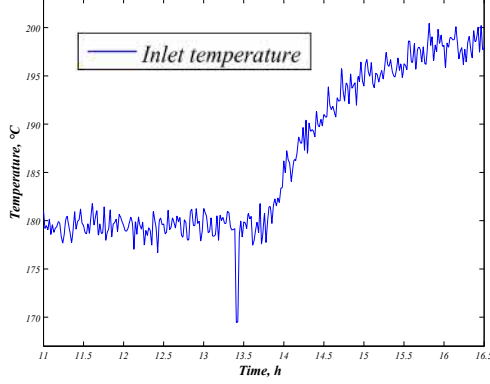
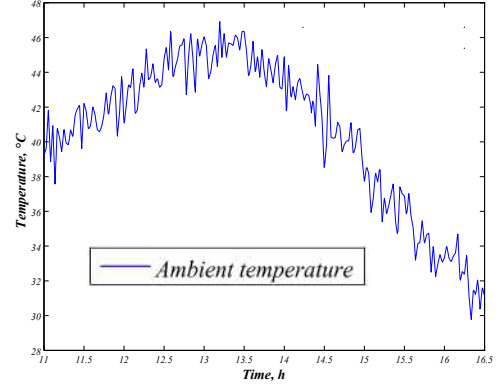
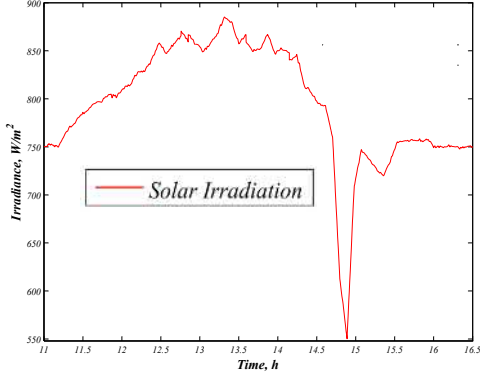
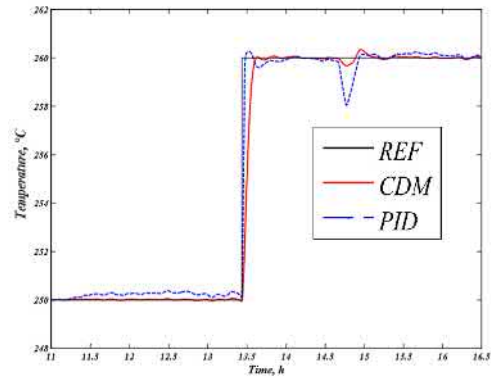
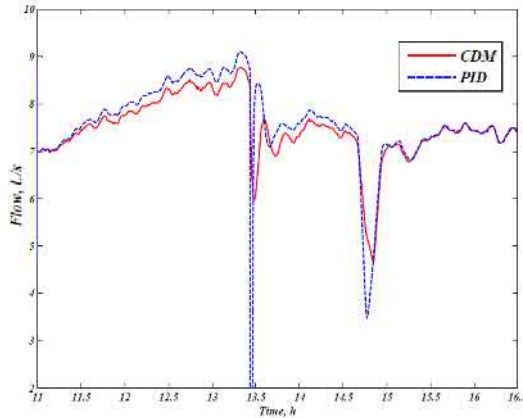
**Figure 5:** Inlet temperature.**Figure 6:** Ambient temperature.**Figure 7:** Solar irradiations.**Figure 8:** Response to a step reference for CDM and PID controllers.

Fig. 8 and Fig. 9 illustrate responses of CDM and PID controllers for a step reference with the corresponding fluid flow.

**Figure 9:** Fluid flow.

As we see in Table 2, the PID controller has better rise time. Nevertheless, the CDM

controller presents better performance indexes in comparison with the PID controller, with a better settling time with no peak overshoots or disturbance's peak. Except that, ISE is little wide because of the large rise time in the case of CDM controller response.

To make more tests to the CDM controller, we did another simulation for the 5 hours and half (between 11:00 and 16:30). The controllers were evaluated with reference variations (between 235°C and 265°C), using the same profiles of variant solar irradiation, inlet temperature and ambient temperature.

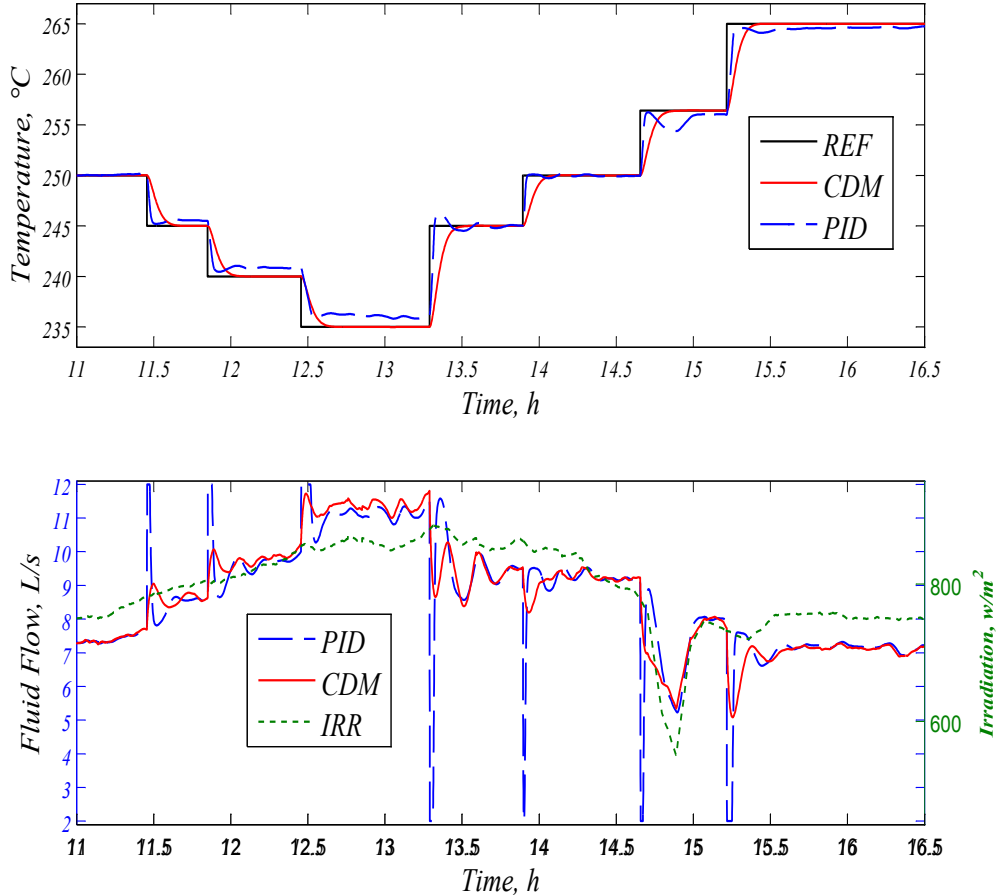


Figure 10: Reference temperature and average outlet temperature for the CDM (impulse-sinusoidal type disturbances) and PID controller.

From Fig. 10 and Table 3, it appears that the CDM exhibits better performance than the PID control, even with a large rise time compared to the first type, especially in the case of the supposed brutal change in the solar irradiance as an effect of the passing clouds (at 14.8 h) or the brutal change in the inlet temperature (at 13.5 h).

We also note that the pump's performance is better and widely admissible with instantaneous small impulses, which may give a considerable lifetime to this pump. Which is not the case in the PID controller with a huge impulses in case of reference variation.

Fig. 11 and Fig. 12 describe the temperature evolution inside the pipe in 2D and

Controller	IAE	ISE	ITAE
CDM	1.087×10^4	4.937×10^4	9.838×10^7
PID	1.375×10^4	2.747×10^4	1.299×10^8

Table 3: Performance of CDM and PID controllers applied on the solar plant B.

3D, respectively. The performance of CDM controller in terms of time response (settling time, even with a small rise time in comparison with the PID), reference tracking and disturbances rejection clearly appears in Fig. 11 where the outlet temperature tracks the reference even with disturbed inlet temperature with an admissible pump control.

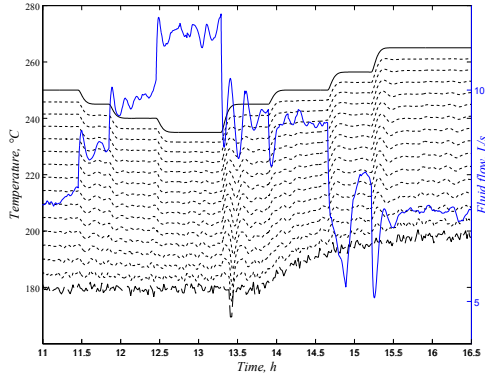


Figure 11: Inlet, outlet and segments temperatures of fluid in 2-D for the tube with the flow.

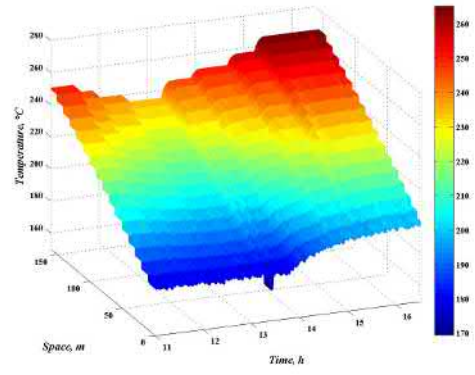


Figure 12: Internal dynamics showing the temperature distribution in 3D.

4.2 Robustness tests

In this part, some robustness tests are given to show the difference between the two controllers. This robustness will be supposed against both the modelling errors and the system parameters variations over time, such as fluid density and thermal capacity.

The first test will correspond to the increase in fluid density by 15 % ($\rho_{f_1} = 1.15 \rho_{f_0}$). see Fig. 13, and the second will correspond to the decrease in fluid thermal capacity by 15 % ($C_{f_1} = 0.85 C_{f_0}$), see Fig. 14.

As seen in the two figures, the CDM controller is more robust against the parameters variations.

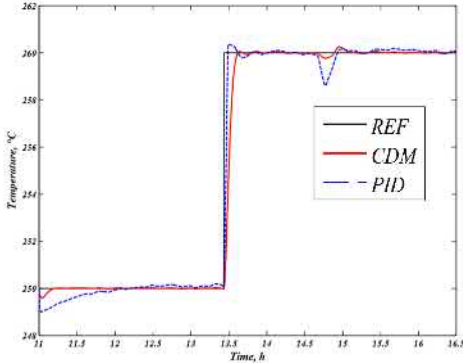


Figure 13: Responses in case of fluid density increase.

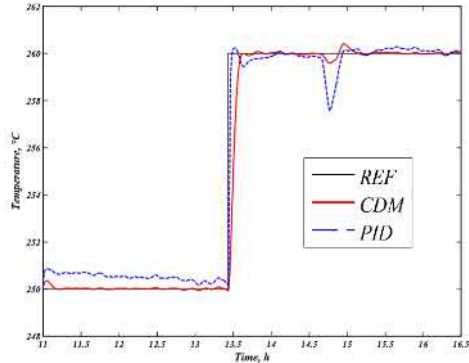


Figure 14: Responses in case of thermal capacity decrease.

5 Conclusion

In this work, a control system for the cylindrical-parabolic collector of a solar plant is designed employing the coefficient diagram method (CDM), which is an algebraic method. The cylindrical-parabolic solar collector is considered as an uncertain non-linear system, represented by two partial differential equations (PDEs), that usually complicates the control.

The performance and robustness of the CDM-controller has been tested with digital simulations using Matlab functions and Simulink programs. The CDM results have been compared with those of the PID-controller. It is shown by the comparative design examples in Section 4, that the controlled system using the CDM exhibits better performance than the PID-control with the external disturbances. The designed controller is simple, easy, robust against parameter variations, capable of decreasing the steady state error to zero and reducing the settling time (even with a large rise time), while supervising an admissible pump control signal applied to the actual plant, which may give a significant life to the pump.

Therefore, the CDM is flexible and can be used perfectly for the precise control in different conditions, replacing the traditional PID and LQG controllers and others (it is important to note that the PID controller may assume the control object as seen in different works, also the LQG controller has the same form as the CDM one, but the CDM controller synthesis is easier and have better performance and more robustness).

We also remind that it is still necessary to make a system of CDM controllers combined with fuzzy logic to ensure the control with all parameter variations such as solar radiation, inlet temperature and reference temperature, as done in [25]

References

- [1] S. Elmetennani and T.M. Laleg-Kirati. Bilinear reduced order approximate model of parabolic distributed solar collectors. *Solar Energy* **131** (2016) 71–80.
- [2] E. F. Camacho, F. R. Rubio, and F. M. Hughes. Self-tuning control of a solar power plant with a distributes collector field. *IEEE Control Systems* (1992) 72–78.
- [3] E. F. Camacho and E. Berenguel. Robust adaptive model predictive control of a solar plant with bounded uncertainties. *International Journal of Adaptive Control and Signal processing* **11**(4) (1997) 311–325.

- [4] E.F. Camacho, F.R. Rubio, M. Berenguel, and L. Valenzuela. A survey on control schemes for distributed solar collector fields. part ii : Advanced control approaches. *Solar Energy* **81** (2007) 1252–1272.
- [5] E.F. Camacho, F.R. Rubio, M. Berenguel, and L. Valenzuela. A survey on control schemes for distributed solar collector fields. part i : Modeling and basic control approaches. *Solar Energy* **81** (2007) 1240–1251.
- [6] C. Cirre, L. Valenzuela, M. Berenguel, and E. F. Camacho. Feedback linearization control for a distributed solar collector field. *IFAC Proceedings Volumes* **38**(1) (2005) 356–361.
- [7] R. N. Silva, L. M. Rato, L. M. Barao, and J. M. Lemos. A physical model based approach to distributed collector solar field control. In: *Proceedings of the American Control Conference, Anchorage, AK* (2002) 3817–3822.
- [8] F. R. Rubio, M. Berenguel, and E. F. Camacho. Fuzzy logic control of a solar power plant. *IEEE Transactions on Fuzzy Systems* **3**(4) (1995) 459–468.
- [9] D. Limon, I. Alvarado, T. Alamo, M. Ruiz, and E. F. Camacho. Robust control of the distributed solar collector field acurex using mpc for tracking. *Proceedings of the 17th World Congress The International Federation of Automatic Control* (2008) 958–963.
- [10] E. F. Camacho and A. J. Gallego. Estimation of effective solar irradiation using an unscented kalman filter in a parabolic-trough field. *Solar Energy* **86** (2012) 3512–3518.
- [11] S. F. AVSAR and M. T. Soylemez. Optimizing cdm controllers under control signal constraints. In: *International Symposium on Innovations in Intelligent Systems and Applications, IEEE*, (2012).
- [12] K. Kalpana and B. Meenakshipriya. Design of coefficient diagram method (cdm) based pid controller for double integrating unstable system. In: *2nd International Conference on Electrical Energy Systems (ICEES), IEEE*, (2014).
- [13] S. Manabe. Coefficient diagram method as applied to the attitude control of controlled-bias-momentum satellite. In: *13th IFAC Symposium on Automatic Control in Aerospace, Palo Alto, California, USA*, (1994) 322–327.
- [14] M. Koksal and S. E. Hamamci. A program for the design of linear time invariant control systems : Cdmcad. *Computer Application and Engeneering Education* **12** (2004) 165–174.
- [15] O. Ocal, M.T Soylemez, and A. Bir. Robust controller tuning based on coefficient diagram method. In: *Proceedings of International Conference on Control, Manchester, UK*, 2008.
- [16] S.E. Hamamci and M. Koksal. Robust control of a dc motor by coefficient diagram method. In: *Proceedings of the 9th Mediterranean Conference on Control and Automation, Dubrownik, Chorwacja*, 2001.
- [17] E. F. Camacho, M. Berenguel, F. R. Rubio, and D. Martinez. *Advanced Control of Solar Thermal, Control of Solar Energy Systems*. Springer, London Dordrecht Heidelberg, New York, 2012.
- [18] A.J. Gallego and E.F. Camacho. Adaptative state-space model predictive control of a parabolic-trough field. *Control Engineering Practice* **20** (2012) 904–911.
- [19] S. Manabe. Brief tutorial and survey of coefficient diagram method. In: *The 4th Asian Control Conference, Singapore* (2002) 1161–1166.
- [20] R. Ali, T. H. Mohamed, Y. S. Qudaih, and Y. Mitani. A new load frequency control approach in an isolated small power systems using coefficient diagram method. *Electrical Power and Energy Systems* **56** (2014) 110–116.
- [21] M. Z. Bernard, T. H. Mohamed, Y. S. Qudaih, and Y. Mitani. Decentralized load frequency control in an interconnected power system using coefficient diagram method. *Electrical Power and Energy Systems* **63** (2014) 165–172.

- [22] H. Kim. The study of control design method. *IEEE, Information Technology, KORUS* (2004) 55–58.
- [23] P.V. Gopi Krishna Rao, M. V. Subramanyam, and K. Satyaprasad. Study on pid controller design and performance based on tuning techniques. In: *International Conference on Control, Instrumentation, Communication and Computational Technologies (ICCICCT)* (2014) 1411–1417.
- [24] C. A. Mosbah, M. Tadjine, M. Chakir, and M. S. Boucherit. On the control of parabolic solar collector : The zipper approach. *International Journal of Renewable Energy Research* **6**(3) (2016) 1100–1108.
- [25] A. L. Cardoso, J. Henriques, and A. Douardo. Fuzzy supervisor and feedforward control of a solar power plant using accessible disturbances. In: *European Control Conference (ECC)*, IEEE, 1999.
- [26] P. Garasi, Y. Qudaih, R. Ali, M. Watanabe, and Y. Mitani. Coefficient diagram method based load frequency control for a modern power system. *Journal Of Electronic Science And Technology* **12**(3) (2014) 270–276.
- [27] A.A. Boichuk and V.F. Zhuravlev. Solvability criterion for integro-differential equations with degenerate kernel in banach spaces. *Nonlinear Dynamics and Systems Theory* **18**(4) (2018) 331–341.
- [28] N. Fallo and R.J. Moitsheki. Approximate analytical solutions for transient heat transfer in two-dimensional straight fins. *Nonlinear Dynamics and Systems Theory* **19** (1-SI) (2019) 133–140.
- [29] E. F. Camacho and A. J. Gallego. Optimal operation in solar trough plants: A case study. *Solar Energy* **95** (2013) 106–117.



Adaptive Sliding Mode Control Synchronization of a Novel, Highly Chaotic 3-D System with Two Exponential Nonlinearities

F. Hannachi*

Larbi Tebessi University – Tebessa, Algeria

Received: May 4, 2019; Revised: December 24, 2019

Abstract: In this paper, a new 3D chaotic system with three nonlinearities is introduced. Basic dynamical properties of this new chaotic system are studied such as equilibrium points and their stability, dissipativity and Lyapunov exponent, Lyapunov exponent spectrum, Kaplan-Yorke dimension. Also, an adaptive integral sliding mode control scheme is proposed for synchronization of the new chaotic system with unknown system parameters based on the Lyapunov stability theory and adaptive control theory of this new chaotic system with unknown system parameters. Finally, numerical simulations are presented to show the effectiveness of the proposed chaos synchronization scheme using Matlab.

Keywords: *chaotic system; strange attractor; Lyapunov exponent; Lyapunov stability theory; adaptive control; synchronization.*

Mathematics Subject Classification (2010): 37B55, 34C28, 34D08, 37B25, 37D45, 93C40, 93D05.

1 Introduction

Chaos as an important nonlinear phenomenon has been studied in mathematics, engineering and in many other disciplines. Synchronization of chaotic systems has become an active research area because of its potential applications in different industrial areas [1, 2, 3]. For the first time chaotic synchronization was illustrated by Fujisaka and Yamada [2] in 1983, then, Pecora and Carroll [3] in 1990, reported a new and very effective method for the synchronization of two chaotic systems with different initial conditions. The control

* Corresponding author: <mailto:fareh.hannachi@univ-tebessa.dz>

scheme has been applied in the recent decade for the synchronization of chaotic or hyperchaotic system, for example, the OYG method [4], adaptive control [5, 13, 14, 15, 19, 20], backstepping design method [6], sliding mode control [7, 20], PC synchronization method [3], passive control [8], fuzzy control [9], nonlinear active control [10], etc. The adaptive control scheme is used when parameters are unknown or initially uncertain. The sliding mode control method is often used because of its inherent advantages of easy realization, fast response and good transient performance, as well as its insensitivity to parameter uncertainties and external disturbances. Also, in the adaptive method, the control law and parameter update law are designed in such a way that the chaotic response system to behave like chaotic drive systems. As a result, the adaptive scheme maintains consistent performance of a system in the presence of uncertainty as well as variations in plant parameters. The adaptive control technique is different from other control methods since it does not need a priori information about the bounds on these uncertain or time varying parameters because this method of control is concerned with the control law changing themselves. Recently, many papers are available on synchronization of chaotic systems using this method of control.

In this paper a new chaotic system is considered for synchronization using the sliding mode control method and adaptive sliding mode control method when system parameters are unknown. Stabilization and convergence of error dynamics are achieved using the Lyapunov stability theory [11, 12]. This paper is organized as follows. The first section deals with the description and some properties of the novel chaotic system. The next two sections deal with the synchronization problem for globally and exponentially synchronizing the identical 3-D novel chaotic systems using the integral sliding mode control and adaptive integral sliding mode control law with unknown system parameters, respectively. Finally, numerical simulations using MATLAB have been shown to illustrate our results for the new chaotic system with unknown parameters.

1.1 Description of the novel chaotic system

A novel 3D autonomous chaotic system is expressed as follows:

$$\begin{cases} \frac{dx}{dt} = a(y - x), \\ \frac{dy}{dt} = cx - y - xz - e^x, \\ \frac{dz}{dt} = e^{xy} - dy - bz, \end{cases} \quad (1)$$

where x, y, z are the state variables and a, b, c are positive real parameters.

There are nine terms on the right-hand side but it mainly relies on three nonlinearities, namely, e^{xy} , e^x and xz , respectively.

System (1) can generate a new strange attractor for the parameters $a = 15, b = 3, c = 300, d = 1$ with the initial conditions $(x(0), y(0), z(0)) = (1, 1, 1)$. The chaotic attractor is displayed in Figure 1. It appears that the new attractor exhibits the interesting complex and abundant chaotic dynamics behavior, which is similar to the Lorenz chaotic attractor, but is different from that of the Lorenz system or any existing systems.

1.2 Basic properties

In this section, some basic properties of the system (1) are given. We start with the equilibrium points of the system and check their stability at the initial values of the parameters a, b, c .

1.3 Equilibrium points

Putting equations of the system (1) equal to zero, i.e.,

$$\begin{cases} a(y - x) = 0, \\ cx - y - xz - e^x = 0, \\ e^{xy} - dy - bz = 0, \end{cases} \quad (2)$$

gives numerically the only equilibrium point

$$p^* = (3.3595 \times 10^{-3}, 3.3595 \times 10^{-3}, 0.33222).$$

1.4 Stability

In order to check the stability of the equilibrium points we derive the Jacobian matrix at a point $p(x, y, z)$ of the system (1)

$$J(p) = \begin{pmatrix} -a & a & 0 \\ c - z - e^x & -1 & -x \\ ye^{xy} & -d + xe^{xy} & -b \end{pmatrix}. \quad (3)$$

For p^* , we obtain three eigenvalues

$$\lambda_1 = 59.297, \lambda_2 = -3.0, \lambda_3 = -75.297. \quad (4)$$

Since all the eigenvalues are real, Hartman-Grobman theorem implies that p is a saddle point which is unstable according to the Lyapunov theorem of stability.

1.4.1 Dissipativity

In vector notation, we may express the system (1) as

$$\dot{X} = f(X) = \begin{pmatrix} f_1(x, y, z) \\ f_2(x, y, z) \\ f_3(x, y, z) \end{pmatrix}.$$

Let Ω be any region in R^3 with a smooth boundary and also, $\Omega(t) = \phi_t(\Omega)$, where ϕ_t is the flow of f . Furthermore, let $V(t)$ denote the volume of $\Omega(t)$. By Liouville's theorem, we have

$$\dot{V}(t) = \int_{\Omega(t)} (\nabla \cdot f) dx dy dz \quad (5)$$

with

$$\nabla \cdot f = \frac{\partial \dot{f}_1}{\partial x} + \frac{\partial \dot{f}_2}{\partial y} + \frac{\partial \dot{f}_3}{\partial z} = -(a + b + 1) < 0 \quad (6)$$

and therefore

$$\dot{V}(t) = \int_{\Omega(t)} (-19) dx dy dz = -19V(t).$$

By integration, we get

$$V(t) = e^{-19t} V(0), \quad (7)$$

then, $V(t) \rightarrow 0$ as $t \rightarrow \infty$. This shows that the novel chaotic system (1) is dissipative.

1.4.2 Lyapunov exponents and Kaplan-Yorke dimension

Lyapunov exponents are used to measure the exponential rates of divergence and convergence of nearby trajectories, which is an important characteristic to judge the system whether it is chaotic or not. The existence of at least one positive Lyapunov exponent implies that the system is chaotic.

For the chosen parameter values of a, b, c, d , the Lyapunov exponents of the novel chaotic system (1) are obtained using Matlab with the initial conditions $(x(0), y(0), z(0)) = (1, 1, 1)$

$$L_1 = 6.6231, L_2 = -0.00206431, L_3 = -20.621. \quad (8)$$

The Lyapunov exponents spectrum is shown in Fig. 1.

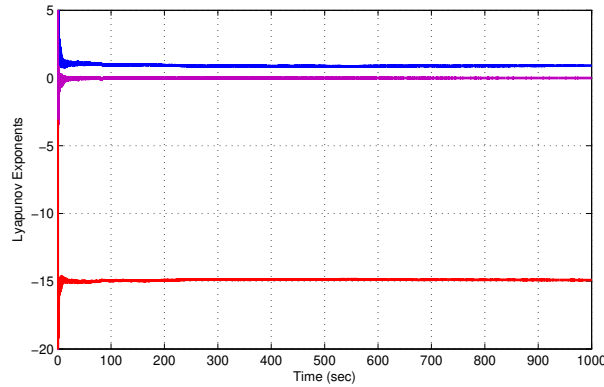


Figure 1: Lyapunov exponents spectrum.

Since the spectrum of Lyapunov exponents (8) has a maximal positive value L_1 , it follows that the 3-D novel system (1) is a highly chaotic . The Kaplan-Yorke dimension of system (1) is calculated as

$$D_{KL} = 2 + \frac{L_1 + L_2}{|L_3|} = 2.3211. \quad (9)$$

In Figs. 2-6, the 2-D projections of the strange chaotic attractor of the novel chaotic system (1) on the $(x; y)$, $(x; z)$, $(y; z)$, $(z; x)$, $(z; y)$ planes are shown, respectively.

1.5 Synchronizing of the identical 3-D novel chaotic systems using integral sliding mode control

In this section, an integral sliding mode controller will be designed for globally and exponentially synchronizing the identical 3-D novel chaotic systems.

Thus, the master system is given by the novel chaotic system dynamics

$$\begin{cases} \frac{dx_1}{dt} = a(x_2 - x_1), \\ \frac{dx_2}{dt} = cx_1 - x_2 - x_1x_3 - e^{x_1}, \\ \frac{dx_3}{dt} = e^{x_1x_2} - dx_2 - bx_3. \end{cases} \quad (10)$$

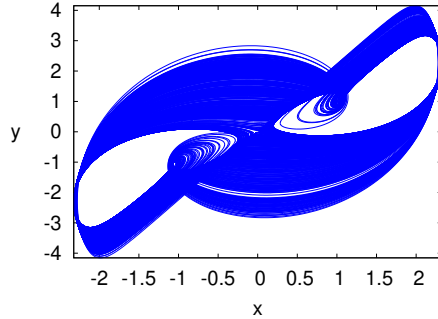


Figure 2: Projection on the $x - y$ plane of the chaotic attractor of system (1).

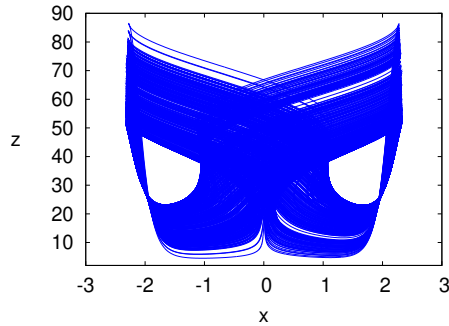


Figure 3: Projection on the $x - z$ plane of the chaotic attractor of system (1).

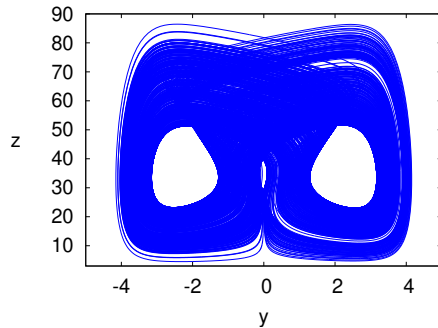


Figure 4: Projection on the $y - z$ plane of the chaotic attractor of system (1).

Also, the slave system is given by the novel chaotic system dynamics

$$\begin{cases} \frac{dy_1}{dt} = a(y_2 - y_1) + u_1, \\ \frac{dy_2}{dt} = cy_1 - y_2 - y_1y_3 - e^{y_1} + u_2, \\ \frac{dy_3}{dt} = e^{y_1y_2} - dy_2 - by_3 + u_3. \end{cases} \quad (11)$$

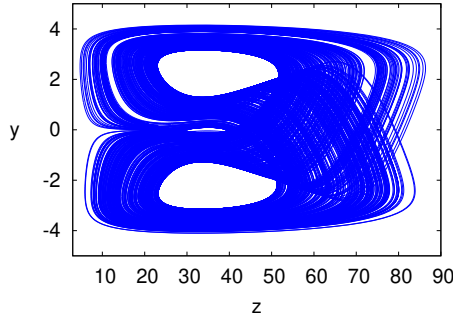


Figure 5: Projection on the $z - y$ plane of the chaotic attractor of system (1).

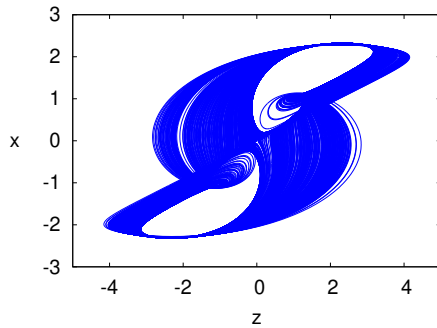


Figure 6: Projection on the $z - x$ plane of the chaotic attractor of system (1).

In (10) and (11), the system parameters a, b, c, d are $a = 15, b = 3, c = 300, d = 1$ and the main objective here is to design the controllers u_1, u_2, u_3 to synchronize two of the identical 3-D novel chaotic systems in equation (11) with equation (10), respectively.

The synchronization error between the novel chaotic systems (10) and (11) is defined as

$$\begin{cases} e_1 = y_1 - x_1, \\ e_2 = y_2 - x_2, \\ e_3 = y_3 - x_3, \end{cases} \quad (12)$$

(12) implies

$$\begin{cases} \dot{e}_1 = \dot{y}_1 - \dot{x}_1, \\ \dot{e}_2 = \dot{y}_2 - \dot{x}_2, \\ \dot{e}_3 = \dot{y}_3 - \dot{x}_3. \end{cases} \quad (13)$$

The sliding surface of the integral sliding mode controller is defined as

$$s_i = \left(\frac{d}{dt} + \lambda_i \right) \left(\int_0^t e_i(\tau) d\tau \right) = e_i + \lambda_i \int_0^t e_i(\tau) d\tau \quad (14)$$

and the reaching law is given by

$$\dot{s}_i = -\eta_i \operatorname{sgn}(s_i) - k_i s_i, \quad i = 1, 2, 3, \quad (15)$$

where $\eta_i > 0$, which indicates that the rate of the system reaching the switching surface $s_i = 0$, and the exponential reaching term, $-k_i s_i$, can guarantee that the system state can tend to the sliding mode with a large rate when s_i is bigger.

The derivative of equation in equation (14) results

$$\dot{s}_i = \dot{e}_i + \lambda_i e_i. \quad (16)$$

The Hurwitz condition is realized if $\lambda_i > 0$ for $i = 1, 2, 3$.

Equation (16) by considering the exponential reaching law presented by equation (15) gives

$$\begin{cases} \dot{e}_1 + \lambda_1 e_1 = -\eta_1 \operatorname{sgn}(s_1) - k_1 s_1, \\ \dot{e}_2 + \lambda_2 e_2 = -\eta_2 \operatorname{sgn}(s_2) - k_2 s_2, \\ \dot{e}_3 + \lambda_3 e_3 = -\eta_3 \operatorname{sgn}(s_3) - k_3 s_3. \end{cases} \quad (17)$$

Writing equation (17) with the provision of equations (12) and (13) yields

$$\begin{cases} a(e_2 - e_1) + u_1 + \lambda_1 e_1 = -\eta_1 \operatorname{sgn}(s_1) - k_1 s_1, \\ ce_1 - e_2 - y_1 y_3 + x_1 x_3 - e^{y_1} + e^{x_1} + u_2 + \lambda_2 e_2 = -\eta_2 \operatorname{sgn}(s_2) - k_2 s_2, \\ -de_2 - be_3 + e^{y_1 y_2} - e^{x_1 x_2} + u_3 + \lambda_3 e_3 = -\eta_3 \operatorname{sgn}(s_3) - k_3 s_3. \end{cases} \quad (18)$$

Then, the following control laws result in

$$\begin{cases} u_1 = -a(e_2 - e_1) - \lambda_1 e_1 - \eta_1 \operatorname{sgn}(s_1) - k_1 s_1, \\ u_2 = -ce_1 + e_2 + y_1 y_3 - x_1 x_3 + e^{y_1} - e^{x_1} - \lambda_2 e_2 - \eta_2 \operatorname{sgn}(s_2) - k_2 s_2, \\ u_3 = de_2 + be_3 - e^{y_1 y_2} + e^{x_1 x_2} - \lambda_3 e_3 - \eta_3 \operatorname{sgn}(s_3) - k_3 s_3. \end{cases} \quad (19)$$

Theorem 1.1 *The response of the system in equation (11) with the arbitrary initial condition $y(0) \in R^3$, using the control laws in equation (19) and with η_i, λ_i and $k_i > 0$, is same as the response of the system in equation (10). This means equation (12) is globally asymptotically stable.*

Proof. We consider the quadratic Lyapunov function given by

$$V(s_1, s_2, s_3) = \frac{1}{2} (s_1^2 + s_2^2 + s_3^2), \quad (20)$$

where $s_i, i = 1, 2, 3$, are the same as the ones in equation (14). Then, the derivative of equation (20) gives

$$\dot{V} = s_1 \dot{s}_1 + s_2 \dot{s}_2 + s_3 \dot{s}_3. \quad (21)$$

By substituting equation (15) into equation (21) we get

$$\begin{aligned} \dot{V} &= s_1 (-\eta_1 \operatorname{sgn}(s_1) - k_1 s_1) + s_2 (-\eta_2 \operatorname{sgn}(s_2) - k_2 s_2) + s_3 (-\eta_3 \operatorname{sgn}(s_3) - k_3 s_3) \\ &= -\eta_1 |s_1| - k_1 s_1^2 - \eta_2 |s_2| - k_2 s_2^2 - \eta_3 |s_3| - k_3 s_3^2, \end{aligned} \quad (22)$$

which is a negative definite function on R^3 for $\eta_i, k_i > 0$, $i = 1, 2, 3$. Hence, by the Lyapunov stability theory [11, 12], it follows that $e_i(t) \rightarrow 0$ as $t \rightarrow \infty$ for $i = 1, 2, 3$. Hence, the proof is complete.

2 Adaptive Synchronization of the Identical 3-D Novel Chaotic Systems

In this section, we derive an adaptive integral sliding mode control law for globally and exponentially synchronizing the identical 3-D novel chaotic systems with unknown system parameters.

Thus, the master system is given by the novel chaotic system dynamics

$$\begin{cases} \frac{dx_1}{dt} = a(x_2 - x_1), \\ \frac{dx_2}{dt} = cx_1 - x_2 - x_1x_3 - e^{x_1}, \\ \frac{dx_3}{dt} = e^{x_1x_2} - dx_2 - bx_3. \end{cases} \quad (23)$$

Also, the slave system is given by the novel chaotic system dynamics

$$\begin{cases} \frac{dy_1}{dt} = a(y_2 - y_1) + u_1, \\ \frac{dy_2}{dt} = cy_1 - y_2 - y_1y_3 - e^{y_1} + u_2, \\ \frac{dy_3}{dt} = e^{y_1y_2} - dy_2 - by_3 + u_3. \end{cases} \quad (24)$$

In (23) and (24), the system parameters a, b, c, d are unknown and the design goal is to find the adaptive feedback controls u_1, u_2, u_3 using the states $x_1, x_2, x_3, y_1, y_2, y_3$ and the estimates $a_1(t), b_1(t), c_1(t), d_1(t)$ of the unknown parameters a, b, c, d , respectively.

The synchronization error between the novel chaotic systems (23) and (24) is defined as

$$\begin{cases} e_1 = y_1 - x_1, \\ e_2 = y_2 - x_2, \\ e_3 = y_3 - x_3, \end{cases} \quad (25)$$

(25) implies

$$\begin{cases} \dot{e}_1 = \dot{y}_1 - \dot{x}_1, \\ \dot{e}_2 = \dot{y}_2 - \dot{x}_2, \\ \dot{e}_3 = \dot{y}_3 - \dot{x}_3. \end{cases} \quad (26)$$

Thus, the synchronization error dynamics is obtained as

$$\begin{cases} \dot{e}_1 = a(e_2 - e_1) + u_1, \\ \dot{e}_2 = ce_1 - e_2 - y_1y_3 + x_1x_3 - e^{y_1} + e^{x_1} + u_2, \\ \dot{e}_3 = -de_2 - be_3 + e^{y_1y_2} - e^{x_1x_2} + u_3. \end{cases} \quad (27)$$

We take the adaptive control law defined by

$$\begin{cases} u_1 = -a_1(e_2 - e_1) - \lambda_1 e_1 - \eta_1 sgn(s_1) - k_1 s_1, \\ u_2 = -c_1 e_1 + e_2 + y_1 y_3 - x_1 x_3 + e^{y_1} - e^{x_1} - \lambda_2 e_2 - \eta_2 sgn(s_2) - k_2 s_2, \\ u_3 = d_1 e_2 + b_1 e_3 - e^{y_1 y_2} + e^{x_1 x_2} - \lambda_3 e_3 - \eta_3 sgn(s_3) - k_3 s_3, \end{cases} \quad (28)$$

where k_1, k_2, k_3 are positive gain constants.

Substituting (28) into (27), we obtain the closed-loop error dynamics as

$$\begin{cases} \dot{e}_1 = (a - a_1)(e_2 - e_1) - \lambda_1 e_1 - \eta_1 sgn(s_1) - k_1 s_1, \\ \dot{e}_2 = (c - c_1)e_1 - \lambda_2 e_2 - \eta_2 sgn(s_2) - k_2 s_2, \\ \dot{e}_3 = (d_1 - d)e_2 - (b - b_1)e_3 - \lambda_3 e_3 - \eta_3 sgn(s_3) - k_3 s_3. \end{cases} \quad (29)$$

The parameter estimation errors are defined as

$$\begin{cases} e_a(t) = a - a_1(t), \\ e_c(t) = c - c_1(t), \\ e_b(t) = b - b_1(t), \\ e_d(t) = d - d_1(t). \end{cases} \quad (30)$$

Differentiating (30) with respect to t , we obtain

$$\begin{cases} \frac{de_a(t)}{dt} = -\frac{da_1(t)}{dt}, \\ \frac{de_c(t)}{dt} = -\frac{dc_1(t)}{dt}, \\ \frac{de_b(t)}{dt} = -\frac{db_1(t)}{dt}, \\ \frac{de_d(t)}{dt} = -\frac{dd_1(t)}{dt}. \end{cases} \quad (31)$$

By using (31), we rewrite the closed-loop system (29) as

$$\begin{cases} \dot{e}_1 = e_a(e_2 - e_1) - \lambda_1 e_1 - \eta_1 sgn(s_1) - k_1 s_1, \\ \dot{e}_2 = e_c e_1 - \lambda_2 e_2 - \eta_2 sgn(s_2) - k_2 s_2, \\ \dot{e}_3 = -e_d e_2 - e_b e_3 - \lambda_3 e_3 - \eta_3 sgn(s_3) - k_3 s_3. \end{cases} \quad (32)$$

We consider the quadratic Lyapunov function given by

$$V(s_1, s_2, s_3, e_a, e_b, e_c, e_d) = \frac{1}{2} (s_1^2 + s_2^2 + s_3^2 + e_a^2 + e_b^2 + e_c^2 + e_d^2), \quad (33)$$

which is a positive definite function on \mathbb{R}^6 .

Differentiating V along the trajectories of the systems (31) and (32), we obtain the following:

$$\begin{cases} \dot{V} = -\sum_{i=1}^3 k_i s_i^2 - (\eta_1 |s_1| + \eta_2 |s_2| + \eta_3 |s_3|) + e_a \left(s_1(e_2 - e_1) - \frac{da_1(t)}{dt} \right), \\ \quad -e_b \left(s_3 e_3 + \frac{db_1(t)}{dt} \right) + e_c \left(s_2 e_1 - \frac{dc_1(t)}{dt} \right) - e_d \left(s_3 e_2 + \frac{dd_1(t)}{dt} \right). \end{cases} \quad (34)$$

In view of (34), we take the parameter update law as follows:

$$\begin{cases} \frac{da_1(t)}{dt} = s_1(e_2 - e_1), \\ \frac{db_1(t)}{dt} = -s_3 e_3, \\ \frac{dc_1(t)}{dt} = s_2 e_1, \\ \frac{dd_1(t)}{dt} = -s_3 e_2. \end{cases} \quad (35)$$

Substituting (35) into (34), we obtain

$$\dot{V} = -\sum_{i=1}^3 k_i s_i^2,$$

which is a negative definite function on \mathbb{R}^3 . Hence, by the Lyapunov stability theory [11, 12], it follows that $e_i(t) \rightarrow 0$ as $t \rightarrow \infty$ for $i = 1, 2, 3$. Hence, we have proved the following theorem.

Theorem 2.1 *The 3-D novel chaotic systems (23) and (24) with unknown parameters are globally and exponentially synchronized for all initial conditions by the adaptive feedback control law (28) and the parameter update law (35), where k_1, k_2, k_3 are positive constants.*

2.1 Numerical simulations

We used the classical fourth-order Runge-Kutta method with step size $h = 10^{-8}$ to solve the system of differential equations (23), (24) and (35) when the adaptive control law (28) is applied.

The parameter values of the novel 3-D chaotic system (23) are chosen as in the chaotic case, i.e., $a = 15, b = 3, c = 300, d = 1$. The positive gain constants are taken as $k_i = 5$, for $i = 1, 2, 3$.

The initial conditions of the drive system (23) are chosen as: $x_1(0) = 2, x_2(0) = -5, x_3(0) = 7$ and $y_1(0) = 12, y_2(0) = 6, y_3(0) = 10$ for the slave system (24). Furthermore, as initial conditions of the parameter estimates of the unknown parameters, we have chosen $a_1(0) = 20, b_1(t) = 5, c_1(t) = 25, d_1(t) = 3$.

In Figs. 7-9, the synchronization of the states of the master system (23) and slave system (24) is depicted, when the adaptive control law (28) and parameter update law (35) are implemented.

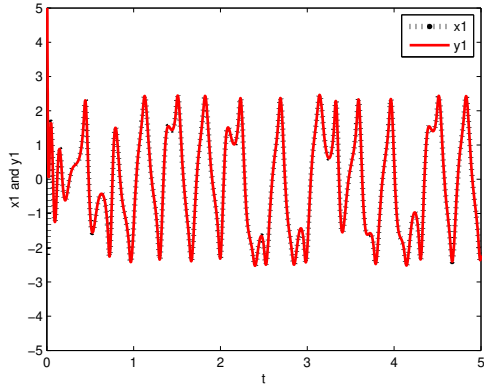


Figure 7: Synchronization of the states $x_1(t)$ and $y_1(t)$.

3 Conclusion

In this paper, a new chaotic system is introduced. Basic properties of this system are studied such as equilibrium points and their stability and the Lyapunov exponent and Kaplan-Yorke dimension. Moreover, the synchronization problem for globally and exponentially synchronizing the identical 3-D novel chaotic systems is solved using the integral sliding mode control and adaptive integral sliding mode control law with unknown system parameter, respectively. Numerical simulations using MATLAB have been shown to illustrate our results for the new chaotic system with unknown parameters. The results of this work are very important and have many applications in many fields such as security and communication. Therefore, further research on the system is still important and insightful and will be taken into consideration in a future work.

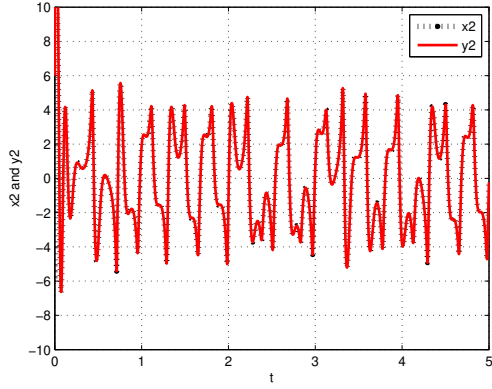


Figure 8: Synchronization of the states $x_2(t)$ and $y_2(t)$.

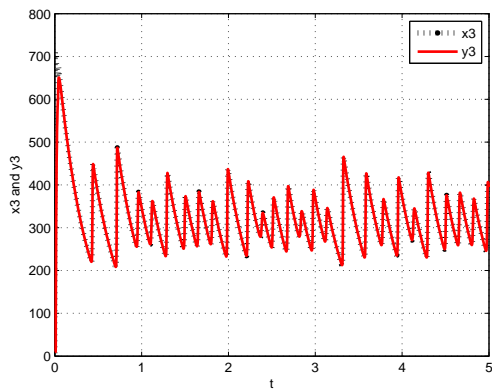


Figure 9: Synchronization of the states $x_3(t)$ and $y_3(t)$.

Acknowledgment

The author would like to thank the editor in chief and the referees for their valuable suggestions and comments.

References

- [1] O. Edward. *Chaos in Dynamical Systems*. Cambridge university press, 2002.
- [2] H. Fujisaka and T. Yamada. Stability theory of synchronized motion in coupled-oscillator systems. *Progress of Theoretical Physics* **69** (1) (1983) 32–47.
- [3] L. M. Pecora and T. L. Carroll. Synchronization in chaotic systems. *Physical Review Letters* **64** (1990) 821–825.
- [4] C. Grebogi and Y. C. Lai. Controlling chaotic dynamical systems. *Systems and control letters* **31** (5) (1997) 307–312.

- [5] H. Adloo and M. Roopaei. Review article on adaptive synchronization of chaotic systems with unknown parameters. *Nonlinear Dynamics* **65** (1) (2011) 141–159.
- [6] X. Wu and J. Lu. Parameter identification and backstepping control of uncertain Lu system. *System, Chaos, Solitons and Fractals* **18** (1) (2003) 721–729.
- [7] J. Sun, Y. Shen, X. Wang, et al. Finitetime combination-combination synchronization of four different chaotic systems with unknown parameters via sliding mode control. *Nonlinear Dynamics* **76** (1) (2014) 383–397.
- [8] F. Wang and C. Liu. Synchronization of unified chaotic system based on passive control. *Physica D: Nonlinear Phenomena* **225** (1) (2007) 55–60.
- [9] H. J. Zimmermann. Fuzzy control. In: *Fuzzy Set Theory and Its Applications*. Springer, Dordrecht, 1996, P. 203–240.
- [10] M. Ho and Y. Hung. Synchronization of two different chaotic systems using generalized active control. *Physics Letters A* **301** (5) (2002) 424–428.
- [11] H. K. Khalil. *Nonlinear Systems*. New York, Prentice Hall, 2002.
- [12] W. Hahn. *The Stability of Motion*. Springer, New York, USA, 1967.
- [13] S. Vaidyanathan, C. Volos, V. Pham and K. Madhavan. Analysis, adaptive control and synchronization of a novel 4-D hyperchaotic hyperjerk system and its SPICE implementation. *Archives of Control Sciences* **25** (1) (2003) 135–158.
- [14] S. Vaidyanathan and C. Volos. Analysis and adaptive control of a novel 3-D conservative noequilibrium chaotic system. *Archives of Control Sciences* **25** (3) (2015) 333–353.
- [15] S. Vaidyanathan. A new six-term 3-D chaotic system with an exponential nonlinearity. *Far East Journal of Mathematical Sciences* **79** (2013) 35–143.
- [16] F. Yu and C. Wang. A novel three dimension autonomous chaotic system with a quadratic exponential nonlinear term. *Engineering, Technology and Applied Science Research* **2** (2) (2012) 209–215.
- [17] I. Ahmed, C. Mu and F. Zhang. A New Chaotic Attractor with Quadratic Exponential Nonlinear Term from Chen’s Attractor. *International Journal of Analysis and Application* **5** (1) (2014) 27–32.
- [18] P. P. Singh, J. P. Singh and B. K. Roy. Adaptive Control Scheme for Anti-synchronization of Identical Bhalekar-Gejji Chaotic Systems. *Research & Reviews: Journal of Physics* **3** (3) (2014) 1–7.
- [19] Y. Toopchi and J. Wang. Chaos control and synchronization of a hyperchaotic Zhou system by integral sliding mode control. *Entropy* **16** (12) (2014) 6539–6552.
- [20] S. Vaidyanathan. Adaptive design of controller and synchronizer for Lu-Xiao chaotic system with unknown parameters. *International Journal of Computer Science & Information Technology* **5** (1) (2013) 197.
- [21] Y. Li, B. Li and Y. Chen. Anticipated function synchronization with unknown parameters of discrete-time chaotic systems. *International Journal of Modern Physics C* **20** (04) (2009) 597–608.
- [22] F. Hannachi. Analysis, dynamics and adaptive control synchronization of a novel chaotic 3-D system. *SN Applied Sciences* **1** (2) (2019) 158.
- [23] S. Vaidyanathan and S. Sampath. Sliding mode controller design for the global chaos synchronization of Couplet systems. In: *International Conference on Computer Science and Information Technology*. Springer, Berlin, Heidelberg, 2012, P. 103–110.
- [24] M. Feki. Sliding mode control and synchronization of chaotic systems with parametric uncertainties. *Chaos, Solitons & Fractals* **41** (3) (2009) 1390–1400.

- [25] A. A. Abdullah and Y. Nishio. On the Chaotic Nature of Biological Signals Using Non-linear Data Analysis Methodology. *Proc. of the International Conference on Man-Machine Systems (ICoMMS)* 11–13 October 2009, Batu Ferringhi, Penang, MALAYSIA.
- [26] S. Sampath, S. Vaidyanathan, C. K. Volos and V. T. Pham. An eight-term novel four-scroll chaotic system with cubic nonlinearity and its circuit simulation. *Journal of Engineering Science and Technology Review* **8** (2) (2015) 1–6.
- [27] S. Vaidyanathan, Q. Zhu and A. T. Azar. Adaptive control of a novel nonlinear double convection chaotic system. In: *Fractional Order Control and Synchronization of Chaotic Systems*. Springer, Cham, 2017, P. 357–385.
- [28] S. Vaidyanathan, K. Rajagopal, C. K. Volos, I.M. Kyprianidis and I. N. Stouboulos. Analysis, Adaptive Control and Synchronization of a Seven-Term Novel 3-D Chaotic System with Three Quadratic Nonlinearities and its Digital Implementation in LabVIEW. *Journal of Engineering Science & Technology Review* **8** (2) (2015).
- [29] S. Vaidyanathan and C. Volos. Analysis and adaptive control of a novel 3-D conservative no-equilibrium chaotic system. *Archives of Control Sciences* **25** (3) (2015) 333–353.
- [30] F. Hannachi. Analysis and Adaptive Control Synchronization of a Novel 3-D Chaotic System. *Nonlinear Dynamics and Systems Theory* **19** (1) (2019) 68–78.



Motion Control Design of UNUSAITS AUV Using Sliding PID

T. Herlambang¹, S. Subchan^{2*}, H. Nurhadi^{3,4} and D. Adzkiya^{2,4}

¹ Department of Information Systems, University of Nahdlatul Ulama Surabaya, Indonesia

² Department of Mathematics, Sepuluh Nopember Institute of Technology, Indonesia

³ Department of Industrial Mechanical Engineering, Sepuluh Nopember Institute of Technology, Indonesia

⁴ Center of Excellence for Mechatronics and Industrial Automation Research Center, Sepuluh Nopember Institute of Technology, Indonesia

Received: October 27, 2019; Revised: January 27, 2020

Abstract: An unmanned submarine commonly called an Autonomous Underwater Vehicle (AUV) is one type of underwater robots used for underwater mapping. The AUV is an underwater vehicle capable of automatically moving in the water, controlled by humans on a vessel. Building an AUV is not easy as many components play important roles in the operation of the AUV. One of them is the motion control system. This paper develops the motion control system of the UNUSAITS AUV by applying a Sliding PID (SPID) control to a linear model with 6-DOF. The linear model is obtained through linearization of the nonlinear model with 6-DOF. The SPID is a combination of the Sliding Mode Control (SMC) and PID. The results of the study indicate that the SPID method can be effectively used as the motion control system of the linear model with an error of 0.2% - 4.2%.

Keywords: autonomous underwater vehicle; control systems; sliding PID; 6-DOF; linear model.

Mathematics Subject Classification (2010): 93C05, 93C15.

* Corresponding author: <mailto:subchan@matematika.its.ac.id>

1 Introduction

Underwater vehicle technology plays an important role for archipelago nations such as Indonesia. Since its water area is much larger than its land area, underwater technology is required to explore and keep or maintain its natural resources. So, an underwater vehicle is needed [1]. Underwater rides widely developed by many researchers and practitioners today are unmanned underwater robots. This robot is known as the Autonomous Underwater Vehicle (AUV). The AUV is one type of underwater robots that have attracted a lot of researchers in recent years [2]. The AUV is a vehicle driven through water with a propulsion system, controlled and driven by an onboard computer with six degrees of freedom (DOF) maneuver, so that it can carry out its determined tasks entirely by itself. The benefits of the AUV are not only for exploring marine resources, but also for underwater mapping and underwater defense system equipment [3,4].

Several studies on the AUV control system that have been conducted within the period of 1990s up to now can be described as follows. Guo, Chiu and Huang examined the AUV motion control by using a Fuzzy Sliding Mode Control for 6-DOF [5]. Then, Mc Gann et al. used an adaptive control for 6-DOF underwater vehicles [6]. Petric dan Stilwell applied PID to the Virginia Tech 475 AUV model with 2-DOF [7]. Oktafianto et al. developed a Sliding Mode Control (SMC) method for a 6-DOF linear model [8]. Herlambang et al. proposed a Particle Swarm Optimization (PSO) and Ant Colony Optimization (ACO) for controlling an AUV system [9].

This study was carried out in the following stages. First, the equation of motion for the 6-DOF nonlinear model was formulated. Then, the model was linearized using the Jacobi matrix to obtain the 6-DOF linear model. Next, the Sliding PID (SPID) method was employed to control the motion of the 6-DOF model to reach the desired set point in the disturbance-free case (when the AUV is moving).

2 Autonomous Underwater Vehicle

Two important things are considered essential to analyze an AUV, that is, the axis system consisting of the Earth Fixed Frame (EFF) and Body Fixed Frame (BFF) as seen in Figure 1 (left) [10]. The EFF is used to show the position and orientation of the AUV, of which the x -axis position leads northward, the y -axis goes to the east, and the z -axis heads toward the center of the earth. The BFF defines the positive x -axis leading to the prowess of the vehicle, the positive y -axis leads to the right side of the vehicle, and the positive z -axis points downward [10]. The BFF system is used to show the speed and acceleration of the AUV with the starting point at the center of gravity. The profile of the UNUSAITS AUV is shown in Figure 1 (right). Figure 1 (left) and Table 1 show that the AUV has six degrees of freedom (6-DOF), that is, surge, sway, heave, roll, pitch and yaw. The equation of AUV motion is influenced by the outer force as follows:

$$\tau = \tau_{hydrostatic} + \tau_{addedmass} + \tau_{drag} + \tau_{lift} + \tau_{control}.$$

The movement of the UNUSAITS AUV has 6 degrees of freedom, that is, 3 (three) degrees of freedom for the direction of translational motion on the x -axis (surge), y -axis (sway), and z -axis (heave) and the other 3 (three) degrees of freedom for rotational motion on the x -axis (roll), y -axis (yaw), and z -axis (pitch). The UNUSAITS AUV specifications include, among others, weight of 16 kg, length of 1.5 m, and a diameter of 20 cm [12]. The general description of the AUV with 6 DOF can be expressed in the

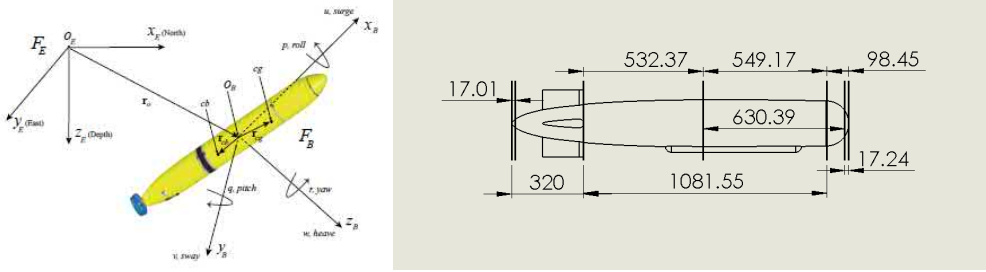


Figure 1: AUV motion with six degrees of freedom [11] and profile of UNUSAITS AUV [12].

Weight	16 Kg
Length	1500 mm
Diameter	200 mm
Controller	Ardupilot Mega 2.0
Communication	Wireless Xbee 2.4 GHz
Camera	TTL Camera
Battery	Li-Pro 11.8 V
Propulsion	12 V DC motor
Propeller	3 Blades OD : 50 mm
Speed	3.1 knots (1.5 m/s)
Maximum depth	8 m

Table 1: Specification of UNUSAITS AUV.

equations [10]:

$$\begin{aligned} \eta &= [\eta_1^T, \eta_2^T]^T, & \eta_1 &= [x, y, z]^T, & \eta_2 &= [\phi, \theta, \psi]^T; \\ v &= [v_1^T, v_2^T]^T, & v_1 &= [u, v, w]^T, & v_2 &= [p, q, r]^T; \\ \tau &= [\tau_1^T, \tau_2^T]^T, & v_1 &= [X, Y, Z]^T, & v_2 &= [K, M, N]^T; \end{aligned}$$

In the equations above, η shows the vector position and orientation on the EFF. Then, τ denotes the force vector and moment working on the AUV on the BFF, namely, surge (u), sway (v), heave (w), roll (p), pitch (q) and yaw (r). The total force and moment working on the AUV can be obtained by combining hydrostatic forces, hydrodynamic forces and thrust forces. In this case, it is assumed that the diagonal inertia tensor (I_o) is zero, to obtain the total force and moment of the whole nonlinear AUV model [2]. The following equations represent the surge, sway, heave, roll, pitch and yaw motions, respectively:

$$\begin{aligned} m[\dot{u} - vr + wq - x_G(q^2 + r^2) + y_G(pr - \dot{r}) + z_G(pr + \dot{q})] &= X_{\text{res}} + X_{|u|u}u|u| + X_{\dot{u}}\dot{u} \\ &\quad + X_{wq}wq + X_{qq}qg + X_{vr}vr + X_{rr}rr + X_{\text{prop}}, \\ m[\dot{v} - wp + ur - y_G(r^2 + p^2) + z_G(qr - \dot{p}) + x_G(pq + \dot{r})] &= Y_{\text{res}} + Y_{|v|v}v|v| + Y_{r|r}r|r| \end{aligned} \quad (1)$$

$$+ Y_i \dot{v} + Y_r \dot{r} + Y_{ur} ur + Y_{wp} wp + Y_{pq} pq + Y_{uv} uv + Y_{uu\delta_{r1}} u^2 \delta_{r1}, \quad (2)$$

$$m[\dot{w} - uq + vp - z_G(p^2 + q^2) + x_G(rp - \dot{q}) + y_G(rq + \dot{p})] = Z_{res} + Z_{|w|w} w |w| + Z_{q|q} q |q| + Z_{\dot{w}} \dot{w} + Z_{\dot{q}} \dot{q} + Z_{uq} uq + Z_{vp} vp + Z_{rp} rp + Z_{uw} uw + Z_{uu\delta_{s1}} u^2 \delta_{s1}, \quad (3)$$

$$I_x \dot{p} + (I_z - I_y) qr + m[y_G(\dot{w} - uq + vp) - z_G(\dot{v} - wp + ur)] = K_{res} + K_{p|p} p |p| + K_{\dot{p}} \dot{p} + K_{prop}, \quad (4)$$

$$I_y \dot{q} + (I_x - I_z) rp + m[z_G(\dot{u} - vr + wq) - x_G(\dot{w} - uq + vp)] = M_{res} + M_{w|w} w |w| + M_{q|q} q |q| + M_{\dot{w}} \dot{w} + M_{\dot{q}} \dot{q} + M_{uq} uq + M_{vp} vp + M_{rp} rp + M_{uw} uw + M_{uu\delta_{s2}} u^2 \delta_{s2}, \quad (5)$$

$$I_z \dot{r} + (I_y - I_z) pq + m[x_G(\dot{v} - wp + ur) - y_G(\dot{u} - vr + wq)] = N_{res} + N_{v|v} v |v| + N_{r|r} r |r| + N_v \dot{v} + N_r \dot{r} + N_{ur} ur + N_{wp} wp + N_{pq} pq + N_{uv} uv + N_{uu\delta_{r2}} u^2 \delta_{r2}. \quad (6)$$

The state variables of the model in (1)-(6) are u (surge), v (sway), w (heave), p (roll), q (pitch) and r (yaw), i.e., $x = [u, v, w, p, q, r]^T$. In this work, we assume that all state variables are measured, i.e., $y = x$. The input variables are X_{prop} , δ_{r1} , δ_{s1} , K_{prop} , δ_{s2} and δ_{r2} , i.e., $u = [X_{prop}, \delta_{r1}, \delta_{s1}, K_{prop}, \delta_{s2}, \delta_{r2}]^T$. It follows that the model in (1)-(6) can be formulated in the following state-space form:

$$\dot{x}(t) = f(x(t), u(t), t), \quad (7)$$

$$y(t) = x(t), \quad (8)$$

where

$$f_1(x, u) = (-m[-vr + wq - x_G(q^2 + r^2) + pqy_G + prz_G] + X_{res} + X_{|u|u} u |u| + X_{wq} wq + X_{qq} qq + X_{vr} vr + X_{rr} rr + X_{prop}) / (m - X_{\dot{u}}), \quad (9)$$

$$f_2(x, u) = (-m[-wp + ur - y_G(r^2 + p^2) + qrz_G + pqx_G] + Y_{res} + Y_{|v|v} v |v| + Y_{r|r} r |r| + Y_r \dot{r} + Y_{ur} ur + Y_{wp} wp + Y_{pq} pq + Y_{uv} uv + Y_{uu\delta_{r1}} u^2 \delta_{r1}) / (m - Y_{\dot{v}}), \quad (10)$$

$$f_3(x, u) = (-m[-uq + vp - z_G(p^2 + q^2) + rpx_G + rqy_G] + Z_{res} + Z_{|w|w} w |w| + Z_{q|q} q |q| + Z_{\dot{q}} \dot{q} + Z_{uq} uq + Z_{vp} vp + Z_{rp} rp + Z_{uw} uw + Z_{uu\delta_{s1}} u^2 \delta_{s1}) / (m - Z_{\dot{w}}), \quad (11)$$

$$f_4(x, u) = (-(I_z - I_y) qr - m[y_G(-uq + vp) - z_G(-wp + ur)] + K_{res} + K_{p|p} p |p| + K_{prop}) / (I_x - K_{\dot{p}}), \quad (12)$$

$$f_5(x, u) = (-(I_x - I_z) rp - m[z_G(-vr + wq) - x_G(-uq + vp)] + M_{res} + M_{w|w} w |w| + M_{q|q} q |q| + M_{\dot{w}} \dot{w} + M_{uq} uq + M_{vp} vp + M_{rp} rp + M_{uw} uw + M_{uu\delta_{s2}} u^2 \delta_{s2}) / (I_y - M_{\dot{q}}), \quad (13)$$

$$f_6(x, u) = (-(I_y - I_z) pq - m[x_G(-wp + ur) - y_G(-vr + wq)] + N_{res} + N_{v|v} v |v| + N_{r|r} r |r| + N_v \dot{v} + N_{ur} ur + N_{wp} wp + N_{pq} pq + N_{uv} uv + N_{uu\delta_{r2}} u^2 \delta_{r2}) / (I_z - N_{\dot{r}}). \quad (14)$$

Notice that the nonlinear AUV model in (7)-(8) is quite complicated. Thus, it is difficult to design a controller for the nonlinear model. Therefore, we linearize the nonlinear AUV model (7)-(8) around a solution by using the Jacobi matrix. The linearized AUV model is given by

$$\dot{x}(t) = Ax(t) + Bu(t), \quad (15)$$

$$y(t) = Cx(t) + Du(t), \quad (16)$$

where

$$A = \begin{bmatrix} 1 & 0 & 0 & 0 & \frac{mz_G}{m-X_{\dot{u}}} & \frac{-my_G}{m-X_{\dot{u}}} \\ 0 & 1 & 0 & -\frac{mz_G}{m-Y_{\dot{v}}} & 0 & \frac{mx_G-Y_{\dot{r}}}{m-Y_{\dot{v}}} \\ 0 & 0 & 1 & \frac{my_G}{m-Z_{\dot{w}}} & \frac{(mx_G+Z_{\dot{q}})}{m-Z_{\dot{w}}} & 0 \\ 0 & -\frac{mz_G}{I_x-K_{\dot{p}}} & \frac{my_G}{I_x-K_{\dot{p}}} & 1 & 0 & 0 \\ \frac{mz_G}{I_y-M_{\dot{q}}} & 0 & -\frac{(mx_G+M_{\dot{w}})}{I_y-M_{\dot{q}}} & 0 & 1 & 0 \\ -\frac{my_G}{I_z-N_{\dot{r}}} & \frac{mx_G-N_{\dot{v}}}{I_z-N_{\dot{r}}} & 0 & 0 & 0 & 1 \end{bmatrix}^{-1}$$

$$\begin{bmatrix} a_1 & b_1 & c_1 & d_1 & e_1 & g_1 \\ a_2 & b_2 & c_2 & d_2 & e_2 & g_2 \\ a_3 & b_3 & c_3 & d_3 & e_3 & g_3 \\ a_4 & b_4 & c_4 & d_4 & e_4 & g_4 \\ a_5 & b_5 & c_5 & d_5 & e_5 & g_5 \\ a_6 & b_6 & c_6 & d_6 & e_6 & g_6 \end{bmatrix}, \quad (17)$$

$$B = \begin{bmatrix} 1 & 0 & 0 & 0 & \frac{mz_G}{m-X_{\dot{u}}} & \frac{-my_G}{m-X_{\dot{u}}} \\ 0 & 1 & 0 & -\frac{mz_G}{m-Y_{\dot{v}}} & 0 & \frac{mx_G-Y_{\dot{r}}}{m-Y_{\dot{v}}} \\ 0 & 0 & 1 & \frac{my_G}{m-Z_{\dot{w}}} & \frac{(mx_G+Z_{\dot{q}})}{m-Z_{\dot{w}}} & 0 \\ 0 & -\frac{mz_G}{I_x-K_{\dot{p}}} & \frac{my_G}{I_x-K_{\dot{p}}} & 1 & 0 & 0 \\ \frac{mz_G}{I_y-M_{\dot{q}}} & 0 & -\frac{(mx_G+M_{\dot{w}})}{I_y-M_{\dot{q}}} & 0 & 1 & 0 \\ -\frac{my_G}{I_z-N_{\dot{r}}} & \frac{mx_G-N_{\dot{v}}}{I_z-N_{\dot{r}}} & 0 & 0 & 0 & 1 \end{bmatrix}^{-1}$$

$$\begin{bmatrix} A_1 & B_1 & C_1 & D_1 & E_1 & G_1 \\ A_2 & B_2 & C_2 & D_2 & E_2 & G_2 \\ A_3 & B_3 & C_3 & D_3 & E_3 & G_3 \\ A_4 & B_4 & C_4 & D_4 & E_4 & G_4 \\ A_5 & B_5 & C_5 & D_5 & E_5 & G_5 \\ A_6 & B_6 & C_6 & D_6 & E_6 & G_6 \end{bmatrix}, \quad (18)$$

$$C = \begin{bmatrix} 1 & 0 & 0 & 0 & 0 & 0 \\ 0 & 1 & 0 & 0 & 0 & 0 \\ 0 & 0 & 1 & 0 & 0 & 0 \\ 0 & 0 & 0 & 1 & 0 & 0 \\ 0 & 0 & 0 & 0 & 1 & 0 \\ 0 & 0 & 0 & 0 & 0 & 1 \end{bmatrix}, \quad D = \begin{bmatrix} 0 & 0 & 0 & 0 & 0 & 0 \\ 0 & 0 & 0 & 0 & 0 & 0 \\ 0 & 0 & 0 & 0 & 0 & 0 \\ 0 & 0 & 0 & 0 & 0 & 0 \\ 0 & 0 & 0 & 0 & 0 & 0 \\ 0 & 0 & 0 & 0 & 0 & 0 \end{bmatrix}. \quad (19)$$

3 Sliding PID

The Sliding-PID control system design is a combination of the SMC and PID. In the first stage, the error signal (the difference between the set point and the output) is used

as an input to the SMC. The SMC produces a signal that will guarantee that the error becomes zero in finite time. Then, the signal generated by the SMC is used as an input to the PID. Finally, the PID generates a signal that will be sent to the model as the input signal. The above process can be compactly displayed as a block diagram of the Sliding PID in Figure 2.

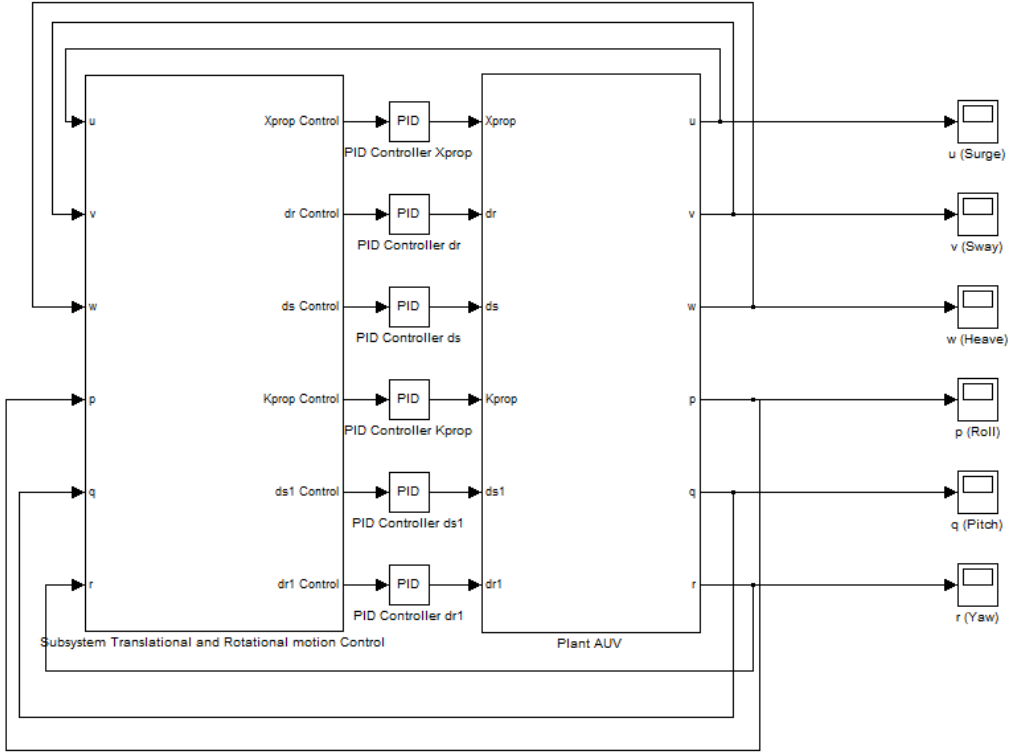


Figure 2: The block diagram of SPID.

Next, we design the SMC control system of the 6-DOF linear model for surge, sway, heave, roll, pitch and yaw. The SMC algorithm is used to compute the control input for those motions. Without going into the details, the control law produced by the SMC for each motion is as follows:

$$\begin{aligned} X_{prop} &= - \left(\frac{aa_1 u + bb_1 v + cc_1 w + dd_1 p + ee_1 q + gg_1 r + BB_1 \delta_{r1} + CC_1 \delta_{s1}}{AA_1} \right) \\ &\quad - \left(\frac{DD_1 K_{prop} + EE_1 \delta_{s2} + GG_1 \delta_{r2}}{AA_1} \right) - \left| \max \frac{\eta}{AA_1} \right| \text{sat} \left(\frac{S}{\phi} \right), \end{aligned} \quad (20)$$

$$\begin{aligned} \delta_{r1} &= - \left(\frac{aa_2 u + bb_2 v + cc_2 w + dd_2 p + ee_2 q + gg_2 r + AA_2 X_{prop} + CC_2 \delta_{s1}}{BB_2} \right) \\ &\quad - \left| \max \frac{\eta}{BB_2} \right| \text{sat} \left(\frac{S}{\phi} \right), \end{aligned} \quad (21)$$

$$\begin{aligned}\delta_{s1} = & - \left(\frac{aa_3u + bb_3v + cc_3w + dd_3p + ee_3q + gg_3r + AA_3X_{prop} + BB_3\delta_{r1}}{CC_3} \right) \\ & - \left(\frac{DD_3K_{prop} + EE_3\delta_{s2} + GG_3\delta_{r2}}{CC_3} \right) - \left| \max \frac{\eta}{CC_3} \right| \operatorname{sat} \left(\frac{S}{\phi} \right),\end{aligned}\quad (22)$$

$$\begin{aligned}K_{prop} = & - \left(\frac{aa_4u + bb_4v + cc_4w + dd_4p + ee_4q + gg_4r + AA_4X_{prop} + BB_4\delta_{r1}}{DD_4} \right) \\ & - \left(\frac{CC_4\delta_{s1} + EE_4\delta_{s2} + GG_4\delta_{r2}}{DD_4} \right) - \left| \max \frac{\eta}{AA_1} \right| \operatorname{sat} \left(\frac{S}{\phi} \right),\end{aligned}\quad (23)$$

$$\begin{aligned}\delta_{s2} = & - \left(\frac{aa_5u + bb_5v + cc_5w + dd_5p + ee_5q + gg_5r + AA_3X_{prop} + BB_5\delta_{r1} + CC_5\delta_{s1}}{EE_5} \right) \\ & - \left(\frac{DD_5K_{prop} + GG_5\delta_{r2}}{EE_5} \right) - \left| \max \frac{\eta}{CC_3} \right| \operatorname{sat} \left(\frac{S}{\phi} \right),\end{aligned}\quad (24)$$

$$\begin{aligned}\delta_{r2} = & - \left(\frac{aa_6u + bb_6v + cc_6w + dd_6p + ee_6q + gg_6r + AA_6X_{prop} + BB_6\delta_{r1} + CC_6\delta_{s1}}{GG_6} \right) \\ & - \left(\frac{DD_6K_{prop} + EE_6\delta_{s2}}{GG_6} \right) - \left| \max \frac{\eta}{BB_2} \right| \operatorname{sat} \left(\frac{S}{\phi} \right).\end{aligned}\quad (25)$$

As shown in Figure 2, the signals generated by the SMC (20)-(25) are fed to the PID controller. In the PID controller, the coefficients for the proportional, integral and derivative terms are shown in Table 2.

	K_p	K_i	K_d
Surge	3.1	0	0
Sway	2.5	0	0
Heave	2.5	0	0
Roll	2.04	0	0
Pitch	2.2	0	0
Yaw	2.2	0	0

Table 2: The coefficients of the proportional, integral and derivative terms.

The designing the SPID control system on the 6-DOF linear model first passes the SMC control system equation then optimized by the PID controller, of which the proportional, integral and derivative values are shown in Table 2. Once the control system equations are obtained, then they are connected to the 6-DOF linear model on the block diagram shown by Figure 2.

4 Computational Results

In this section, we present the simulation results of the closed-loop system by using the SPID controller designed in the previous section. First of all, we define the set point for surge, sway, heave, roll, pitch and yaw. The set point of surge, sway and heave is 1 m/s. The set point for roll rotation motion is 1 rad/s, whereas those of pitch and yaw are -1 rad/s. For each simulation result, we compare the time delay, rise time, peak time and settling time. The simulation results by using SPID control systems are as shown in Figure 3.

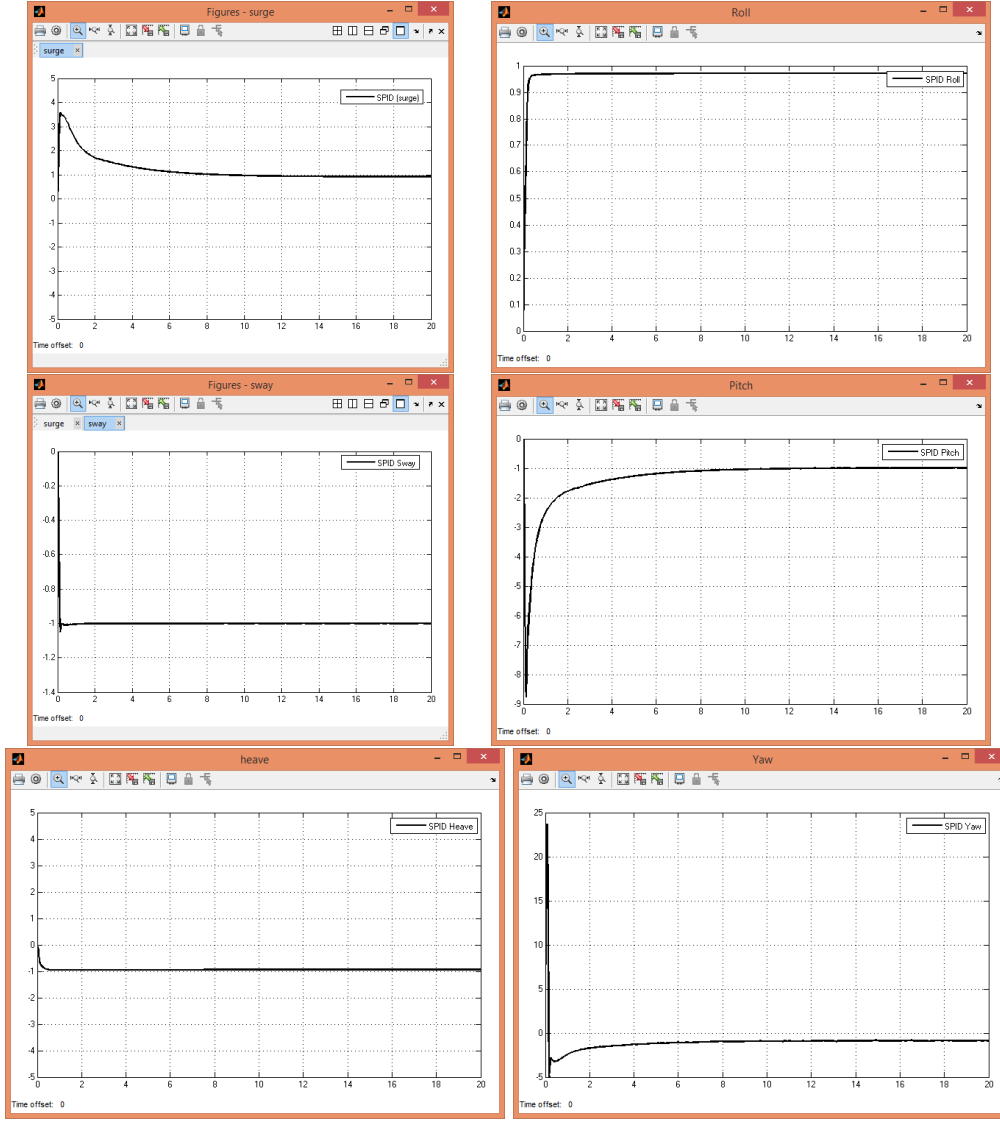


Figure 3: The results of the simulation by using the Sliding PID control system for surge and sway.

Figure 3 shows that the surge responses by the SPID were more stable at a set point of 1 m/s, reaching a settling time in 6 seconds with a maximum overshoot of 3.5 m/s, and had an error of 3.2%. The sway response is stable at the set point of -1 m/s , reaching the settling time in 0.1 of a second, and having an error of 0.1%. The heave response is also stable at the set point of -1 m/s , reaching a settling time in approximately 0.2 of a second, and having an error of 0.2%. These results show that the responses generated by the SPID in surge, sway, and heave motion were stable for surge, sway and heave motions. In this case, the overshoot was not the main consideration for the autonomous platform

performance. The prioritized ones were the settling time and the resulting error.

The results of simulation for rotational motion are shown in Figure 3. For the roll response, the result of simulation with the SPID shows that the roll responses were stable at the set point of 1 rad/s, reached a settling time in 0.15 of a second with a maximum overshoot of 1.2 rad/s, and had an error of 0.5%. The pitch responses by the SPID were also stable at set point of -1 rad/s, reached a settling time in 1.5 of a second with a maximum overshoot of -4.8 rad/s, and had an error of 4.1%. Finally, the yaw responses by the SPID were stable at the set point of -1 rad/s, reached a settling time in 0.25 of a second with a maximum overshoot of -5.6 rad/s, and had an error of 4.2%. In summary, the responses by the SPID in roll, pitch, and yaw were stable. The complete results of the transient responses are shown in Table 3, which shows that the error is very small.

	Surge	Sway	Heave	Roll	Pitch	Yaw
Delay time	0.04 s	0.042 s	0.043 s	0.045 s	0.09 s	0.003 s
Rise time	0.06 s	0.07 s	0.3 s	0.18 s	1.4 s	0.09 s
Peak time	0.1 s	0.01 s	0 s	0 s	0.3 s	0.1 s
Maximum peak	3.5 m/s	-1.08 m/s	0 m/s	0 m/s	-4.8 m/s	-5.6 m/s
Settling time	6 s	0.1 s	0.2 s	0.15 s	1.5 s	0.25 s
Error	3.2 %	0.1 %	0.2 %	0.5 %	4.1 %	4.2 %

Table 3: Specification of the transient responses in surge, sway, heave, roll, pitch, and yaw motions.

5 Conclusion

Based on the results of simulation and discussion about designing the Sliding Proportional, Integral, and Derivative (SPID) control system, regarding the linear model of 6-DOF, it could be concluded that the SPID method could be used as a motion control system of the 6-DOF linear model with a significant accuracy and an error of about 0.2% – 4.2%.

Acknowledgment

This work was supported by the Ministry of Research and High Education (Kemenristekdikti) for the funding support for the research conducted in the year of 2019 with the following contract numbers 061/SP2H/LT/MONO/L7/2019, 945/PKS/ITS/2019, 946/PKS/ITS/2019.

References

- [1] T. Herlambang, H. Nurhadi and Subchan. Preliminary Numerical Study on Designing Navigation and Stability Control Systems for ITS AUV. *Applied Mechanics and Materials* **493** (2014) 420–452.
- [2] T. Herlambang, E. B. Djatmiko and H. Nurhadi. Ensemble Kalman filter with a square root scheme (enkf-sr) for trajectory estimation of AUV SEGOROGENI ITS. *International Review of Mechanical Engineering* **9** (6) (2015) 553–560.

- [3] T. Herlambang, E. B. Djatmiko and H. Nurhadi. Navigation and guidance control system of AUV with trajectory estimation of linear modelling. In: *Proc. International Conf. on Advanced Mechatronics, Intelligent Manufacture, and Industrial Automation (ICAMIMIA)* Surabaya, Indonesia, 2015, 184–187.
- [4] Z. Ermayanti, E. Apriliani, H. Nurhadi and T. Herlambang. Estimate and control position autonomous underwater vehicle based on determined trajectory using fuzzy Kalman filter method. In: *Proc. International Conf. on Advanced Mechatronics, Intelligent Manufacture, and Industrial Automation (ICAMIMIA)* Surabaya, Indonesia, 2015, 156–161.
- [5] J. Guo, F.-C. Chiu and C.-C. Huang. Design of a sliding mode fuzzy controller for the guidance and control of an autonomous underwater vehicle. *Ocean Engineering* **30** (16) (2003) 2137–2155.
- [6] C. McGann, F. Py, K. Rajan, J. P. Ryan and R. Henthorn. Adaptive control for autonomous underwater vehicles. In: *Proc. Twenty-Third AAAI Conf. on Artificial Intelligence* 2008, 1319–1324.
- [7] J. Petrich and D. J. Stilwell. Model simplification for AUV pitch-axis control design. *Ocean Engineering* **37** (7) (2010) 638–651.
- [8] K. Oktafianto, T. Herlambang, Mardlijah and H. Nurhadi. Design of Autonomous Underwater Vehicle motion control using Sliding Mode Control method. In: *Proc. International Conf. on Advanced Mechatronics, Intelligent Manufacture, and Industrial Automation (ICAMIMIA)* Surabaya, Indonesia, 2015, 162–166.
- [9] T. Herlambang, D. Rahmalia and T. Yulianto. Particle Swarm Optimization (PSO) and Ant Colony Optimization (ACO) for Optimizing PID Parameters on Autonomous Underwater Vehicle (AUV) Control System. *Journal of Physics: Conference Series* **1211** (1) (2019) 012039.
- [10] C. Yang. Modular modelling and control for autonomous vehicle (AUV). *Department of Mechanical Engineering National University of Singapore* (2007).
- [11] U. Ansari and A. H. Bajodah. Robust generalized dynamic inversion control of autonomous underwater vehicles. *IFAC-PapersOnLine* **50** (1) (2017) 10658–10665.
- [12] T. Herlambang, S. Subchan and H. Nurhadi. Design of Motion Control Using Proportional Integral Derivative for UNUSAITS AUV. *International Review of Mechanical Engineering (IREME)* **12** (11) (2018) 928–938.



Alternative Legendre Functions for Solving Nonlinear Fractional Fredholm Integro-Differential Equations

Khawlah H. Hussain*

Department of Mechanical Technology, Basra Technical Institute, Southern Technical University, AL-Basrah, Iraq

Received: September 12, 2019; Revised: December 18, 2019

Abstract: This paper mainly focuses on the numerical technique based on a new set of functions called the fractional alternative Legendre functions for solving the nonlinear Fredholm integro-differential equations of fractional order. Also, the convergence analysis of the proposed technique is carried out. Finally, an example is included to demonstrate the validity and applicability of the proposed technique.

Keywords: *Fredholm integro-differential equations, alternative Legendre polynomials, Caputo fractional derivative, operational matrix.*

Mathematics Subject Classification (2010): 26A33, 45J05, 35C11.

1 Introduction

In recent years, fractional calculus and differential equations have found enormous applications in mathematics, physics, chemistry and engineering because of the fact that a realistic modeling of a physical phenomenon having dependence not only on the time instant but also on the previous time history can be successfully achieved by using fractional calculus. The developed analytical solutions are very few and are restricted to the solution of simple fractional Volterra integro-differential equations, therefore the development of effective and easy to use numerical schemes for solving such equations has acquired an increasing interest in recent years. Some fundamental works on various aspects of the fractional calculus are given by [2, 3, 9, 12, 15–20, 22].

Several numerical schemes have been presented for solving these problems, for example,

Mittal and Nigam [21] used the Adomian decomposition method for solving

$$D^\alpha u(x) = f(x)u(x) + g(x) + \int_0^x k(x,s)G(u(s))ds, \quad 0 < \alpha < 1.$$

* Corresponding author: <mailto:khawlah.hussain@stu.edu.iq>

$$u(0) = \Upsilon.$$

In [24] a computational method was employed for the numerical solution of the following equation:

$$\begin{aligned} D^\alpha u(x) &= f(x) + \lambda \int_0^x k(x, s)G(u(s))ds, \quad n-1 < \alpha \leq n, \\ u^{(i)}(0) &= \Upsilon_i, \quad i = 0, 1, \dots, n-1. \end{aligned}$$

Hamoud and Ghadle [3] used the Adomian decomposition method and modified Laplace Adomian decomposition method for the following equation:

$$\begin{aligned} D^\alpha u(x) &= f(x)u(x) + g(x) + \int_0^x k_1(x, s)G_1(u(s))ds + \int_0^1 k_2(x, s)G_2(u(s))ds, \\ u^{(i)}(0) &= \Upsilon_i, \quad n-1 < \alpha \leq n, \quad i = 0, 1, \dots, n-1. \end{aligned}$$

Motivated by the above works, in this paper we discuss a new set of functions called the fractional alternative Legendre functions for solving the nonlinear Fredholm integro-differential equations of fractional order of the form

$$D^\alpha u(x) = F\left(x, u(x) + \int_0^1 K(x, s)G(s, u(s))ds\right), \quad n-1 < \alpha \leq n, \quad (1)$$

with the initial conditions

$$u^{(i)}(x) = \Upsilon_i, \quad i = 0, 1, \dots, n-1. \quad (2)$$

During the last decades, several methods have been used for solving fractional differential equations, fractional integro-differential equations, fractional partial differential equations and dynamic systems containing fractional derivatives such as: the homotopy analysis method [2], Chebyshev wavelets [15], Sinc functions [17], Legendre wavelets [19], shifted second kind Chebyshev polynomials [20], Legendre collocation method [23]. For considering existence and uniqueness of the solutions of fractional integro-differential equations we refer the reader to [1, 4–8, 14].

The main objective of the present paper is to study the new fractional-order functions based on the alternative Legendre polynomials for solving the nonlinear fractional Fredholm integro-differential equations (FFIDEs). This method is accurate and easy to implement in solving the FVIDEs. First, the fractional derivative of the unknown function in the underlying FFIDE is approximated by finite linear combinations of the fractional-order alternative Legendre functions (FALFs). Then, we obtain the FALFs operational matrix of fractional integration. Finally, the problem is converted to a system of algebraic equations by using the FALFs operational matrix together with the collocation method.

2 Basic Definitions

The mathematical definitions of fractional derivative and fractional integration are the subject of several different approaches. The most frequently used definitions of the fractional calculus involve the Riemann-Liouville fractional derivative and Caputo derivative [3, 9–11, 13, 15].

Definition 2.1 [3] (**Riemann-Liouville fractional integral**). The Riemann-Liouville fractional integral of order $\alpha > 0$ of a function f is defined as

$$\begin{aligned} J^\alpha f(x) &= \frac{1}{\Gamma(\alpha)} \int_0^x (x-t)^{\alpha-1} f(t) dt, \quad x > 0, \quad \alpha \in \mathbb{R}^+, \\ J^0 f(x) &= f(x), \end{aligned} \quad (3)$$

where \mathbb{R}^+ is the set of positive real numbers.

Definition 2.2 [3] (**Caputo fractional derivative**). The fractional derivative of $f(x)$ in the Caputo sense is defined by

$$\begin{aligned} {}^c D_x^\alpha f(x) &= J^{m-\alpha} D^m f(x) \\ &= \begin{cases} \frac{1}{\Gamma(m-\alpha)} \int_0^x (x-t)^{m-\alpha-1} \frac{d^m f(t)}{dt^m} dt, & m-1 < \alpha < m, \\ \frac{d^m f(x)}{dx^m}, & \alpha = m, \quad m \in \mathbb{N}, \end{cases} \end{aligned} \quad (4)$$

where the parameter α is the order of the derivative and is allowed to be real or even complex. In this paper, only real and positive α will be considered. Hence, we have the following properties:

1. $J^\alpha J^\nu f = J^{\alpha+\nu} f, \quad \alpha, \nu > 0.$
2. $J^\alpha x^\beta = \frac{\Gamma(\beta+1)}{\Gamma(\beta+\alpha+1)} x^{\beta+\alpha}.$
3. $D^\alpha x^\beta = \frac{\Gamma(\beta+1)}{\Gamma(\beta-\alpha+1)} x^{\beta-\alpha}, \quad \alpha > 0, \quad \beta > -1, \quad x > 0.$
4. $J^\alpha D^\alpha f(x) = f(x) - \sum_{k=0}^{m-1} f^{(k)}(0^+) \frac{x^k}{k!}, \quad x > 0, \quad m-1 < \alpha \leq m.$

Definition 2.3 [3] (**Riemann-Liouville fractional derivative**). The Riemann-Liouville fractional derivative of order $\alpha > 0$ is normally defined as

$$D^\alpha f(x) = D^m J^{m-\alpha} f(x), \quad m-1 < \alpha \leq m, \quad m \in \mathbb{N}. \quad (5)$$

3 Fractional Alternative Legendre Polynomials

Let m be a fixed non-negative integer. The set $P_m = \{p_{m,i}(t)\}_{i=0}^m$ of alternative Legendre polynomials is

$$\begin{aligned} p_{m,i}(t) &= \sum_{r=0}^{m-i} (-1)^r \binom{m-i}{r} \binom{m+i+r+1}{m-i} t^{i+r} \\ &= \sum_{r=i}^m (-1)^{r-i} \binom{m-i}{r-i} \binom{m+r+1}{m-i} t^r, \quad i = 0, 1, \dots, m. \end{aligned} \quad (6)$$

These polynomials are orthogonal on the interval $[0, 1]$ with respect to the weight function $w(t) = 1$, and satisfy the orthogonality relationships

$$\int_0^1 p_{m,k}(t) p_{m,l}(t) dt = \frac{1}{k+l+1} \delta_{k,l}, \quad k, l = 0, 1, \dots, m. \quad (7)$$

Here $\delta_{k,l}$ denotes the Kronecker delta [23]. It should be noted that, in contrast to common sets of orthogonal polynomials, every member in P_m has degree m . For example, when $m = 3$, we have

$$\begin{aligned} p_{3,0}(t) &= 4 - 30t + 60t^2 - 35t^3, \\ p_{3,1}(t) &= 10t - 30t^2 + 21t^3, \\ p_{3,2}(t) &= 6t^2 - 7t^3, \\ p_{3,3}(t) &= t^3. \end{aligned} \quad (8)$$

Eq. (6) obtains Rodrigues's type representation

$$p_{m,i}(t) = \frac{1}{(m-i)!} \frac{1}{t^{i+1}} \frac{d^{m-i}}{dt^{m-i}} (t^{m+i+1} (1-t)^{m-i}), \quad i = 0, 1, \dots, m. \quad (9)$$

It follows from (9) that

$$\int_0^1 p_{m,i}(t) dt = \int_0^1 t^m dt = \frac{1}{m+1}, \quad i = 0, 1, 2, \dots, m. \quad (10)$$

Now, we define a new set of fractional functions based on the alternative Legendre polynomials to obtain the solution of NVIDEs. The FALFs are obtained by a change of variable t to $x^\alpha (\alpha > 0)$, on the alternative Legendre polynomials. We denote $p_{m,i}(x^\alpha)$ by $p_{m,i}^\alpha(x)$. Therefore we have

$$\begin{aligned} p_{m,i}^\alpha(x) &= \sum_{r=0}^{m-i} (-1)^r \binom{m-i}{r} \binom{m+i+r+1}{m-i} x^{(i+r)\alpha} \\ &= \sum_{r=i}^m (-1)^{r-i} \binom{m-i}{r-i} \binom{m+r+1}{m-i} x^{r\alpha}, \quad i = 0, 1, \dots, m. \end{aligned} \quad (11)$$

The set of FALFs is orthogonal with respect to the weight function $w(x) = x^{\alpha-1}$ on the interval $[0, 1]$ with the orthogonality property

$$\int_0^1 p_{m,k}^\alpha(x) p_{m,l}^\alpha(x) x^{\alpha-1} dx = \frac{1}{(k+l+1)\alpha} \delta_{k,l}, \quad k, l = 0, 1, \dots, m. \quad (12)$$

For example, when $m = 3$, we have

$$\begin{aligned} p_{3,0}^\alpha(x) &= 4 - 30x^\alpha + 60x^{2\alpha} - 35x^{3\alpha}, \\ p_{3,1}^\alpha(x) &= 10x^\alpha - 30x^{2\alpha} + 21x^{3\alpha}, \\ p_{3,2}^\alpha(x) &= 6x^{2\alpha} - 7x^{3\alpha}, \\ p_{3,3}^\alpha(x) &= x^{3\alpha}. \end{aligned} \quad (13)$$

Any $f \in L^2[0, 1]$ may be expanded in terms of the fractional-order alternative Legendre functions as

$$f(x) = \sum_{i=0}^{\infty} c_i p_{m,i}^\alpha(x), \quad (14)$$

where the coefficients c_i are given by

$$c_i = \langle f, p_{m,i}^\alpha \rangle = (2i+1)^\alpha \int_0^1 f(x) p_{m,i}^\alpha(x) x^{\alpha-1} dx,$$

where \langle , \rangle denotes the inner product in $L^2[0, 1]$. If the infinite series in Eq. (14) is truncated, then it can be written as

$$f(x) \simeq \sum_{i=0}^m c_i p_{m,i}^\alpha(x) = C^T \Phi^\alpha(x), \quad (15)$$

where T indicates transposition, C and $\Phi^\alpha(x)$ are $(m+1) \times 1$ vectors given by

$$C = [c_0, c_1, c_2, \dots, c_m]^T, \quad (16)$$

and

$$\Phi^\alpha(x) = [p_{m,0}^\alpha(x), p_{m,1}^\alpha(x), p_{m,2}^\alpha(x), \dots, p_{m,m}^\alpha(x)]^T. \quad (17)$$

Now we will derive the fractional-order alternative Legendre functions operational matrix of the fractional integration. The Riemann-Liouville fractional integration of the vector $\Phi^\alpha(x)$ given in equation (17) is obtained by

$$I^\nu \Phi^\alpha(x) = F^{(\nu, \alpha)} \Phi^\alpha(x), \quad (18)$$

where $F^{(\nu, \alpha)}$ is the $(m+1) \times (m+1)$ operational matrix of the fractional integration of order α in the Riemann-Liouville sense.

By using Eq. (11) and linearity of the Riemann-Liouville fractional integral, for $i = 0, 1, \dots, m$, we get

$$\begin{aligned} I^\nu p_{m,i}^\alpha(x) &= \sum_{r=i}^m (-1)^{r-i} \binom{m-i}{r-i} \binom{m+r+1}{m-i} I^\alpha x^{r\alpha} \\ &= \sum_{r=i}^m (-1)^{r-i} \binom{m-i}{r-i} \binom{m+r+1}{m-i} \frac{\Gamma(r\alpha+1)}{\Gamma(r\alpha+\nu+1)} x^{r\alpha+\nu} \\ &= \sum_{r=i}^m \gamma_{mi,r}^{(\nu, \alpha)} x^{r\alpha+\nu}, \end{aligned} \quad (19)$$

where

$$\gamma_{mi,r}^{(\nu, \alpha)} = (-1)^{r-i} \binom{m-i}{r-i} \binom{m+r+1}{m-i} \frac{\Gamma(r\alpha+1)}{\Gamma(r\alpha+\nu+1)}.$$

Now, approximating $x^{r\alpha+\nu}$ by $m+1$ terms of the fractional-order alternative Legendre functions, we get

$$x^{r\alpha+\nu} \simeq \sum_{j=0}^m \delta_{r,j}^{(\nu, \alpha)} p_{m,j}^\alpha(x). \quad (20)$$

Substituting Eq. (20) into Eq. (19) for $i = 0, 1, \dots, m$, we obtain

$$I^\nu p_{m,i}^\alpha(x) \simeq \sum_{r=i}^m \gamma_{mi,r}^{(\nu, \alpha)} \sum_{j=0}^m \delta_{r,j}^{(\nu, \alpha)} p_{m,j}^\alpha(x) = \sum_{j=0}^m \left(\sum_{r=i}^m \omega_{mi,j,r}^{(\nu, \alpha)} \right) p_{m,j}^\alpha(x), \quad (21)$$

where

$$\omega_{mi,j,r}^{(\nu,\alpha)} = \gamma_{mi,r}^{(\nu,\alpha)} \delta_{r,j}^{(\nu,\alpha)}.$$

Eq. (21) can be rewritten as

$$I^\nu p_{m,i}^\alpha(x) \simeq [\sum_{r=i}^m \omega_{mi,0,r}^{(\nu,\alpha)}, \sum_{r=i}^m \omega_{mi,1,r}^{(\nu,\alpha)}, \dots, \sum_{r=i}^m \omega_{mi,m,r}^{(\nu,\alpha)}] \Phi^\alpha(x).$$

Finally, we get

$$F^{(\nu,\alpha)} = \begin{bmatrix} \sum_{r=0}^m \omega_{m0,0,r}^{(\nu,\alpha)} & \sum_{r=0}^m \omega_{m0,1,r}^{(\nu,\alpha)} & \cdots & \sum_{r=0}^m \omega_{mi,m,r}^{(\nu,\alpha)} \\ \sum_{r=1}^m \omega_{m1,0,r}^{(\nu,\alpha)} & \sum_{r=1}^m \omega_{m1,1,r}^{(\nu,\alpha)} & \cdots & \sum_{r=1}^m \omega_{m1,m,r}^{(\nu,\alpha)} \\ \vdots & \vdots & \ddots & \vdots \\ \omega_{mm,0,r}^{(\nu,\alpha)} & \omega_{mm,1,r}^{(\nu,\alpha)} & \cdots & \omega_{mm,m,r}^{(\nu,\alpha)} \end{bmatrix}.$$

4 Description of the Method

In this section, we present a numerical method for solving the fractional Fredholm integro-differential equation (1)-(2). To solve this equation, we first expand $D^\alpha u(x)$ by the fractional-order alternative Legendre functions as

$$D^\nu u(x) \simeq D^\nu u_m(x) = C^T \Phi^\alpha(x), \quad (22)$$

with C and $\Phi^\alpha(x)$ defined in the previous section. By applying I^α on both sides of (22), we obtain

$$u(x) \simeq u_m(x) = C^T F^{(\nu,\alpha)} \Phi^\alpha(x) + \sum_{k=0}^{n-1} \frac{x^k}{k!} \Upsilon_k, \quad (23)$$

where $F^{(\nu,\alpha)}$ is the operational matrix of fractional integration of order α of the fractional-order alternative Legendre functions. Now, by substituting Eqs.(22)-(23) into (1), we have

$$\begin{aligned} C^T \Phi^\alpha(x) &= F\left(x, C^T F^{(\nu,\alpha)} \Phi^\alpha(x) + \sum_{k=0}^{n-1} \frac{x^k}{k!} \Upsilon_k, \right. \\ &\quad \left. \int_0^1 K(x,s)G(s,C^T F^{(\nu,\alpha)} \Phi^\alpha(s) + \sum_{k=0}^{n-1} \frac{x^k}{k!} \Upsilon_k) ds \right) \\ &\quad + Res_m(x), \end{aligned} \quad (24)$$

where $Res_m(x)$, $x \in [0, 1]$, is a residual error; that is, the error made when substituting the approximate solution into the governing equation. By using the Gauss-Legendre

numerical integration for evaluating the integral in Eq. (24), we get

$$\begin{aligned}
C^T \Phi^\alpha(x) &= F\left(x, C^T F^{(\nu, \alpha)} \Phi^\alpha(x) + \sum_{k=0}^{n-1} \frac{x^k}{k!} \Upsilon_k, \right. \\
&\quad \left. \frac{1}{2} \sum_{j=1}^{\tilde{m}} \omega_j K(x, \frac{1+\zeta_j}{2}) G\left(\frac{1+\zeta_j}{2}, C^T F^{(\nu, \alpha)} \Phi^\alpha\left(\frac{1+\zeta_j}{2}\right)\right) \right. \\
&\quad \left. + \sum_{k=0}^{n-1} \frac{\left(\frac{1+\zeta_j}{2}\right)^k}{k!} \Upsilon_k \right) \\
&\quad + E_{\tilde{m}} + Res_m(x),
\end{aligned} \tag{25}$$

where $\zeta_j, j = 1, 2, \dots, \tilde{m}$ are zeros of the Legendre polynomial $P_{\tilde{m}}(x)$ and $\omega_j = \frac{-2}{(\tilde{m}+1)P_{\tilde{m}}(\zeta_j)P_{\tilde{m}+1}(\zeta_j)}$ and $E_{\tilde{m}}$ is the error between the Gauss-Legendre rule and the exact integral given in [24]. By collocating Eq. (25) at the zeros of the shifted Legendre polynomials $L_{m+1}(x); (x_i, i = 0, 1, \dots, m)$ we have

$$\begin{aligned}
C^T \Phi^\alpha(x_i) &= F\left(x_i, C^T F^{(\nu, \alpha)} \Phi^\alpha(x_i) + \sum_{k=0}^{n-1} \frac{x_i^k}{k!} \Upsilon_k, \right. \\
&\quad \left. \frac{1}{2} \sum_{j=1}^{\tilde{m}} \omega_j K(x_i, \frac{1+\zeta_j}{2}) G\left(\frac{1+\zeta_j}{2}, C^T F^{(\nu, \alpha)} \Phi^\alpha\left(\frac{1+\zeta_j}{2}\right)\right) \right. \\
&\quad \left. + \sum_{k=0}^{n-1} \frac{\left(\frac{1+\zeta_j}{2}\right)^k}{k!} \Upsilon_k \right).
\end{aligned} \tag{26}$$

Eqs. (26) are nonlinear equations which can be solved for the unknown C using Newton's iterative method. By determining C , the values of $u(x)$ can be obtained from Eq. (23).

5 Convergence Analysis

In this section we investigate the convergence of the proposed method for solving FFIDEs. Before starting and proving the main results, we introduce the following hypotheses:

- (H1) There exists a constant K_1 such that $K_1 = \max |K(x, s)|; (x, s) \in [0, 1] \times [0, 1]$.
- (H2) u is a bounded function for all x in $[0, 1]$.
- (H3) F and G satisfy the Lipschitz conditions with the Lipschitz constants η and η_1 , respectively.

Theorem 5.1 *Assume that (H1)–(H3) hold, and let u and u_m be the exact and approximate solution of (1)–(2), respectively. If $\Gamma(\alpha) - \eta - K_1 \eta \eta_1 \neq 0$, then $\|u - u_m\| \rightarrow 0$.*

Proof. Let e_m denote the error function as

$$e_m(x) = u(x) - u_m(x),$$

so from (1) we can write

$$\begin{aligned} D^\alpha e_m(x) &= F\left(x, u(x), \int_0^1 K(x, s)G(s, u(s))ds\right) \\ &\quad - F\left(x, u_m(x), \int_0^1 K(x, s)G(s, u_m(s))ds\right) - E_{\tilde{m}} - Res_m(x). \end{aligned} \quad (27)$$

Using the definitions of the fractional derivative and integral, it is suitable to rewrite (27) in the integral form

$$\begin{aligned} e_m(x) &= I^\alpha \left(F\left(x, u(x), \int_0^1 K(x, s)G(s, u(s))ds\right) \right. \\ &\quad \left. - F\left(x, u_m(x), \int_0^1 K(x, s)G(s, u_m(s))ds\right) \right) - I^\alpha E_{\tilde{m}} - I^\alpha Res_m(x). \end{aligned} \quad (28)$$

It follows from (28) that

$$e_m(x) = \Lambda_1(x) - \Lambda_2(x) - \Lambda_3(x), \quad (29)$$

where

$$\begin{aligned} \Lambda_1(x) &= I^\alpha \left(F\left(x, u(x), \int_0^1 K(x, s)G(s, u(s))ds\right) \right. \\ &\quad \left. - F\left(x, u_m(x), \int_0^1 K(x, s)G(s, u_m(s))ds\right) \right), \end{aligned} \quad (30)$$

$$\Lambda_2(x) = I^\alpha E_{\tilde{m}}, \quad (31)$$

$$\Lambda_3(x) = I^\alpha Res_m(x). \quad (32)$$

We now estimate the three terms one by one. For Λ_1 , we have

$$\begin{aligned} |\Lambda_1(x)| &= \left| \frac{1}{\Gamma(\alpha)} \int_0^x (x-t)^{\alpha-1} \left(F\left(t, u(t), \int_0^1 K(t, s)G(s, u(s))ds\right) \right. \right. \\ &\quad \left. \left. - F\left(t, u_m(t), \int_0^1 K(t, s)G(s, u_m(s))ds\right) \right) dt \right| \\ &\leq \frac{1}{\Gamma(\alpha)} \int_0^x |x-t|^{\alpha-1} \left| \left(F\left(t, u(t), \int_0^1 K(t, s)G(s, u(s))ds\right) \right. \right. \\ &\quad \left. \left. - F\left(t, u_m(t), \int_0^1 K(t, s)G(s, u_m(s))ds\right) \right) \right| dt. \end{aligned} \quad (33)$$

Since $|x-t| \leq 1$ and F and G satisfy the Lipschitz conditions, we obtain

$$|\Lambda_1(x)| = \frac{1}{\Gamma(\alpha)} \int_0^1 (\eta + K_1 \eta \eta_1) |u(t) - u_m(t)| dt. \quad (34)$$

Using $0 \leq t \leq x \leq 1$ leads to

$$|\Lambda_1(x)| = \frac{1}{\Gamma(\alpha)} \int_0^1 (\eta + K_1 \eta \eta_1) |e_m(t)| dt. \quad (35)$$

So, we have

$$\|\Lambda_1\| \leq \frac{1}{\Gamma(\alpha)}(\eta + K_1\eta\eta_1)\|e_m\|. \quad (36)$$

For Λ_2 and Λ_3 , we have

$$\|\Lambda_2\| \leq \frac{1}{\Gamma(\alpha)}\|E_{\tilde{m}}\|, \quad \|\Lambda_3\| \leq \frac{1}{\Gamma(\alpha)}\|Res_m\|. \quad (37)$$

Then,

$$\|e_m\| \leq \frac{1}{\Gamma(\alpha)}(\eta + K_1\eta\eta_1)\|e_m\| + \frac{1}{\Gamma(\alpha)}\|E_{\tilde{m}}\| + \frac{1}{\Gamma(\alpha)}\|Res_m\|. \quad (38)$$

Consequently,

$$\|e_m\| \leq \frac{\|E_{\tilde{m}}\| + \|Res_m\|}{\Gamma(\alpha) - \eta - K_1\eta\eta_1}. \quad (39)$$

If we choose \tilde{m} sufficiently large, then by [24], $E_{\tilde{m}}$ tends to 0. So, if Res_m tends to 0, then $\|e_m\| = \|u - u_m\| \rightarrow 0$. The numerical results reveal that Res_m tends to 0.

6 Numerical Example

In this section, we give a numerical example and apply the technique for solving it.

Example 1. Consider the following nonlinear FFIDE:

$$D^\alpha u(x) = f(x) + \int_0^1 (x+s)^2 u^3(s) ds \quad (40)$$

with the initial conditions $u(0) = u'(0) = 0$, where $f(x) = \frac{6x^{\frac{1}{3}}}{\Gamma(\frac{1}{3})} - \frac{x^2}{7} - \frac{x}{4} - \frac{1}{9}$, and the exact solution is $u(x) = x^2$ when $\alpha = \frac{5}{3}$.

Table 1: The absolute errors with $m = 6$ for Example 1.

x	$\alpha = 1$	$\alpha = \frac{1}{2}$	$\alpha = \frac{1}{3}$	$\alpha = \frac{5}{3}$
0.1	2.96×10^{-4}	5.13×10^{-5}	1.12×10^{-14}	5.54×10^{-5}
0.2	4.73×10^{-4}	8.40×10^{-5}	2.11×10^{-14}	1.25×10^{-3}
0.3	6.61×10^{-4}	1.16×10^{-4}	3.23×10^{-14}	1.25×10^{-3}
0.4	8.60×10^{-4}	1.51×10^{-4}	4.53×10^{-14}	7.17×10^{-4}
0.5	1.07×10^{-3}	1.88×10^{-4}	6.03×10^{-14}	1.68×10^{-4}
0.6	1.28×10^{-3}	2.29×10^{-4}	7.75×10^{-14}	4.72×10^{-4}
0.7	1.53×10^{-3}	2.74×10^{-4}	9.74×10^{-14}	2.16×10^{-3}
0.8	1.82×10^{-3}	3.24×10^{-4}	1.20×10^{-13}	3.37×10^{-3}
0.9	2.15×10^{-3}	3.80×10^{-4}	1.45×10^{-13}	8.49×10^{-4}
1.0	2.46×10^{-3}	4.44×10^{-4}	1.74×10^{-13}	5.70×10^{-3}

Table 1 shows the absolute errors between the exact and approximate solutions $|u(x) - u_m(x)|$ for $m = 6$ and various choices of α .

7 Conclusion

In this paper, we derive a general formulation for the fractional alternative Legendre functions and obtain their operational matrix of fractional integration $F(\nu, \alpha)$. Then, a numerical method based on the FALFs expansions together with this matrix and the collocation method is proposed to obtain the numerical solution of the nonlinear fractional Fredholm integro-differential equations. Several examples are given to demonstrate the validity and applicability of the proposed method for solving the fractional Fredholm integro-differential equations. Some of the advantages of the present approach are summarized as follows. It is shown that only a small value of the fractional alternative Legendre functions is needed to achieve high accuracy and satisfactory results.

References

- [1] K. Al-Khaled and M. Yousef. Sumudu decomposition method for solving higher-order nonlinear Volterra-Fredholm fractional integro-differential equations. *Nonlinear Dynamics and Systems Theory* **19** (3) (2019) 348–361.
- [2] M. Dehghan, J. Manafian and A. Saadatmandi. Solving nonlinear fractional partial differential equations using the homotopy analysis method. *Numer. Methods Partial Differential Equations* **26** (2) (2010) 448–479.
- [3] A. Hamoud and K. Ghadle. Modified Laplace decomposition method for fractional Volterra-Fredholm integro-differential equations. *J. Math. Model.* **6** (1) (2018) 91–104.
- [4] A. Hamoud and K. Ghadle. Some new existence, uniqueness and convergence results for fractional Volterra-Fredholm integro-differential equations. *J. Appl. Comput. Mech.* **5** (1) (2019) 58–69.
- [5] A. Hamoud and K. Ghadle. Existence and uniqueness of solutions for fractional mixed Volterra-Fredholm integro-differential equations. *Indian J. Math.* **60** (3) (2018) 375–395.
- [6] A. Hamoud and K. Ghadle. The approximate solutions of fractional Volterra-Fredholm integro-differential equations by using analytical techniques. *Probl. Anal. Issues Anal.* **7** (25) (2018) 41–58.
- [7] A. Hamoud and K. Ghadle. Existence and uniqueness of the solution for Volterra-Fredholm integro-differential equations, *Journal of Siberian Federal University. Mathematics & Physics* **11** (6) (2018) 692–701.
- [8] A. Hamoud, A. Azeez and K. Ghadle. A study of some iterative methods for solving fuzzy Volterra-Fredholm integral equations. *Indonesian J. Elec. Eng. & Comp. Sci.* **11** (3) (2018) 1228–1235.
- [9] A. Hamoud and K. Ghadle. Usage of the homotopy analysis method for solving fractional Volterra-Fredholm integro-differential equation of the second kind. *Tamkang Journal of Mathematics* **49** (4) (2018) 301–315.
- [10] A. Hamoud, K. Ghadle and P. Pathade. An existence and convergence results for Caputo fractional Volterra integro-differential equations. *Jordan Journal of Mathematics and Statistics* **12** (3) (2019) 307–327.
- [11] A. Hamoud, K. Hussain, N. Mohammed and K. Ghadle. Solving Fredholm integro-differential equations by using numerical techniques. *Nonlinear Functional Analysis and Applications* **24** (3) (2019) 533–542.
- [12] A. Hamoud, N. Mohammed and K. Ghadle. A study of some effective techniques for solving Volterra-Fredholm integral equations. *Dynamics of Continuous, Discrete and Impulsive Systems Series A: Mathematical Analysis* **26** (2019) 389–406.

- [13] A. Hamoud, K. Ghadle and S. Atshan. The approximate solutions of fractional integro-differential equations by using modified Adomian decomposition method. *Advances in Operator Theory* **5** (2019) 21–39.
- [14] K. Hussain, A. Hamoud and N. Mohammed. Some new uniqueness results for fractional integro-differential equations. *Nonlinear Functional Analysis and Applications* **24** (4) (2019) 827–836.
- [15] M. Heydari, M. Hooshmandasl, F. Mohammadi and C. Cattani. Wavelets method for solving systems of nonlinear singular fractional Volterra integro-differential equations. *Commun. Nonl. Sci. Numer. Simulat.* **19** (2014) 37–48.
- [16] I. Horng and J. Chou. Shifted Chebyshev direct method for solving variational problems. *Int. J. Sys. Sci.* **16** (1985) 855–861.
- [17] Y. Jalilian and M. Ghasemi. On the solutions of a nonlinear fractional integro-differential equation of pantograph type. *Mediterr. J. Math.* **14** (2017).
- [18] M. Khader and N. Sweilam. On the approximate solutions for system of fractional integro-differential equations using Chebyshev pseudo-spectral method. *Appl. Math. Model.* **37** (2013) 9819–9828.
- [19] M. Lakestani, B. Nemati Saray and M. Dehghan. Numerical solution for the weakly singular Fredholm integro-differential equations using Legendre multi wavelets. *J. Comput. Appl. Math.* **235** (11) (2011) 3291–3303.
- [20] K. Maleknejad, K. Nouri and L. Torkzadeh. Operational matrix of fractional integration based on the shifted second kind Chebyshev polynomials for solving fractional differential equations. *Mediterr. J. Math.* **13** (3) (2016) 1377–1390.
- [21] R. Mittal and R. Nigam. Solution of fractional integro-differential equations by Adomian decomposition method. *Int. J. Appl. Math. Mech.* **4** (2008) 87–94.
- [22] P. Pathade, K. Ghadle and A. Hamoud. Optimal solution solved by triangular intuitionistic fuzzy transportation problem. *Advances in Intelligent Systems and Computing* **1025** (2020) 379–385.
- [23] A. Saadatmandi and M. Dehghan. A Legendre collocation method for fractional integro-differential equations. *J. Vib. Control* **17** (13) (2011) 2050–2058.
- [24] H. Saeedi and M. Mohseni Moghadam. Numerical solution of nonlinear Volterra integro-differential equations of arbitrary order by CAS wavelets. *Commun. Nonl. Sci. Numer. Simul.* **16** (2011) 1216–1226.



On the Boundedness of a Novel Four-Dimensional Hyperchaotic System

S. Rezzag*

*Department of Mathematics and Informatics,
University of Larbi Ben M'hidi, 04000, Oum-El-Bouaghi, Algeria*

Received: June 24, 2019; Revised: January 10, 2020

Abstract: To estimate the ultimate bound and positively invariant set for a dynamical system is an important but quite challenging task in general. This paper attempts to investigate the bounds of a novel four-dimensional hyperchaotic system using a technique combining the generalized Lyapunov function theory and the Lagrange multiplier method. Finally, a numerical example is provided to illustrate the main result.

Keywords: *4D hyperchaotic system; boundedness of solutions; Lyapunov stability; Lagrange multiplier method.*

Mathematics Subject Classification (2010): 65P20, 65P30, 65P40.

1 Introduction

Hyperchaos characterized by more than one positive Lyapunov exponent has attracted an increasing attention of various scientific and engineering communities. It is very important to generate hyperchaos with more complicated dynamics as a model for theoretical research and practical implication. Hyperchaos was firstly reported by Rossler [18] in 1979, and the first circuit implementation of hyperchaos was realized by Matsumoto et al. [10]. Since then, some other hyperchaos generators have also been found. Typical examples are the hyperchaotic Lorenz-Haken system [11], hyperchaotic Chua's circuit [6], hyperchaotic modified Chua's circuit [20], these examples in themselves indicate that hyperchaos has a broad range of applications in such fields as nonlinear circuit [2], secure communications [21], lasers [22], neural network [1], control [4], synchronization [5] and so on. In fact, the study of hyperchaos has recently become a central topic of the research in nonlinear sciences.

* Corresponding author: <mailto:rezzag.samia@gmail.com>

In particular, the ultimate boundedness is very important for the study of the qualitative behavior of a chaotic system. If one can show that a chaotic or a hyperchaotic system under consideration has a globally attractive set, one knows that the system cannot have the equilibrium points, periodic or quasi-periodic solutions, or other chaotic or hyperchaotic attractors existing outside the attractive set. This greatly simplifies the analysis of dynamics of a chaotic or hyperchaotic system [9]. The boundedness of a chaotic system also plays an important role in chaos control and chaos synchronization.

Such an estimation is quite difficult to achieve technically, however, several works on this topic were realized for some 3D and 4D dynamical systems [3], [7], [8], [12], [13], [14], [15], [16], [17], [19], [23], [25].

Furthermore, there are no unified methods for constructing the Lyapunov functions to study the boundedness of the chaotic systems. Therefore, it is necessary to study the boundedness of the hyperchaotic systems.

In the present paper, we study the bounds of solutions of a new of hyperchaotic system based on a technique combining the generalized Lyapunov function theory and optimization. The paper is organized as follows : the problem formulation and main result are presented in Section 2. A numerical example is given in Section 3 to illustrate the main result. Finally, conclusion is made in Section 4.

2 Problem Formulation and Main Result

A novel four-dimensional hyperchaotic system with four nonlinearity terms presented in [24] by Wenjuan, Zengqiang and Zhuzhi can be described by the following system:

$$\begin{cases} x' = ay - ax + eyz - kw, \\ y' = cx - xz - dy, \\ z' = xy - bz, \\ w' = ry + fz, \end{cases} \quad (1)$$

where a, b, c, d, e, f, k and r are all real constant parameters. For the chosen $a = 56$, $b = 16$, $c = 49$, $d = 9$, $k = 8$, $e = 30$, $f = 40$ and $r = 48$ system (1) exhibits complex hyperchaotic dynamical behaviors. The corresponding three-dimensional phase diagrams in $(x - y - w)$, $(y - z - w)$ spaces are shown in Figure 1.

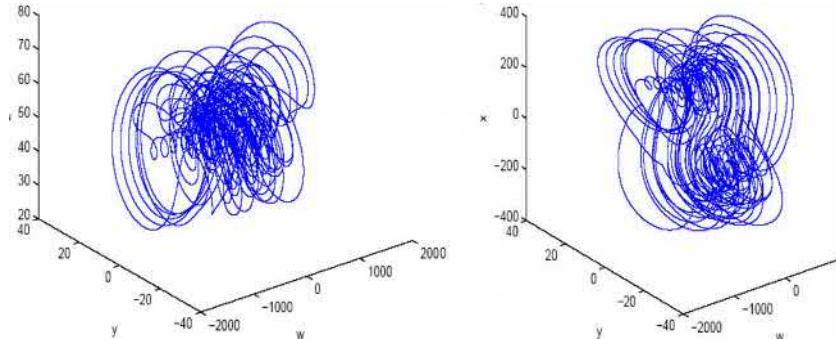


Fig. 1. Phase portrait of the system (1) in the $x - y - z$ space with parameters $\alpha = 5$, $\beta = 0.7$, $\gamma = 26$.

Some basic dynamical properties of the novel four-dimensional hyperchaotic system (1) were studied in [24]. But many properties of the system (1) remain to be uncovered. In the following, we will discuss the boundedness of the novel hyperchaotic system (1).

Lemma 2.1 Define a set

$$\Gamma = \left\{ (y, z) / \frac{y^2}{b^2} + \frac{(z - c)^2}{c^2} = 1, b > 0, c > 0 \right\} \quad (2)$$

and $G = y^2 + z^2$, $H = y^2 + (z - 2c)^2$, $(y, z) \in \Gamma$. Then we have

$$\max_{(y,z) \in \Gamma} G = \max_{(xy,z) \in \Gamma} H = \begin{cases} \frac{b^4}{b^2 - c^2}, & b \geq \sqrt{2}c, \\ 4c^2, & b < \sqrt{2}c. \end{cases} \quad (3)$$

Proof. It can be easily calculated by the Lagrange multiplier method.

Theorem 2.1 When $a > 0$, $b > 0$, $c > 0$, $d > 0$, $k > 0$, $e > 0$, $f > 0$, $r > 0$, the following set defined by

$$\Omega = \left\{ (x, y, z, w) / y^2 + (z - c)^2 \leq R^2, (ax + kw)^2 \leq \left(\frac{aB + kA}{a}\right)^2 \right\} \quad (2)$$

is the bound for system (1), where

$$R^2 = \begin{cases} \frac{b^2 c^2}{4d(b-d)}, & \text{if } b \geq 2d, \\ c^2, & \text{if } b < 2d, \end{cases} \quad (3)$$

$$A = R[r + f(R + c)], B = aR + eR(R + c). \quad (4)$$

Proof. Define the following Lyapunov function

$$V_1(y, z) = y^2 + (z - c)^2. \quad (5)$$

Then, its time derivative along the orbits of system (1) is

$$\begin{aligned} \dot{V}_1 &= 2yy' + 2(z - c)z' \\ &= -2dy^2 - 2bz^2 + 2cbz \\ &= -2dy^2 - 2b\left(z - \frac{c}{2}\right)^2 + \frac{bc^2}{2}. \end{aligned} \quad (6)$$

That is to say, for $a > 0$, $b > 0$, $c > 0$, $d > 0$, $k > 0$, $e > 0$, $f > 0$, $r > 0$, the equation $\dot{V}_1 = 0$ holds, that means the surface

$$\Gamma = \left\{ (y, z) / \frac{y^2}{bc^2} + \frac{\left(z - \frac{c}{2}\right)^2}{\frac{4d}{4}} = 1 \right\} \quad (7)$$

is an ellipsoid in $2D$ space for certain values of a , b , c , d , k , e , f and r . Outside Γ , we have $\dot{V}_1 < 0$, while inside Γ , we have $\dot{V}_1 > 0$. Since the function $V_1 = y^2 + (z - c)^2$ is

continuous on the closed set Γ , V_1 can reach its maximum on the surface Γ . Denote the maximum value of V as R^2 , that is, $R^2 = \max_{(y,z) \in \Gamma} V_1(y,z)$.

By Lemma 1, we can easily get

$$V_1(y, z) \leq R^2 = \begin{cases} \frac{b^2 c^2}{4d(b-d)}, & \text{if } b \geq 2d, \\ c^2, & \text{if } b < 2d. \end{cases} \quad (8)$$

From the formula (8), we obtain

$$|y| \leq R, |z| \leq R + c. \quad (9)$$

At the same time, the first equation of formula (1) and (9) yield

$$\begin{aligned} x' &= ay - ax + eyz - kw \\ &\leq a|y| + e|y||z| - ax - kw \\ &\leq aR + eR(R+c) - ax - kw \\ &= B - ax - kw, \end{aligned}$$

where

$$B = aR + eR(R+c).$$

Also, the fourth equation of formula (1) and (9) yield

$$\begin{aligned} w' &= ry + fyz \leq r|y| + f|y||z| \\ &\leq rR + fR(R+c) = A. \end{aligned}$$

Let

$$V_2 = ax + kw.$$

Then

$$V'_2 = ax' + kw' \leq aB + kA - aV_2. \quad (10)$$

Integrating both sides of formula (10), we have

$$V_2(t) \leq \frac{aB + kA}{a} + \left(V_2(t_0) - \frac{aB + kA}{a} \right) e^{-a(t-t_0)}. \quad (11)$$

So, we get

$$\lim_{t \rightarrow +\infty} V_2(t) \leq \frac{aB + kA}{a}. \quad (12)$$

That is to say, the inequality $(ax + kw)^2 \leq \left(\frac{aB + kA}{a}\right)^2$ holds as $t \rightarrow +\infty$. Therefore, we have the conclusion that

$$\Omega = \left\{ (x, y, z, w) / y^2 + (z - c)^2 \leq R^2, (ax + kw)^2 \leq \left(\frac{aB + kA}{a}\right)^2 \right\} \quad (13)$$

is the bound for the hyperchaotic systems (1). This completes the proof.

3 Example

Consider the system (1), when $a = 56$, $b = 16$, $c = 49$, $d = 9$, $k = 8$, $e = 30$, $f = 40$ and $r = 48$, we have

$$\Omega = \left\{ (x, y, z, w) / y^2 + (z - 49)^2 \leq 49^2, (56x + 8w)^2 \leq \left(\frac{56B + 8A}{56} \right)^2 \right\}$$

is the bound for the hyperchaotic system (1).

Consequently, we have

$$\begin{cases} (56x + 8w)^2 \leq 174580^2, \\ |y| \leq 49, \\ 0 \leq z \leq 98. \end{cases}$$

It is obvious that the orbits of system (1) locate in the section where $z \geq 0$.

4 Conclusion

In this paper, we have investigated the boundedness for a novel four-dimensional hyperchaotic system using a combination of the Lyapunov stability theory with optimization. Finally, a numerical example is provided to illustrate the main result.

References

- [1] P. Arena, S. Baglio, L. Fortuna and G. Manganaro. Hyperchaos from cellular networks. *Electron. Lett.* **31** (1995) 250–251.
- [2] A. Cenys, A. Tamasesvicius, A. Baziliauskas, R. Krivickas and E. Lindberg. Hyperchaos in coupled Colpitts oscillators. *Chaos, Solitons & Fract.* **17** (2-3) (2003) 349–353.
- [3] Z. Elhadj and J. C. Sprott. About the boundedness of 3D continuous time quadratic systems. *Nonlinear Oscil.* **13** (2-3) (2010) 515–521.
- [4] J. Y. Hsieh, C. C. Hwang, A. P. Li and W. J. Li. Controlling hyper-chaos of the Rossler system. *Int. J. Control.* **72** (1999) 882–886.
- [5] P. Q. Jiang, B. H. Wang, S. L. Bu, Q. H. Xia and X. S. Luo. Hyperchaotic synchronization in deterministic small-world dynamical networks. *Int. J. Modern Phys. B* **18** (2004) 2674–2679.
- [6] T. Kapitaniak and L. O. Chua. Hyper-chaotic attractor of unidirectionally-coupled Chua's circuit. *Int. J. Bifurcation Chaos* **4** (1994) 477–482.
- [7] D. Li, J. A. Lu, X. Wu and G. Chen. Estimating the bounds for the Lorenz family of chaotic systems. *Chaos, Solitons & Fract.* **23** (2005) 529–534.
- [8] D. Li, X. Wu and J. Lu. Estimating the ultimating bound and positively invariant set for the hyperchaotic Lorenz-Haken system. *Chaos, Solitons & Fract.* **39** (2009) 1290–1296.
- [9] X. Liao, Y. Fu, S. Xie and P. Yu. Globally exponentially attractive sets of the family of Lorenz systems. *Sci. China, Ser. F* **51** (2008) 283–292.
- [10] T. Matsumoto, L. O. Chua and K. Kobayashi. Hyperchaos: laboratory experiment and numerical confirmation. *IEEE Trans. Circ. Syst.* **33** (1986) 1143–1147.
- [11] C. Z. Ning and H. Haken. Detuned lasers and the complex Lorenz equations: subcritical and super-critical Hopf bifurcations. *Phys. Rev. A* **41** (1990) 3826–3837.

- [12] A. Y. Pogromsky, G. Santoboni and H. Nijmeijer. An ultimate bound on the trajectories of the Lorenz systems and its applications. *Non-linearity* **16** (2003) 1597–1605.
- [13] S. Rezzag. Solution bounds of the hyper-chaotic Rabinovich system. *Nonlinear studies* **24**(4) (2017) 903–909.
- [14] S. Rezzag. Boundedness of the new modified hyperchaotic Pan System. *Nonlinear Dyn. Syst. Theory* **17** (3) (2017) 402–408.
- [15] S. Rezzag, O. Zehrour and A. Aliouche. Estimating the bounds for the general 4-D hyper-chaotic system. *Nonlinear studies* **22** (1) (2015) 41–48.
- [16] S. Rezzag, O. Zehrour and A. Aliouche. Estimating the Bounds for the General 4-D Continuous-Time Autonomous System. *Nonlinear Dyn. Syst. Theory* **15** (3) (2015) 313–320.
- [17] S. Rezzag. Boundedness Results for a New Hyperchaotic System and Their Application in Chaos Synchronization. *Nonlinear Dyn. Syst. Theory* **18** (4) (2018) 409–417.
- [18] O. E. Rossler. An equation for hyperchaos. *Phys. Lett. A* **71** (1979) 155–157.
- [19] Y. J. Sun. Solution bounds of generalized Lorenz chaotic system. *Chaos, Solitons & Fract.* **40** (2009) 691–696.
- [20] K. Thamilmaran, M. Lakshmanan and A. Venkatesan. Hyperchaos in a modified Canonical Chua’s circuit. *Int. J. Bifurcation Chaos* **14** (2004) 221–243.
- [21] V. S. Udal’tsov, J. P. Goedgebuer, L. Larger, J. B. Cuenot, P. Levy, J. B. Cuenot, P. Levy and W. T. Rhodes. Communicating with hyperchaos: the dynamics of a DNLFemitter and recovery of transmitted information. *Opt. Spectrosc.* **95** (2003) 114–118.
- [22] R. Vicente, J. Dauden, P. Colet and R. Toral. Analysis and characterization of thehyperchaos generated by a semiconductor laser subject to delayed feedbackloop. *IEEE J. Quantum Electron.* **41** (2005) 541–548.
- [23] P. Wang, D. Li and Q. Hu. Bounds of the hyper-chaotic Lorenz-Stenflo system. *Commun. Nonlinear Sci. Numer. Simul.* **15** (2010) 2514–2520.
- [24] W. Wenjuan, C. Zengqiang and Y. Zhuzhi. The evolution of a novel four-dimensional autonomous system: Among 3-torus, limit cycle, 2-torus, chaos and hyperchaos. *Chaos, Solitons & Fract.* **39** (2009) 2340–2356.
- [25] F. Zhang, Y. Li and C. Mu. Bounds of Solutions of a Kind of Hyper-Chaotic Systems and Application. *Journal of Mathematical Research with Applications* **33** (3) (2013) 345–352.



Periodic Solutions in Non-Homogeneous Hill Equation

A. Rodriguez * and J. Collado

*Automatic Control Department, CINVESTAV-IPN,
Av. IPN 2508, ZACATENCO, Mexico City, 07360, Mexico.*

Received: December 15, 2017; Revised: January 13, 2020

Abstract: Properties of T and $2T$ periodic solutions in the homogeneous Hill equation have been entirely determined, but there is hardly any information about the existence of periodic solutions with different period. In this work, kT periodic solutions in the Hill equation will be explicitly characterized, here k is a natural number. Moreover, it will be shown that those kT periodic solutions become unstable when the system is forced with a function having the same period (or an integer multiple of it) of any of those solutions. As a consequence, two types of instability will be presented for the first time on the Ince-Strutt diagram: the well-known parametric resonance and the linear resonance due to the forcing signal.

Keywords: *non-homogeneous Hill equation; kT -periodic solutions; linear and parametric resonance; Ince-Strutt diagram; Floquet multipliers.*

Mathematics Subject Classification (2010): 34C25, 11J20.

1 Introduction

1.1 Hill equation

The general class of homogeneous second order linear differential equations with real periodic coefficients can be characterized by the Hill equation (1), it describes dynamical systems with intrinsic periodicity and parametric behaviour such as the modulation of radio carrier waves, transverse vibrations of a tense elastic member, the stability of a periodic motion in a non-linear system (linearization in a neighbourhood of a periodic motion) and the focus and defocus of particle beams in particle accelerators. Also, this equation can be seen as a particular case of the Schrödinger equation with periodic potential.

* Corresponding author: <mailto:a.rodriguezm@ctrl.cinvestav.mx>

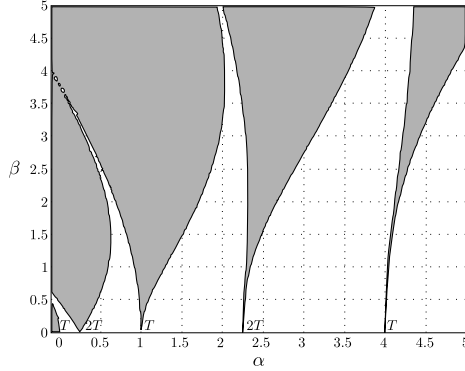


Figure 1: Stability-chart of the Mathieu equation: $\ddot{x} + [\alpha + \beta \cos(t)] x = 0$.

The Hill equation name arose after the transcendent publication "of the memoir on the motion of the lunar perigee" by G. W. Hill [1], in which he established the mathematical foundations of the stability theory of parametric systems.

The Hill equation is denoted by

$$\ddot{x} + [\alpha + \beta f(t)]x = 0, \quad f(t) = f(t + T), \quad \int_0^T f(t)dt = 0, \quad (1)$$

where α and β are two independent parameters. $\sqrt{\alpha}$ is the natural frequency of the system of free oscillation in the absence of excitation, β is the amplitude of the parametric excitation (in most cases it is small). $T > 0$ is the minimum period.

There are two particular forms of equation (1): the Mathieu equation [2]

$$\ddot{x} + [\alpha + \beta \cos(\omega t)]x = 0, \quad (2)$$

when the function $f(t)$ is purely sinusoidal and the Meissner equation, in its implest form: $\ddot{x} + [\alpha + \beta \operatorname{sgn}(\cos(t))]x$.

Stability of the solutions in the Hill equation can be seen in a two-parameter bifurcation chart known as the Ince-Strutt diagram [3], see Fig. 1. The white areas represent the values of parameters at which the solution is stable and the gray regions are the Arnold tongues or parametric resonance tongues [4], they depict unstable solutions.

Equation (2) admits at least one non-trivial periodic solution on the tongue boundaries. The tongues that born at $\alpha = n^2, \beta = 0$, for $n = 1, 2, \dots$, have one T -periodic solution, and the instability that occurs upon crossing such a tongue boundary is referred to as a harmonic instability. The other boundaries whose tongues arise at $\alpha = (2n + 1)^2/4$ have one $2T$ -periodic solution, see Fig. 1.

1.2 Parametric and linear resonance

Parametric resonance is a topic well studied and inherent to the homogeneous Hill equation. However, as we will see later, linear resonance can also be linked to the Hill type systems.

With a few exceptions, [5–8], the forced Hill equation has not been widely studied in the literature; in this work the kT -periodically forced system will be analysed, with $k \in \mathbb{Z}_+ \setminus \{1, 2\}$.

Parametric excitation of a system differs from direct forcing in that the fluctuations appear as a temporal modulation (usually periodic) of a parameter rather than as a direct additive term. The time dependence is explicit, which implies an external energy source and the possibility of unstable behaviour known as parametric resonance which is dependent upon the frequency of the parameter variation and the natural frequency of the system.

The rate of increase in amplitude of the response of a linear system with parametric resonance is exponential [9], whereas the typical resonance is characterized by a linear growth rate. Examples of parametric and linear resonance can be found in [10] and [11] respectively.

Through the Ince-Strutt diagram, only T or $2T$ -periodic solutions appear, however the system (1) admits other kT -periodic solutions ($k \in \mathbb{Z}_+ \setminus \{1, 2\}$), as it was specified in [12].

Such kT -periodic solutions come out as very slim lines on the stable zones in the stability diagram. The lines become unstable if the system (1) is forced by a periodic function containing at least one spectral line in its Fourier series with the same period as any of these kT -periodic lines, see Figures 5a and 5b. Further details will be provided in Section 3.

Even though, the existence of periodic solutions inside the stable regions was already known, the first one in obtaining (numerically) the values of parameters α, β for which these periodic solutions arise was Jazar [13], he called them splitting lines. However, in this text they will be termed as *resonance lines* for the reasons that will be clear later.

It is important to highlight that before this work, the above-mentioned kT -periodic solutions were not studied in the context of stability for the Hill equation.

So far, we have only remarked the properties of the homogeneous Hill equation. Nevertheless, the study of the forced equation (3) also leads to interesting features.

$$\ddot{x} + \delta \dot{x} + [\alpha + \beta f(t)] x = g(t), \quad g(t) = g(t + T), \quad \int_0^T g(t) dt = 0, \quad (3)$$

Few studies have been developed around the non-homogeneous case, among them, one can find the results of Slane and Tragesser [8] who modified the Floquet theory so as to analytically examine the transitory and steady-state behaviour of a non-autonomous inhomogeneous system, but only for $g(t+T) = g(t)$. Younesian et al. [7] used the strained parameter technique to seek the asymptotic periodic solutions in the forced Mathieu equation, Shadman and Mehri [5] worked with fixed point theorems to investigate the existence of periodic solutions of the non-homogeneous Hill equation, Kwong and Wong [6] applied the Floquet theory to prove the conjecture that all solutions of a second order forced linear differential equation of Hill type are oscillatory on $[0, \infty)$. In addition, the damped forcing Hill equation can be obtained, after some light modifications, from the more general equation analyzed in [14].

Notice that in these previous contributions no damping effect was examined. Herein, the stability of a specific type of the non-homogeneous Hill equation with a linear dissipative term (δ) will be studied.

Finally, the results will be illustrated through the forced Kapitza pendulum which motivates the work. The behaviour of the pendulum is illustrated by numerical simulations for some specific values of α, β and δ .

2 Preliminaries

2.1 Floquet theory

A state-space representation of (1) is

$$\dot{x} = A(t)x \quad x \in \mathbb{R}^2 \quad \text{and} \quad A(t) = A(t+T) \in \mathbb{R}^{2 \times 2}, \quad (4)$$

where $A(t)$ is a piecewise continuous matrix and T is the fundamental period.

For any initial condition, the general solutions of (4) can be written in terms of the state-transition matrix $\Phi(t, t_0)$, with $\Phi(t_0, t_0) = I_2$. Thus,

$$x(t) = \Phi(t, t_0)x(t_0). \quad (5)$$

The state-transition matrix evaluated at the end of a period, $M = \Phi(T + t_0, t_0)$, is known as *monodromy matrix*. Its eigenvalues, known as the *Floquet multipliers* or *characteristic multipliers*, determine the stability of the system (1), see [12] and [15]. They are independent of t_0 [16], then it is possible and convenient to write $M = \Phi(T, 0)$.

Theorem 2.1 (Floquet [15]) *The state-transition matrix $\Phi(t, t_0)$ of the system (4) can be written as the product of two $n \times n$ -matrices,*

$$\Phi(t, 0) = P(t)e^{Rt}, \quad (6)$$

where $P(t)$ is a T -periodic $n \times n$ -matrix function and $R = \ln[\Phi(T)]/T$ is a constant $n \times n$ -matrix, not necessarily real [17].

Any solution $x(t)$ of (4) can be expressed as $x(t) = \Phi(t, 0)x(0)$. Then, for all $t \geq 0$, $t = kT + \tau$, $k \in \mathbb{Z}_+ \triangleq \{m \in \mathbb{Z} : m \geq 0\}$ and $\tau \in [0, T]$,

$$\begin{aligned} x(t) &= \Phi(kT + \tau, kT)\Phi(kT, (k-1)T) \cdot \Phi((k-1)T, (k-2)T) \dots \Phi(T, 0)x(0) \\ &= \Phi(kT + \tau, kT)M^kx(0), \end{aligned} \quad (7)$$

it follows that the boundedness of $\|x(t)\|$ depends exclusively on the boundedness of M^k .

In other words, let $x(0)$ be the bounded initial conditions and $\sigma(M) = \{\lambda_1, \lambda_2, \dots, \lambda_n\}$ are the spectrum of M (the set of all its eigenvalues), then

1. $x(t) \rightarrow 0 \Leftrightarrow \sigma(M) \subset \mathring{D}_1 \triangleq \{z \in \mathbb{C} : |z| < 1\}$.
2. $x(t)$ is bounded $\Leftrightarrow \sigma(M) \subset \bar{D}_1$ and $\forall \lambda \subset \partial D_1$ being simple roots of the minimal polynomial of M . ∂D_1 is the boundary of the set D_1 .
3. $x(t) \rightarrow \infty \Leftrightarrow \exists \lambda \in \sigma(M) : |\lambda| > 1$ or $\sigma(M) \subset \bar{D}_1 \& \exists |\lambda| = 1$: is a multiple root of the minimal polynomial of M .

An equivalent stability analysis can be carried out using the eigenvalues of matrix R in (6) known as the *Floquet characteristic exponents* and defined by $\mu = \ln(\lambda)/T$. In this version the position of the eigenvalues about the imaginary axis is examined. The imaginary parts of the characteristic exponents are not determined uniquely, we can add $2\pi i/T$ to each of them [15]. Nevertheless, the real part is unique.

2.2 Symplectic and ε -symplectic matrices

Definition 2.1 ([18]) The matrix $Q \in \mathbb{R}^{2n \times 2n}$, $n \in \mathbb{N}$, is said to be symplectic if

$$Q^\top J Q = J, \quad J \triangleq \begin{bmatrix} \mathbf{0} & I_n \\ -I_n & \mathbf{0} \end{bmatrix}, \quad J^\top = -J = J^{-1}. \quad (8)$$

Theorem 2.2 Let $Q \in \mathbb{R}^{2n \times 2n}$ be a symplectic matrix, then it follows that

$$\lambda \in \sigma(Q) \Rightarrow \frac{1}{\lambda} \in \sigma(Q) \quad \text{and} \quad \bar{\lambda} \in \sigma(Q) \Rightarrow \frac{1}{\bar{\lambda}} \in \sigma(Q). \quad (9)$$

In words, the eigenvalues of Q are symmetric with respect to the unit circle.

Lemma 2.1 A matrix $Q \in \mathbb{R}^{2 \times 2}$ is symplectic if and only if its determinant is 1.

Definition 2.2 A matrix $Q \in \mathbb{R}^{2n \times 2n}$ is called symplectic with a multiplier ε (or ε -symplectic) if

$$Q^\top J Q = \varepsilon J, \quad \varepsilon > 0. \quad (10)$$

Lemma 2.2 For $\varepsilon > 0$, $Q \in \mathbb{R}^{2 \times 2}$ is ε -symplectic if and only if $\det[Q] = \varepsilon$.

The eigenvalues of a ε -symplectic matrix $Q \in \mathbb{R}^{2n \times 2n}$ are symmetric with respect to the circle of radius $\sqrt[2n]{\varepsilon}$.

3 Stability Analysis

3.1 Unstable periodic solutions in the non-homogeneous Hill equation

According to the Floquet theory, the state-transition matrix satisfies $\Phi(t + T) = \Phi(t)\Phi(T)$. Therefore, for every solution $x(t)$ of (1) with the initial condition $x(0) = v$ (v is an eigenvector of $\Phi(T)$ associated to λ), the relation $x(t + T) = \lambda x(t)$ holds. By iteration

$$\begin{aligned} x(t + T) &= \lambda x(t), \\ x(t + 2T) &= \lambda^2 x(t), \\ &\vdots \\ x(t + kT) &= \lambda^k x(t). \end{aligned} \quad (11)$$

It is easy to see that the kT -periodic solutions are obtained when $\lambda^k = 1$.

Then, from the last element of (11) and using the Euler formula,

$$x(t + kT) = \lambda^k x(t) = r^k e^{jk\theta} x(t). \quad (12)$$

Recalling that there are coordinates in which the Hill equation is Hamiltonian [15] and the state-transition matrix of a linear Hamiltonian system is symplectic [18], it follows that $r^k = 1$ provided that $\lambda^k \equiv 1$ for any $k \in \mathbb{N}$.

Then $|e^{jk\theta}| = |\cos(k\theta) + j \sin(k\theta)| = 1$ and it is true when $k\theta = \pm 2n\pi$ ($n \in \mathbb{Z}$), hence

$$\theta = \pm \frac{2\pi}{k}, \quad (13)$$

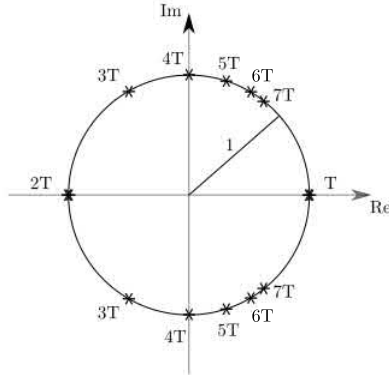


Figure 2: The unit circle shows the eigenvalues' positions for several kT -periodic solutions corresponding to the curves shown on the Ince-Strutt diagram of the forced Mathieu equation.

n is neglected because it only represents full rotations, i.e. spins of 2π radians. *The angle condition* (13) determines for certain values of α and β , the kT -periodic solutions (see Fig. 2). Thereby, the values of λ associated to the kT -periodic solutions are concluded as follows

$$\begin{aligned}
 k = 1, \theta = 2\pi &\Rightarrow \lambda_{1,2} = \{1, 1\}, \\
 k = 2, \theta = \pi &\Rightarrow \lambda_{1,2} = \{-1, -1\}, \\
 k = 3, \theta = \frac{2\pi}{3} &\Rightarrow \lambda_{1,2} = \left\{ -\frac{1}{2} \pm j\frac{\sqrt{3}}{2} \right\}, \\
 k = 4, \theta = \frac{\pi}{2} &\Rightarrow \lambda_{1,2} = \{j, -j\}. \\
 &\vdots
 \end{aligned}$$

Remark 3.1 As k is increased, the kT -periodic solutions come close to the T -periodic solutions. This can be appreciated principally in Fig. 2, but also in Fig. 5.

Now, consider the non-homogeneous Mathieu equation

$$\ddot{x} + [\alpha + \beta \cos(\omega_0 t)] x = \sum_{i=1}^r \gamma_i \cos(\omega_i t), \quad \omega_i = 2\pi/T_i, \quad (14)$$

$T_i = 2\pi/\omega_i$, $T_0 \triangleq T$ and ω_i are the frequencies of the forcing component.

The systems represented by (14) exhibit typical resonance in the same sense as the linear constant parameter systems.

Proposition 3.1 *Linear resonance in the system (14) will arise when any forcing term in the summation satisfies $T_i = k_i T_0$ for some $k_i \in \mathbb{Z}_+$.*

The condition (13) and the relation $k_i = \omega_0/\omega_i$ allow to deduce

$$\theta_i = 2\pi \frac{\omega_i}{\omega_0}, \quad (15)$$

which establishes the T_i -periodic curves for the non-homogeneous system.

Two very important considerations arise from the previous analysis. First, the non-homogeneous Hill equation has two sources of instability: a) the parametric resonance which arises regardless of whether or not there is an input, and b) the linear resonance that appears when condition (15) is satisfied and, the parameters (α_0, β_0) must be such that they generate solutions of period T_i . Secondly, for every system, equivalently for every stable point (α, β) on the Ince-Strutt diagram, there is *only one* frequency for the system to come into resonance.

Notice that the parametric resonance appears when the system is evaluated at some coordinate (α, β) on the dark regions of the stability diagram. The growth rate of the response of a system that undergoes parametric resonance is exponential unlike the linear resonance.

If the forcing signal has a T_0 -periodic term, the boundaries corresponding to the T -periodic Arnold tongues become unstable [8]. Similarly, $2T_0$ -periodic terms make the boundaries of the $2T$ -periodic Arnold tongues unstable.

3.2 Non-homogeneous Mathieu equation with damping term

In this section, the dissipative effect on the inhomogeneous Mathieu equation is evaluated.

Consider the forced Mathieu equation and its state-space representation

$$\ddot{x} + \delta \dot{x} + [\alpha + \beta \cos(\omega_0 t)] x = \sum_{i=1}^r \gamma_i \cos(\omega_i t), \quad \delta > 0, \quad (16)$$

$$\begin{bmatrix} \dot{x}_1 \\ \dot{x}_2 \end{bmatrix} = \begin{bmatrix} 0 & 1 \\ -[\alpha + \beta \cos(t)] & -\delta \end{bmatrix} \begin{bmatrix} x_1 \\ x_2 \end{bmatrix} + \begin{bmatrix} 0 \\ 1 \end{bmatrix} \sum_{i=1}^r \gamma_i \cos(\omega_i t). \quad (17)$$

The results achieved in [8] suggest that the behaviour of the non-homogeneous Mathieu equation is practically the same as the homogeneous version, except when the characteristic multipliers equal to 1 are simple roots of the minimal polynomial of M . This justifies that the analysis is focused on system

$$\dot{x}_h = A(t)x_h, \quad A(t) = \begin{bmatrix} 0 & 1 \\ -\alpha - \beta \cos(t) & -\delta \end{bmatrix} \quad (18)$$

whose monodromy matrix is

$$M = M(T) = \begin{bmatrix} X_{1h}(T) & X_{2h}(T) \\ \dot{X}_{1h}(T) & \dot{X}_{2h}(T) \end{bmatrix}, \quad M(0) = \begin{bmatrix} 1 & 0 \\ 0 & 1 \end{bmatrix}. \quad (19)$$

Using the *Jacobi-Liouville* formula [15], $\det[M(T)] = \det[M(0)]e^{\int_0^T \text{tr}[A(u)]du}$, we get

$$\det[M(T)] = e^{-\delta T} < 1, \quad \delta > 0,$$

since $\det[M(0)] = 1$ and $\text{tr}[A(t)] = -\delta$.

To estimate the Floquet multipliers and determine the stability of (18) we compute $P_M(\lambda) = \lambda^2 - \text{tr}(M)\lambda + \det[M] = \lambda^2 - [X_{1h}(T) + \dot{X}_{2h}(T)]\lambda + e^{-\delta T}$, the characteristic polynomial of M .

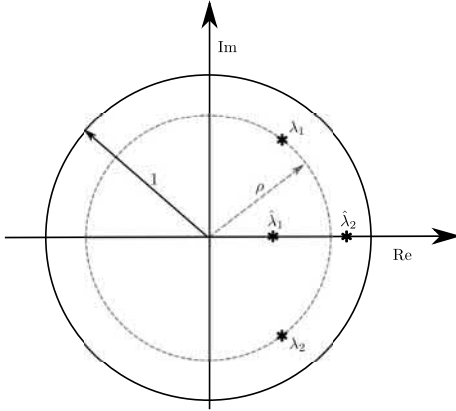


Figure 3: Eigenvalues of the ρ^1 -monodromy matrix on the circle of radius ρ (inside the unitary circle), when they are complex $\{\lambda_1, \lambda_2\}$ or on real-axis when they are real $\{\bar{\lambda}_1, \bar{\lambda}_2\}$.

Proposition 3.2 Let $0 < \rho < 1$, then the monodromy matrix $M \in \mathbb{R}^{2 \times 2}$ is ρ^2 -symplectic $\Leftrightarrow \det[M] = \rho^2$.

Remark 3.2 All the complex eigenvalues of $M \in \mathbb{R}^{2 \times 2}$ are on the circle of radius ρ .

Proof. If $\lambda_1 \in \mathbb{C} \Rightarrow \lambda_2 = \bar{\lambda}_1$, thus $\lambda_1 \bar{\lambda}_1 = \|\lambda_1\|^2 = \rho^2 \Rightarrow \|\lambda_1\| = \rho$.

From previous analysis and Fig. 3, we can see that the characteristic multipliers $\{\lambda_1, \lambda_2\} \in \mathbb{C}$ (on the ρ -radius circle) and the pair $\{\bar{\lambda}_1, \bar{\lambda}_2\} \in \mathbb{C}$ (on real axis) are within the stable region, i.e., inside the unit circle.

The Arnold tongues of the direct forced Mathieu equation affected by distinct damping coefficients are displayed in Fig. 7. Notice that the resonance lines disappeared, this is owing to the Floquet multipliers that were on the unitary circle in Fig. 2 (which caused the resonance) were translated to the circle of radius ρ in Fig. 3. That is, the damping effect causes the characteristic multipliers move from the boundary of the unit circle to the circle with radius ρ .

The damping effect reduces the Arnold tongues by an order of $1/e^{-\delta T}$, see Fig. 7.

4 The Kapitza Pendulum

The Kapitza pendulum is an inverted pendulum whose suspension point is changed periodically in the vertical direction. The objective from the point of view of control theory is the dynamic stabilization of the inverted position, usually when the suspension point is constrained to vibrate with a high frequency along the vertical axis. Its name is due to Pjotr Kapitza who explained in detail the particular behaviour of the system [19].

4.1 General equation of the Kapitza pendulum

Fig. 4 shows a simple diagram of the inverted pendulum, where l is the length of a massless rigid rod with a small bob of mass m at the end, g is the gravitational constant, $q(t)$ is the harmonic excitation function and (x, y) are the coordinates of the system.

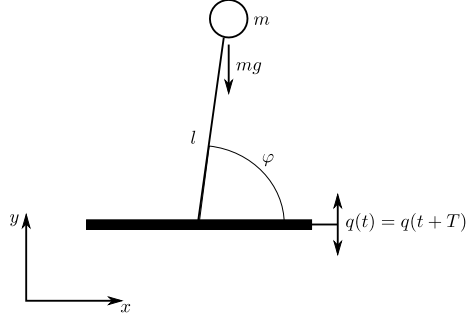


Figure 4: The Kapitza pendulum.

From Fig. 4, it can be deduced that

$$x = l \cos(\varphi), \dot{x} = -l \sin(\varphi)\dot{\varphi}; \quad y = l \sin(\varphi) - q, \dot{y} = l \cos(\varphi)\dot{\varphi} - \dot{q}.$$

Recalling the kinetic and potential energy: $K = 1/2m(\dot{x}^2 + \dot{y}^2)$, $U = mgl(l \sin(\varphi) - p)$, applying the Euler-Lagrange equation $d/dt \cdot \partial L / \partial \dot{\varphi} - \partial L / \partial \varphi = 0$, where $L = K - U$. Linearizing the system around the upper equilibrium position, we obtain

$$\ddot{\varphi} + (-g/l + \ddot{q}/l) \varphi = 0.$$

This is the general equation of motion. However, it is useful to make some variable changes in order to recover the system (1). Hence, the Hill equation describes the Kapitza pendulum linearized around its upper equilibrium position.

4.2 Numerical results of the forced Kapitza pendulum

Since the Hill equation features the inverted pendulum, the system (3) describes its corresponding forced case.

The expressions

$$\ddot{x} + \delta \dot{x} + [\alpha + \beta \cos(t)] x = \sum_{k \in \{3, 5, 9, 14\}} \cos(t/k), \quad (20)$$

$$\ddot{x} + \delta \dot{x} + [\alpha + \beta \operatorname{sgn}(\sin(t))] x = \sum_{k \in \{3, 5, 9, 14\}} \cos(t/k), \quad (21)$$

are tested to investigate the dynamics of the Kapitza pendulum.

Figures 5a and 5b show the stability diagram for the forced pendulum represented by systems (20) and (21), respectively. The kT -periodic solutions in the homogeneous system being forced by any kT -periodic external function become unstable leading to the resonance lines represented by very slim dashed curves in Figures 5a and 5b. Each line has a corresponding pair of eigenvalues on the unit circle, see Figure 2.

Fig. 6a exhibits the periodic behaviour of the homogeneous Kapitza pendulum at the point $(\alpha, \beta) = (3, 2)$ on the Ince-Strutt diagram, notice that this point is intercepted by a $3T$ -periodic solution. Whereas Figures 6b and 6c show the response of the forced system, with the same (α, β) -coordinates. The first graph illustrates the linear resonance

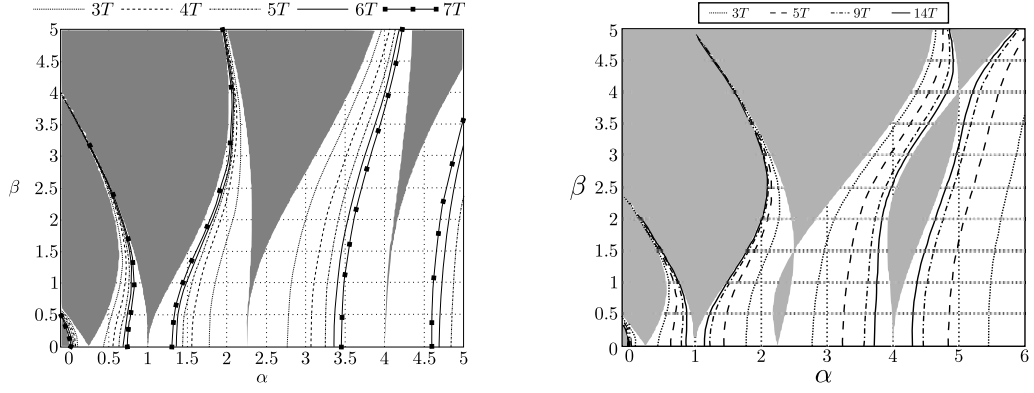


Figure 5: The Ince-Strutt diagrams of: (a) $\ddot{x} + \delta\dot{x} + [\alpha + \beta \cos(t)] x = \sum_{k=3}^7 \cos(t/k)$ and (b) $\ddot{x} + \delta\dot{x} + [\alpha + \beta \operatorname{sgn}(\sin t)] x = \sum_{k \in \{3,5,9,14\}} \cos(t/k)$, $\delta = 0$.

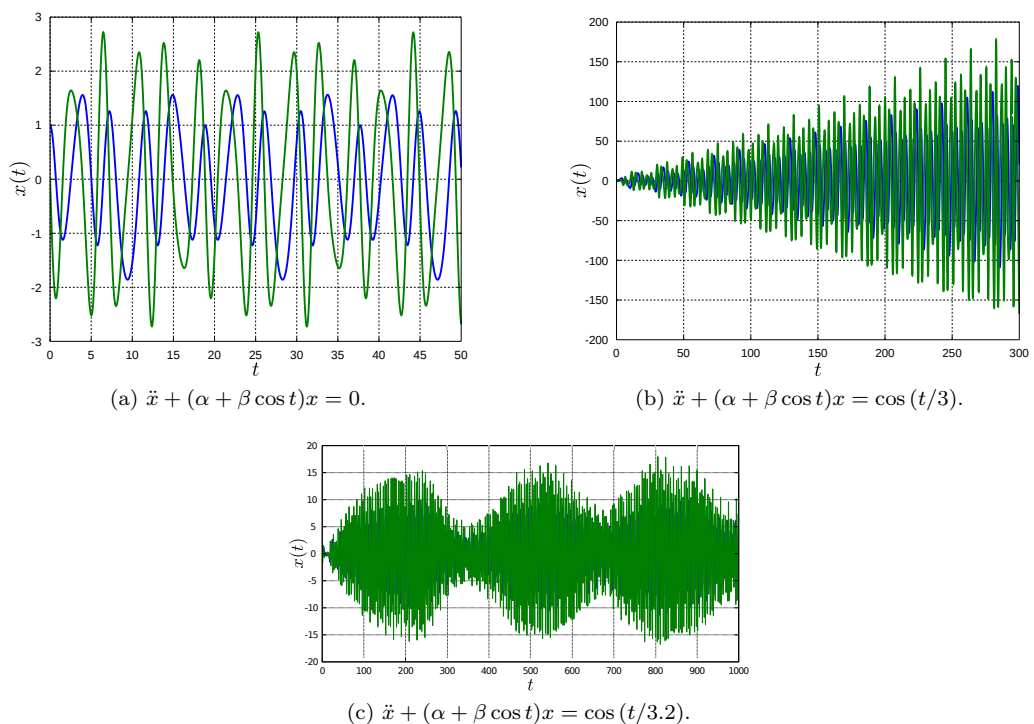


Figure 6: Response of the Kapitza pendulum: (a) homogeneous system, α and β belong to a $3T$ -periodic solution, (b) non-homogeneous system, the forced term is $3T$ -periodic, hence linear resonance arises and (c) non-homogeneous system, the forced term is $3.2T$ -periodic, in this case there can be no resonance. $\alpha = 3$, $\beta = 2$ in all the cases.

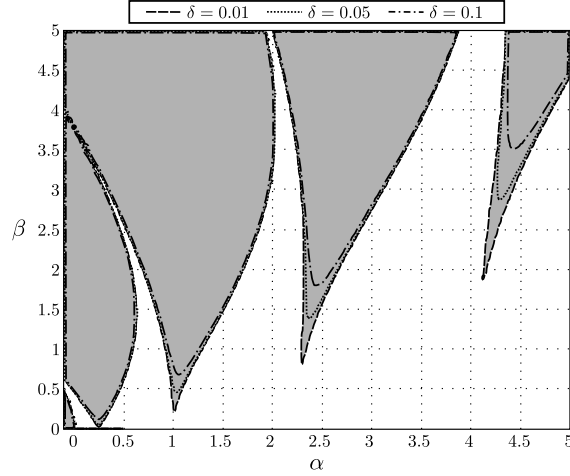


Figure 7: Stability diagram of the forced Kapitza pendulum: $\ddot{x} + \delta\dot{x} + [\alpha + \beta \cos(t)]x = \sum_{i=3}^7 \cos(t/i)$ for different values of damping.

which arises due to the coincidence of the $3T$ -periodic solution (in the non-homogeneous system) and the forcing signal (cosine) with the same period. In the second graph we see that the coincidence between the periods is lost (because the period of the cosine is $T = 3.2$), consequently, the linear instability disappears.

Damping effect plays an essential role in the stability of the inverted pendulum, this reduces the area of parametric resonance in relation to the δ -value (the greater dissipation means the less area of parametric instability). Regarding the linear resonance, it vanishes even with a relatively small value of dissipation, hence, the resonance lines disappear from the stability diagram, see Fig. 7. This fact is a direct consequence of Remark 3.2.

Remark 4.1 A diagram similar to that of Fig. 5a for the forced Mathieu equation (20), for $\alpha \in [-0.8, 0.6]$ and $\beta \in [0, 1.5]$, was obtained in [20], but no analysis was shown.

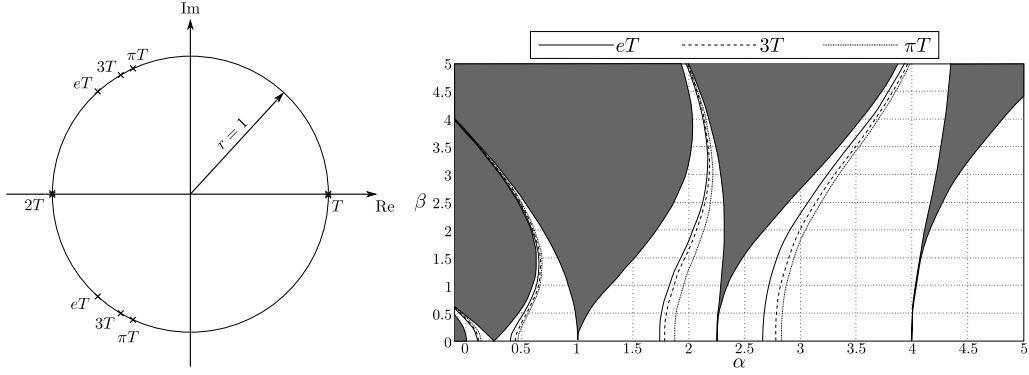
5 Further Results

In this section, we will analyze the system $\ddot{x} + [\alpha + \beta f(t)]x = g(t)$, where $f(t) = f(t+T)$ and $g(t) = g(t+\mathcal{T})$ with T and \mathcal{T} non-commensurable. More specifically, we will evaluate

$$\ddot{x} + [\alpha + \beta \cos(t)]x = \sin(\pi t), \quad \mathcal{T}_1 = 2, \quad (22)$$

$$\ddot{x} + [\alpha + \beta \cos(t)]x = \sin(et), \quad \mathcal{T}_2 = 2\pi/e, \quad (23)$$

where $e \approx 2,7182818$ is the Euler number and $\pi \approx 3.1415926$, both are irrational numbers, and \mathcal{T}_1 and \mathcal{T}_2 are the fundamental periods of the forcing signals in (22) and (23) respectively. Since the minimal period of the parametric excitation term is $T = 2\pi$, it can be seen in a straight way that neither T and \mathcal{T}_1 nor T and \mathcal{T}_2 are commensurable.



(a) Positions of the eigenvalues for eT , (b) Resonance lines generated by the external signals: $3T$ and πT -periodic solutions. $\sin(et)$, $\sin(3t)$, $\sin(\pi t)$.

Figure 8: (a) Multipliers on the unitary disk representing eT , $3T$ and πT -periodic solutions of the homogeneous Kapitza pendulum. (b) stability diagram of the inverted pendulum forced with signals whose period is not commensurable with the parametric excitation term.

Use the condition $\theta = 2\pi/k$ to obtain π and e -periodic solutions

$$\begin{aligned} k = \pi, \theta = \frac{2\pi}{\pi} &\Rightarrow \lambda_{1,2} \approx \{-0.4161 \pm j0.9092\}, \\ k = e, \theta = \frac{2\pi}{e} &\Rightarrow \lambda_{1,2} \approx \{-0.6747 \pm j0.7380\}. \end{aligned}$$

Fig. 8a shows the Floquet multipliers positions associated with πT , $3T$ and eT -periodic signals. The multipliers of $3T$ -periodic signals are plotted as a reference.

Notice that the behavior referring to the periodic solutions (in the homogeneous Hill equation) or the linear resonance (in the non-homogeneous Hill equation) is preserved in spite of the forcing signals and the parametric excitations are incommensurable, i.e., the kT -periodic solutions can appear with k not necessary integer provided that the eigenvalues of the monodromy matrix are on the unit circle. These solutions will resonate if a forcing term, with the same (or multiple) period, is applied to the system.

Fig. 9 traces the trajectories $x(t)$ of the solutions of (22) when $\alpha = 2$ and $\beta = 1.8$, which is a point located on one of πT -periodic lines on the stability diagram, see Fig. 8b, clearly these trajectories describe the linear resonance or instability caused by the forcing signal.

6 Conclusion

The present note covers the non-homogeneous Hill equation, this particular case presents new features in the stability diagram providing that the periodicity condition between the parametric and forcing signal is fulfilled, when this occurs, very thin curves (here called resonance lines) will appear inside the stable areas, such lines depict the linear resonance and emerge independently whether or not there is a commensurable relation between the forcing term and the parametric excitation signal. Then, it can be concluded that there are two types of instability associated with the forced Hill equation: the parametric resonance (well-known) and the linear resonance introduced in this paper.

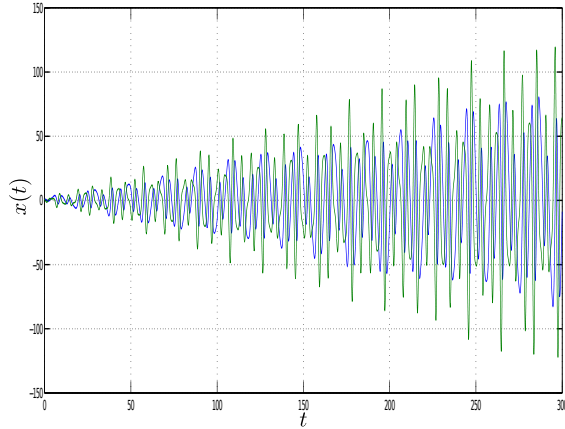


Figure 9: Response of the forced Kapitza pendulum: $\ddot{x} + [\alpha + \beta \cos(t)]x = \cos(\pi t)$, $\alpha = 2$ and $\beta = 1.8$.

This work also generalizes the results presented by Slane and Tragesser [8], about the inhomogeneous Hill equation, they described the changes operated only in the T and $2T$ periodic solutions (the boundaries of the Arnold tongues).

Additionally, it was shown that the multipliers lying on the unit circle were shifted inside the circle when the damping effect was introduced in the non-homogeneous Hill equation. Consequently, the resonance lines disappeared.

A challenging problem appears when we try to characterize the periodic solutions and the resonance lines in the higher order Hill equation. Due to the fact that these systems experience a phenomena that does not occur in the two degree of freedom systems. Therefore, a greater effort is required.

References

- [1] G.H. Hill. On the part of the motion of the lunar perigee which is a function of the mean motions of the sun and moon. *Acta Mathematica* **8** (1986) 1–36.
- [2] E. Mathieu. Mémoire sur le Mouvement Vibratoire d'une Membrane de Forme Elliptique. *Journal de Mathématiques Pures et Appliquées* **13** (1868) 137–203.
- [3] J.W. Strutt. On the crispations of fluid resting upon a vibrating support. *Philosophical Magazine* **16** (1883) 50–58.
- [4] V. I. Arnol'd. Remarks on the perturbation theory for problems of Mathieu type. *Russian Math. Surveys* **38** (4) (1983) 215–233.
- [5] D. Shadman and B. Mehri. A non-homogeneous Hill's equation. *Applied Mathematics and Computation* **167** (2005) 68–75.
- [6] M.K. Kwong and J.S.W. Wong. On the oscillation of Hill's equation under periodic forcing. *Journal of Mathematical and Applications* **320** (2006) 37–55.
- [7] D. Younesian, E. Esmailzadeh and B. Sedaghati. Asymptotic solutions and stability analysis for generalized non-homogeneous Mathieu equation. *Communications in Nonlinear Science and Numerical Simulation*. **12** (2007) 58–71.

- [8] J. Slane and S. Tragesser. Analysis of Periodic Nonautonomous Inhomogeneous Systems. *Nonlinear Dynamics and Systems Theory* **11** (2) (2011) 183–198.
- [9] R. A. Ibrahim and A.D.S. Barr. Parametric vibration. Part 1: Mechanics of linear problems. *The Shock and Vibration Digest*. **10** (1978) 15–29.
- [10] A. Champneys. Dynamics of parametric excitation. *Math. of Comp. and Dyn. Sys.* (2011) 183–204.
- [11] C. Kaur, B. K. Sharma and S. Yadav. Resonance in the Motion of a Geo-Centric Satellite Due to the Poynting-Robertson Drag and Oblateness of the Earth. *Nonlinear Dynamics and Systems Theory* **19** (4) (2019) 497–511.
- [12] W. Magnus and S. Winkler. *Hill's Equation*. John Wiley & Sons, New York, 1966.
- [13] G.N. Jazar. Stability chart of parametric vibrating systems using energy-rate method. *International Journal of Non-Linear Mechanics* **39** (2004) 1319–1331.
- [14] K. Khachnaoui. Homoclinic Orbits for Damped Vibration Systems with Small Forcing Terms. *Nonlinear Dynamics and Systems Theory* **18** (1) (2018) 80–91.
- [15] V.A. Yakubovich and V.M. Starzhinskii. *Linear Differential Equations with Periodic Coefficients*. J. Wiley, New York, 1975.
- [16] R.W. Brockett. *Finite dimensional linear systems*. John Wiley and Sons, USA, 1970.
- [17] V. A. Yakubovich. Remark on a theorem of Floquet-Lyapunov. *Vestnik Leningrad Univ.* **25** (1970) 97–101.
- [18] K.R. Meyer, G.R. Hall and D. Offin. *Introduction to Hamiltonian Dynamical Systems and the N-Body Problem*. 2nd Ed., Springer, USA: Boston, 2009.
- [19] P. L. Kapitza. Dynamic stability of the pendulum with vibrating suspension point. *Sov. Phys. JETP*. **21**(5) (1951) 588–597.
- [20] E.I. Butikov. *Simulations of Oscillatory Systems*. CRC Press, New York, 2015.



Estimates of Accuracy for Asymptotic Soliton-Like Solutions to the Singularly Perturbed Benjamin-Bona-Mahony Equation

V. H. Samoilenko^{1*}, Yu. I. Samoilenko¹ and L. V. Vovk²

¹ Taras Shevchenko National University of Kyiv, 64 Volodymyrs'ka St., 01601, Kyiv, Ukraine

² Kyiv National University of Culture and Arts, 36 Yevgen Konovalets' St., 01601, Kyiv, Ukraine

Received: March 17, 2019; Revised: December 25, 2019

Abstract: The paper deals with the singularly perturbed Benjamin-Bona-Mahony equation with variable coefficients. It plays an important role in various applications, in particular, for the description of waves in liquid. The equation appears in mathematical modeling of the wave processes in the media with small dispersion and variable characteristics. In the case of constant coefficients, this equation is known as the regularized long-wave equation or the regularized Korteweg-de Vries equation. We study the problem of estimating the difference between the exact solution and asymptotic soliton-like solution to the Cauchy problem for the singularly perturbed Benjamin-Bona-Mahony equation with variable coefficients. The initial data for the Cauchy problem are defined according to the concept of asymptotic soliton-like solution. It means that the approximate solutions are deformations of the soliton solutions to the Benjamin-Bona-Mahony equation with corresponding constant coefficients. Asymptotic estimates for the difference between the exact solution to the Benjamin-Bona-Mahony equation and the N-th approximation for the asymptotic soliton-like solution are obtained. In particular, the case of the main term of the solution is considered in detail. Similarly to the case of the singularly perturbed Korteweg-de Vries equation with variable coefficients these estimates are local. Nevertheless, they show that the asymptotic soliton-like solutions constructed through the nonlinear WKB method for the singularly perturbed Benjamin-Bona-Mahony equation with variable coefficients are sufficiently suitable as approximate solutions.

Keywords: *Benjamin-Bona-Mahony equation; asymptotic solutions; soliton-like solutions; Cauchy problem; asymptotic estimates.*

Mathematics Subject Classification (2010): 35Q53, 41A60.

* Corresponding author: valsamyul@gmail.com

1 Introduction

The paper deals with asymptotic estimates for the difference between the exact solution and asymptotic soliton-like solution to the singularly perturbed Benjamin-Bona-Mahony equation with variable coefficients

$$a(x, t, \varepsilon)u_t + b(x, t, \varepsilon)u_x + c(x, t, \varepsilon)uu_x - \varepsilon^2u_{xxt} = 0, \quad (x, t) \in \mathbf{R} \times (0; T), \quad (1)$$

where $a(x, t, \varepsilon)$, $b(x, t, \varepsilon)$, $c(x, t, \varepsilon)$ are some functions described below, and $\varepsilon > 0$ is a small parameter. At $\varepsilon = 1$ and constant coefficients, equation (1) coincides with the following one:

$$u_t + u_x + uu_x - u_{xxt} = 0, \quad (2)$$

that has been deduced in [1], where it was studied through the numerical methods for the case of the wave form initial data.

In the sequel, Benjamin T.B., Bona J.L., and Mahony J.J. [2] studied the initial value problem for equation (2) whose solution was supposed to be a real smooth non-periodic function. In particular, they pointed the following: “*We shall refer to (2) as the regularized long wave equation, reflecting in this term our view that the Korteweg-de Vries equation is an unsuitably posed model for long waves*”. Therefore, at present, equation (2) is known as the regularized long wave equation or the regularized Korteweg-de Vries equation. It is also called the Benjamin-Bona-Mahony equation [3], abbreviated to the BBM equation.

The different properties of equation (2), as well as those of its generalizations, were studied by Eilbeck J.C., and McGuire G.R. [4], [5], Wang B. [6], Wazwaz A.M. [7, 8], Arora R., and Kumar A. [9], Seadway A.R., and Sayed A. [10], El G.A., Hoefer M.A., and Shearer M. [11], and other authors. It was found that the BBM equation possesses soliton solutions [7]

$$u(x, t) = 3(a - 1) \cosh^{-2} \left(\frac{1}{2} \sqrt{\frac{a - 1}{a}} (x - at) + C \right), \quad (3)$$

where a , C are some real constants, and the inelastic collision of two solitary waves of the BBM equation was discovered [12], but it has neither two- nor multi-soliton solutions [13].

Equation (2), as well as the Korteweg-de Vries equation, describes propagation of soliton waves and cnoidal waves in different media, in particular, in shallow water. Similar waves have also appeared in many areas of science such as solid physics, biology [14], telecommunications [15], etc. Therefore, in the case of the medium with variable characteristics [16] and small dispersion [17, 18] the equation of type (1) should be studied.

One of the most effective methods of constructing approximate solutions to the singularly perturbed equations is the asymptotic analysis [19, 20]. Asymptotic soliton-like solutions to equation (1) were constructed in paper [21] through the approach based on the nonlinear WKB method that has been successfully applied for constructing asymptotic soliton-like solutions to many different problems (see, for example, [22], [23], [24], [25]). In the sequel, the nonlinear WKB technique was used for constructing the asymptotic soliton-like solutions to a number of partial differential equations of integrable type with singular perturbation [23].

Elaboration of algorithms for finding asymptotic expansions of different kinds and their justification consisting of determining asymptotic accuracy with which the solutions satisfy the equation under consideration are the main tasks of the perturbation

theory. This traditionally completes the asymptotic analysis of equations with small perturbations.

On the other hand, in many cases it is necessary to examine the question of how much the constructed approximate solution differs from the exact solution to the equation. This problem is usually given much less attention than the previous one [26] since it is necessary to study the equation under additional conditions, for example, under the initial data. Thus, a problem on studying asymptotic solutions to the Cauchy problem for equations with small perturbations appears.

For the case of the asymptotic soliton-like solutions we need to take into account the properties of soliton solutions to the corresponding equation with constant coefficients [21]. Therefore, the initial conditions for the appropriate Cauchy problem should be selected in a special way. In particular, the initial functions must belong to certain functional spaces, for example, the space of quickly decreasing functions.

The problem on estimation of the difference between the exact solution and asymptotic approximation under the same initial condition appears naturally. Namely, this task is considered in the present paper.

The paper is organized as follows. Firstly, the problem under consideration is formulated, then necessary definitions and notations are given. In the sequel, the algorithm of constructing the asymptotic soliton-like solutions to equation (1) is briefly described, and statements on asymptotic estimates for the norm of difference between the exact solution and its constructed asymptotic approximation are finally proved. There is considered the case of the main term of the asymptotic solution as well as the case of the N -th asymptotic approximation.

2 Formulation of the Problem, Preliminary Notes and Definitions

We are facing a problem of constructing the asymptotic soliton-like solution to the Cauchy problem for the singularly perturbed BBM equation with variable coefficients (1) under the initial condition

$$u(x, t, \varepsilon)|_{t=0} = f(x, \varepsilon), \quad x \in \mathbf{R}. \quad (4)$$

It should be noted that the choice of the initial condition essentially influences the asymptotic estimate between the exact solution to the Cauchy problem [27] in question and its constructed asymptotic approximation. We consider the problem with the initial function $f(x, \varepsilon)$ obtained from the formulae for asymptotic soliton-like solution [21] to equation (1). The coefficients $a(x, t, \varepsilon)$, $b(x, t, \varepsilon)$, $c(x, t, \varepsilon)$ of equation (1) are supposed to be represented as

$$\begin{aligned} a(x, t, \varepsilon) &= \sum_{k=0}^N \varepsilon^k a_k(x, t) + O(\varepsilon^{N+1}), & b(x, t, \varepsilon) &= \sum_{k=0}^N \varepsilon^k b_k(x, t) + O(\varepsilon^{N+1}), \\ c(x, t, \varepsilon) &= \sum_{k=0}^N \varepsilon^k c_k(x, t) + O(\varepsilon^{N+1}), \end{aligned} \quad (5)$$

where the functions $a_0(x, t)$, $b_0(x, t)$, $c_0(x, t)$ do not equal zero for all $(x, t) \in \mathbf{R} \times [0; T]$.

Now we recall some notions and definitions.

Let $S = S(\mathbf{R})$ be a space of quickly decreasing functions, i.e., the space of infinitely differentiable on \mathbf{R} functions satisfying, for any integers $m, n \geq 0$, the condition

$$\sup_{x \in \mathbf{R}} \left| x^m \frac{d^n}{dx^n} u(x) \right| < +\infty.$$

By $C^\infty(\mathbf{R} \times (0; T); S)$ we denote a space of infinitely differentiable functions of $(x, t) \in \mathbf{R} \times (0; T)$ such that, for any integers $k, m, n \geq 0$, the following inequality

$$\sup_{t \in [0; T]} \left(\int_{-\infty}^{+\infty} \left(\frac{\partial^{n+k} u}{\partial x^n \partial t^k} \right)^2 dx + \int_{-\infty}^{+\infty} (1+x^2)^m \left(\frac{\partial^k u}{\partial t^k} \right)^2 dx \right) < +\infty$$

holds.

Let $G_1 = G_1(\mathbf{R} \times [0; T] \times \mathbf{R})$ be a space of infinitely differentiable functions $f = f(x, t, \tau)$, $(x, t, \tau) \in \mathbf{R} \times [0; T] \times \mathbf{R}$, for which the following conditions are fulfilled [23]:
1⁰. the relation

$$\lim_{\tau \rightarrow +\infty} \tau^n \frac{\partial^p}{\partial x^p} \frac{\partial^q}{\partial t^q} \frac{\partial^r}{\partial \tau^r} f(x, t, \tau) = 0, \quad (x, t) \in K,$$

takes place;

2⁰. there exists a differentiable function $f^-(x, t)$ such that the condition

$$\lim_{\tau \rightarrow -\infty} \tau^n \frac{\partial^p}{\partial x^p} \frac{\partial^q}{\partial t^q} \frac{\partial^r}{\partial \tau^r} (f(x, t, \tau) - f^-(x, t)) = 0, \quad (x, t) \in K,$$

is satisfied uniformly in $(x, t) \in K$ for any non-negative integers n, p, q, r and every compact set $K \subset \mathbf{R} \times [0; T]$.

Let $G_1^0 = G_1^0(\mathbf{R} \times [0; T] \times \mathbf{R}) \subset G_1$ be a space of functions $f = f(x, t, \tau) \in G_1$, $(x, t, \tau) \in \mathbf{R} \times [0; T] \times \mathbf{R}$, for which the following condition $\lim_{\tau \rightarrow -\infty} f(x, t, \tau) = 0$ takes place uniformly in (x, t) on every compact $K \subset \mathbf{R} \times [0; T]$.

Definition 2.1 A function $u = u(x, t, \varepsilon)$, where ε is a small parameter, is called an asymptotic soliton-like function [23] if for any integer $N \geq 0$, it can be represented in the form

$$u(x, t, \varepsilon) = \sum_{j=0}^N \varepsilon^j [u_j(x, t) + V_j(x, t, \tau)] + O(\varepsilon^{N+1}), \quad \tau = \frac{x - \varphi(t)}{\varepsilon}, \quad (6)$$

where $\varphi(t) \in C^\infty([0; T])$ is a scalar real function; $u_j(x, t) \in C^\infty(\mathbf{R} \times [0; T])$, $j = \overline{0, N}$; $V_0(x, t, \tau) \in G_1^0$; $V_j(x, t, \tau) \in G_1$, $j = \overline{1, N}$.

The function $x - \varphi(t)$ is called a phase of the soliton-like function $u(x, t, \varepsilon)$, and the curve $\Gamma = \{(x, t) : x = \varphi(t), t \in [0; T]\}$ is called a discontinuity curve.

Here and below we use the notation $\Psi(x, t, \varepsilon) = O(\varepsilon^N)$. It means that $|\Psi(x, t, \varepsilon)| \leq C_N \varepsilon^N$ for all $\varepsilon \in (0; \varepsilon_0)$, where C_N, ε_0 are some positive values, $(x, t) \in K \subset \mathbf{R} \times [0; T]$ and K is a compact set.

The constant C_N depends only on the number N and the set K .

Remark 2.1 The term “soliton-like solution” reflects the following property of the asymptotic solution to the equations with constant coefficients having soliton solutions. In the case of such a partial differential equation in the presence of variable coefficients, it is expected that its solutions are certain deformations of the soliton-type solutions. Therefore, it is natural to look for asymptotic solutions to the singularly perturbed Benjamin-Bona-Mahony equation with variable coefficients in the form that is similar to the representation of soliton solutions. Moreover, in the case of constant coefficients, the singular part of the asymptotic solution constructed through the nonlinear WKB method coincides with soliton solution (3) to the singularly perturbed Benjamin-Bona-Mahony equation with account of calibrate transformations.

2.1 Scheme of constructing the asymptotic solution

Now we briefly describe the algorithm of constructing the asymptotic soliton-like solution to the BBM equation (1). The asymptotic solution is represented as [21]

$$u(x, t, \varepsilon) = \sum_{j=0}^N \varepsilon^j [u_j(x, t) + V_j(x, t, \tau)] + O(\varepsilon^{N+1}), \quad \tau = \frac{x - \varphi(t)}{\varepsilon}. \quad (7)$$

Here the function $U_N(x, t, \varepsilon) = \sum_{j=0}^N \varepsilon^j u_j(x, t)$ is called a regular part of asymptotic solution (7) and the function $V_N(x, t, \tau, \varepsilon) = \sum_{j=0}^N \varepsilon^j V_j(x, t, \tau)$ gives a singular part of asymptotic solution (7). The terms of the regular part solve the equations

$$a_0(x, t) \frac{\partial u_0}{\partial t} + b_0(x, t) \frac{\partial u_0}{\partial x} + c_0(x, t) u_0 \frac{\partial u_0}{\partial x} = 0, \quad (8)$$

$$\begin{aligned} a_0(x, t) \frac{\partial u_j}{\partial t} + b_0(x, t) \frac{\partial u_j}{\partial x} + c_0(x, t) \left(u_j \frac{\partial u_0}{\partial x} + u_0 \frac{\partial u_j}{\partial x} \right) &= \\ &= f_j(x, t, u_0, u_1, \dots, u_{j-1}), \quad j = \overline{1, N}, \end{aligned} \quad (9)$$

and the terms of the singular part satisfy the equations

$$\varphi' \frac{\partial^3 V_0}{\partial \tau^3} + [b_0(x, t) - a_0(x, t) \varphi'(t)] \frac{\partial V_0}{\partial \tau} + c_0(x, t) [u_0 + V_0] \frac{\partial V_0}{\partial \tau} = 0, \quad (10)$$

$$\varphi' \frac{\partial^3 V_j}{\partial \tau^3} + (b_0(x, t) - a_0(x, t) \varphi'(t)) \frac{\partial V_j}{\partial \tau} + c_0(x, t) \left(u_0 \frac{\partial V_j}{\partial \tau} + \frac{\partial}{\partial \tau} (V_0 V_j) \right) = F_j(x, t, \tau), \quad (11)$$

where the functions $f_j(x, t, u_0, u_1, \dots, u_{j-1})$, $j = \overline{1, N}$, are obtained recurrently through the terms $u_0(x, t)$, $u_1(x, t)$, ..., $u_{j-1}(x, t)$, $j = \overline{1, N}$, and the functions $F_j(x, t, \tau) = F_j(t, V_0(x, t, \tau), \dots, V_{j-1}(x, t, \tau), u_0(x, t), \dots, u_j(x, t))$, are determined recurrently through the terms $u_0(x, t)$, $u_1(x, t)$, ..., $u_j(x, t)$, $V_0(x, t, \tau)$, $V_1(x, t, \tau)$, ..., $V_{j-1}(x, t, \tau)$, $j = \overline{1, N}$.

Solutions to equations (8), (9) can be found through the method of characteristics. The singular part of asymptotic solution (7) is constructed in a special way [21]. Firstly, equations (10), (11) are studied on the discontinuity curve Γ that is determined through

the solution $\varphi = \varphi(t)$, $t \in [0; T]$, of certain second order ordinary differential equation (see equation (29)). The functions $v_j = v_j(t, \tau) = V_j(x, t, \tau)|_{\Gamma}$, $j = \overline{0, N}$, solve the following partial differential equations:

$$\varphi'(t) \frac{\partial^3 v_0}{\partial \tau^3} + (b_0(\varphi, t) - a_0(\varphi, t)\varphi'(t) + c_0(\varphi, t)u_0(\varphi, t)) \frac{\partial v_0}{\partial \tau} + c_0(\varphi, t)v_0 \frac{\partial v_0}{\partial \tau} = 0, \quad (12)$$

$$\varphi'(t) \frac{\partial^3 v_j}{\partial \tau^3} + (b_0(\varphi, t) - a_0(\varphi, t)\varphi'(t) + c_0(\varphi, t)u_0(\varphi, t)) \frac{\partial v_j}{\partial \tau} + c_0(\varphi, t) \frac{\partial}{\partial \tau} (v_0 v_j) = \mathcal{F}_j(t, \tau), \quad (13)$$

where $\mathcal{F}_j(t, \tau) = F_j(x, t, \tau)|_{\Gamma}$. In particular,

$$\begin{aligned} \mathcal{F}_1(t, \tau) = & -a_0(\varphi, t)v_{0t} - c_0(\varphi, t)u_{0x}(\varphi, t)v_0 - \\ & -[c_{0x}u_0(\varphi, t) + c_0(\varphi, t)u_{0x}(\varphi, t) - a_{0x}(\varphi, t)\varphi'(t) + b_{0x}(\varphi, t)]\tau v_{0\tau} - \\ & -[c_{0x}(\varphi, t)\tau + c_1(\varphi, t)]v_0 v_{0\tau} - [c_0(\varphi, t)u_1(\varphi, t) + c_1(\varphi, t)u_0(\varphi, t) - \\ & -a_1(\varphi, t)\varphi'(t) + b_1(\varphi, t)]v_{0\tau} + v_{0\tau\tau}. \end{aligned} \quad (14)$$

Later, an extension of the functions $v_j(t, \tau)$, $j = \overline{0, N}$, is constructed from the curve Γ into its neighborhood.

All details of the algorithm can be found in [21].

3 Principal Results

3.1 Main term of the asymptotic solution (7)

At first, we consider a main term of asymptotic expansion (7). The term is determined through the solution to equation (12) and is given by the formula

$$V_0(x, t, \tau) = V_0(t, \tau) = v_0(t, \tau) = 3 \frac{A(\varphi, t)}{c_0(\varphi, t)} \cosh^{-2} \left(\sqrt{\frac{A(\varphi, t)}{\varphi'(t)}} \frac{\tau - \tau_0}{2} \right), \quad (15)$$

where $A(\varphi, t) = a_0(\varphi, t)\varphi' - b_0(\varphi, t) - c_0(\varphi, t)u_0(\varphi, t)$, τ_0 is a constant of integration, and function $u_0(x, t)$ is found through the method of characteristics from the Hopf type equation (8). Here the following condition

$$A(\varphi, t)\varphi'(t) > 0, \quad t \in [0; T], \quad (16)$$

is supposed to be satisfied.

Remark 3.1 The function $V_0(t, \tau)$ is an exact solution to equation (12) in the space G_1^0 . Its partial derivative $V_{0\tau}(t, \tau)$ satisfies equation (13) as the right side function $\mathcal{F}_j(t, \tau) = 0$. The last property can be easily verified by direct calculations.

Now we define the initial data of problem (1), (4) more exactly. Let us put

$$f_0(x, \varepsilon) = 3 \frac{A(\varphi_0, 0)}{c_0(\varphi_0, 0)} \cosh^{-2} \left(\sqrt{\frac{A(\varphi_0, 0)}{\varphi'_0}} \left(\frac{x - \varphi_0}{2\varepsilon} - \frac{\tau_0}{2} \right) \right), \quad (17)$$

where $\varphi_0 = \varphi(0)$, $\varphi'_0 = \varphi'(0) \neq 0$, $\tau_0 \in \mathbf{R}$ are parameters, and let us denote the set of functions (17) by $\mathcal{M}_0(\varepsilon)$.

The following statements are true.

Theorem 3.1 *Let us suppose the following propositions are fulfilled:*

- 1⁰. *the functions $a_0(x, t)$, $b_0(x, t)$, $c_0(x, t) \in C^\infty(\mathbf{R} \times [0; T])$ and they do not equal zero for all $(x, t) \in \mathbf{R} \times [0; T]$;*
- 2⁰. *the function $f(x, \varepsilon)$ in initial condition (4) can be represented as $f(x, \varepsilon) = g_0(x) + f_0(x, \varepsilon)$, where $g_0(x) \in C^\infty(\mathbf{R})$, $f_0(x, \varepsilon) \in \mathcal{M}_0(\varepsilon)$;*
- 3⁰. *the Cauchy problem for equation (8) with the initial condition $u_0(x, 0) = g_0(x)$ has the solution $u_0(x, t) \in C^\infty(\mathbf{R} \times [0; T])$;*
- 4⁰. *there exists a function $\varphi(t) \in C^\infty([0; T])$ satisfying (16) and $\varphi(0) = \varphi_0$, $\varphi'(0) = \varphi'_0 \neq 0$.*

Then the main term of the asymptotic soliton-like solution to the Cauchy problem (1), (4) is given by the formula

$$Y_0(x, t, \varepsilon) = u_0(x, t) + V_0(t, \tau), \quad (18)$$

where $u_0(x, t)$ is a solution to equation (8) with the initial condition $u(x, 0) = g_0(x)$ and $V_0(t, \tau)$ is defined through formula (15).

Function (18) satisfies the Cauchy problem (1), (4) with accuracy $O(1)$ on the set $\mathbf{R} \times [0; T]$. Moreover, as $\tau \rightarrow \pm\infty$, it satisfies the Cauchy problem (1), (4) with accuracy $O(\varepsilon)$ on the set $\mathbf{R} \times [0; T]$.

Proof. It is clear that function (18) satisfies initial condition (4). The other statement of Theorem 3.1 is proved according to the scheme of proof for Theorem 1 in [21]. That is why we omit the details here.

Theorem 3.2 *Let the following propositions hold:*

- 1⁰. *the functions $a(x, t, \varepsilon)$, $b(x, t, \varepsilon)$, $c(x, t, \varepsilon)$ satisfy the assumptions $a(x, t, \varepsilon) = a(x, \varepsilon) \in C^\infty(\mathbf{R})$, $b(x, t, \varepsilon) \in C^\infty(\mathbf{R} \times [0; T])$, $c(x, t, \varepsilon) = c(t, \varepsilon) \in C^\infty([0; T])$;*
- 2⁰. *the inequalities $r_1 \leq a(x, \varepsilon) \leq r_2$, $|b(x, t, \varepsilon)| < l_1$, $|b_x(x, t, \varepsilon)| < l_2$ take place for all $x \in \mathbf{R}$, $t \in [0; T]$, where r_1 , r_2 , l_1 , l_2 are some positive constants;*
- 3⁰. *the Cauchy problem (1), (4) has a solution $u(x, t, \varepsilon) \in C^\infty(0, T; S)$;*
- 4⁰. *the functions $a_0(x) \in C^\infty(\mathbf{R})$, $b_0(x, t) \in C^\infty(\mathbf{R} \times [0; T])$, $c_0(t) \in C^\infty([0; T])$ do not equal zero for all $x \in \mathbf{R}$, $t \in [0; T]$ and $a_0(x)$, $b_0(x, t)$ are absolutely bounded for all $x \in \mathbf{R}$, $t \in [0; T]$;*
- 5⁰. *the function $f(x, \varepsilon)$ in initial condition (4) can be represented as $f(x, \varepsilon) = g_0(x) + f_0(x, \varepsilon)$, where $g_0(x) \in S(\mathbf{R})$, $f_0(x, \varepsilon) \in \mathcal{M}_0(\varepsilon)$;*
- 6⁰. *the Cauchy problem for equation (8) with the initial condition $u_0(x, 0) = g_0(x)$, $x \in \mathbf{R}$, has a solution in the space $C^\infty(0, T; S)$;*
- 7⁰. *there exists a function $\varphi(t) \in C^\infty([0; T])$ satisfying (16) and $\varphi(0) = \varphi_0$, $\varphi'(0) = \varphi'_0 \neq 0$.*

Then for the exact solution and the asymptotic soliton-like solution to the Cauchy problem (1), (4) the following estimate

$$\|u(x, t, \varepsilon) - Y_0(x, t, \varepsilon)\| \leq C\varepsilon, \quad t \in [0; \varepsilon\Theta], \quad (19)$$

is true, where C is a constat not depending on the parameter ε , $\Theta > 0$ is a real number, and

$$\|f\|^2 = \|\sqrt{a(x, \varepsilon)} f\|^2 + \varepsilon^2 \|f_x\|^2, \quad \|f\|^2 = \int_{\mathbf{R}} |f(x, t, \varepsilon)|^2 dx.$$

Proof. For proving the theorem let us consider the function

$$\omega(x, t, \varepsilon) = u(x, t, \varepsilon) - Y_0(x, t, \varepsilon), \quad (20)$$

where $u(x, t, \varepsilon)$ is an exact solution to the Cauchy problem (1), (4) and $Y_0(x, t, \varepsilon)$ is given by formula (18). Substituting $u(x, t, \varepsilon) = \omega(x, t, \varepsilon) + Y_0(x, t, \varepsilon)$ into (1), multiplying both sides by $\omega(x, t, \varepsilon)$ and integrating the obtained expression in x from $-\infty$ to $+\infty$, we get

$$\begin{aligned} -\frac{\varepsilon^2}{2} \frac{d}{dt} \int_{-\infty}^{+\infty} \omega_x^2(x, t, \varepsilon) dx &= \frac{1}{2} \frac{d}{dt} \int_{-\infty}^{+\infty} a(x, \varepsilon) \omega^2(x, t, \varepsilon) dx - \\ -\frac{1}{2} \int_{-\infty}^{+\infty} b_x(x, t, \varepsilon) \omega^2(x, t, \varepsilon) dx &- \int_{-\infty}^{+\infty} c(t, \varepsilon) Y_0(x, t, \varepsilon) \omega(x, t, \varepsilon) \omega_x(x, t, \varepsilon) dx + \\ &+ \int_{-\infty}^{+\infty} g(x, t, \varepsilon) \omega(x, t, \varepsilon) dx, \end{aligned} \quad (21)$$

where

$$\begin{aligned} g(x, t, \varepsilon) &= -\varepsilon^2 Y_{0xt}(x, t, \varepsilon) + a(x, \varepsilon) Y_{0t}(x, t, \varepsilon) + \\ &+ b(x, t, \varepsilon) Y_{0x}(x, t, \varepsilon) + c(t, \varepsilon) Y_0(x, t, \varepsilon) Y_{0x}(x, t, \varepsilon). \end{aligned}$$

Taking into account the conditions of Theorem 3.2 and the technique of constructing the asymptotic soliton-like solution to the Cauchy problem (1), (4) we conclude that the function $g(x, t, \varepsilon)$ belongs to the space $C^\infty(0, T; S)$. Moreover, it satisfies the asymptotic relation $g(x, t, \varepsilon) = O(1)$ as $\varepsilon \rightarrow 0$.

From equality (21) we find

$$\frac{1}{2} \frac{d}{dt} E^2 \leq p E^2 + qE, \quad (22)$$

where

$$E^2 = \|\omega(x, t, \varepsilon)\|^2 = \|\sqrt{a(x, \varepsilon)} \omega(x, t, \varepsilon)\|^2 + \varepsilon^2 \|\omega_x(x, t, \varepsilon)\|^2, \quad (23)$$

$$p = \frac{1}{2} \max_{(x, t) \in \mathbf{R} \times [0; T]} \left| \frac{b_x(x, t, \varepsilon)}{a(x, \varepsilon)} \right| + \max_{(x, t) \in \mathbf{R} \times [0; T]} \left| c(t, \varepsilon) \frac{Y_0(x, t, \varepsilon)}{a(x, \varepsilon)} \right| + \quad (24)$$

$$+ \frac{1}{\varepsilon} \max_{(x, t) \in \mathbf{R} \times [0; T]} |c(t, \varepsilon) Y_0(x, t, \varepsilon)|,$$

$$q = \max_{t \in [0; T]} \left(\int_{-\infty}^{+\infty} \left| \frac{g(x, t, \varepsilon)}{\sqrt{a(x, \varepsilon)}} \right|^2 dx \right)^{1/2}.$$

According to the algorithm of constructing the main term of the asymptotic solution (7) the values p, q satisfy the following asymptotic relations:

$$p = O\left(\frac{1}{\varepsilon}\right), \quad q = O(1) \quad \text{as } \varepsilon \rightarrow 0.$$

To estimate the value $y = E(t, \varepsilon)$ we consider the differential inequality

$$\frac{dy}{dt} \leq py + q$$

under the initial condition $y(0) = 0$ according to notations (20) and (23).

Similarly to the proof of the Gronwall-Bellman lemma we find the relation

$$y(t) \leq \frac{q}{p} (e^{pt} - 1).$$

As a result, we obtain estimate (19).

3.2 Higher terms of the asymptotic soliton-like solution

Let us describe the initial data of the Cauchy problem (1), (4) corresponding to the higher terms of asymptotic soliton-like solutions (7). As in the previous case, the initial data is a sum of two functions. One of these functions is a sufficiently smooth one connected with the regular part of asymptotic solution (7). The other function belongs to the defined above space G_1 and is associated with the singular part of asymptotic solution (7).

To clarify the type of the last element of the initial data we go back to the algorithm of constructing the singular part of asymptotic solution (7) and recall some results of paper [21]. The terms of the singular part are represented as follows:

$$V_j(x, t, \tau) = u_j^-(x, t)\eta_j(t, \tau) + \psi_j(t, \tau), \quad j = \overline{1, N}, \quad (25)$$

where $u_j^-(x, t)$, $j = \overline{1, N}$, is a solution to the Cauchy problem

$$\Lambda u_j^-(x, t) = f_j^-(x, t), \quad (26)$$

$$u_j^-(x, t)|_{\Gamma} = \nu_j(t), \quad j = \overline{1, N}. \quad (27)$$

Here the differential operator Λ is written as

$$\Lambda = a_0(x, t) \frac{\partial}{\partial t} + [b_0(x, t) + c_0(x, t)u_0(x, t)] \frac{\partial}{\partial x} + c_0(x, t)u_{0x}(x, t),$$

the right side functions $f_j^-(x, t)$, $j = \overline{1, N}$, are recursively determined, and, for example, $f_1^-(x, t) = 0$,

$$f_2^-(x, t) = -a_1(x, t) \frac{\partial u_1^-}{\partial t} - b_1(x, t) \frac{\partial u_1^-}{\partial x} - c_1(x, t)u_1^- \frac{\partial u_0}{\partial x} - \dots \quad (28)$$

$$\begin{aligned}
& -c_0(x, t) u_1^- \frac{\partial u_1}{\partial x} - c_0(x, t) u_1 \frac{\partial u_1^-}{\partial x} - c_0(x, t) u_1^- \frac{\partial u_1^-}{\partial x} - c_1(x, t) u_0 \frac{\partial u_1^-}{\partial x}; \\
\nu_j(t) &= [-a_0(\varphi, t)\varphi'(t) + b_0(\varphi, t) + c_0(\varphi, t)u_0(\varphi, t)]^{-1} \lim_{\tau \rightarrow -\infty} \Phi_j(t, \tau), \\
\Phi_j(t, \tau) &= - \int_{\tau}^{+\infty} \mathcal{F}_j(t, \xi) d\xi, \quad j = \overline{1, N};
\end{aligned}$$

$\eta_j(t, \tau) \in G_1$ is a function such that $\lim_{\tau \rightarrow -\infty} \eta_j(t, \tau) = 1$; the function $\psi_j(t, \tau)$ belongs to the space G_1^0 , and $u_0(x, t)$ is the main term of the regular part of asymptotic solution (7).

Besides, the function $\varphi = \varphi(t)$, $t \in [0; T]$, is a solution to the second order ordinary differential equation of the following form:

$$[A_1 \varphi'^2 + A_2 \varphi' + A_3] \varphi'' + A_4 \varphi'^4 + A_5 \varphi'^3 + A_6 \varphi'^2 + A_7 \varphi' = 0, \quad (29)$$

where the coefficients $A_k = A_k(\varphi, t)$, $k = \overline{1, 7}$, are given as follows:

$$\begin{aligned}
A_1 &= 24 a_0^2 c_0, \quad A_2 = -8 a_0 c_0 \alpha, \quad A_3 = -c_0 \alpha^2, \quad A_4 = -40 c_{0x} a_0^2 + 30 a_0 a_{0x} c_0, \\
A_5 &= 60 a_0 c_{0x} \alpha + 20 a_0 a_{0t} c_0 - 24 a_0^2 c_{0t} - 30 a_0 c_0 \alpha_x - 15 a_{0x} c_0 \alpha + 20 a_0 c_0^2 u_{0x}, \\
A_6 &= -20 a_0 c_0 \alpha_t - 5 a_{0t} c_0 \alpha + 15 c_0 \alpha \alpha_x + 28 a_0 c_{0t} \alpha - 20 c_0^2 u_{0x} \alpha - 20 c_{0x} \alpha^2, \\
A_7 &= 5 c_0 \alpha \alpha_t - 20 c_{0t} \alpha^2,
\end{aligned}$$

where $\alpha = b_0 + c_0 u_0$, $a_0 = a_0(\varphi, t)$, $b_0 = b_0(\varphi, t)$, $c_0 = c_0(\varphi, t)$, $u_0 = u_0(\varphi, t)$.

Ordinary differential equation (29) is nonlinear and, in general, it possesses a solution on the finite time interval denoted by $[0; T]$.

We suppose that the Cauchy problem (26), (27) has a solution in the domain $\{(x, t) : x < \varphi(t), t \in [0; T]\}$. In the case, asymptotic solution (7) to the Cauchy problem (1), (4) is written as

$$Y_N(x, t, \varepsilon) = \begin{cases} \sum_{j=0}^N \varepsilon^j [u_j(x, t) + V_j(x, t, \tau)], & (x, t) \in \Omega_\mu(\Gamma), \\ u_0(x, t) + \sum_{j=1}^N \varepsilon^j [u_j(x, t) + u_j^-(x, t)], & (x, t) \in D^- \setminus \Omega_\mu(\Gamma), \\ \sum_{j=0}^N \varepsilon^j u_j(x, t), & (x, t) \in D^+ \setminus \Omega_\mu(\Gamma), \end{cases} \quad (30)$$

where

$$\begin{aligned}
\Omega_\mu(\Gamma) &= \{(x, t) \in \mathbf{R} \times [0; T] : |x - \varphi(t)| < \mu\}, \\
D^- &= \{(x, t) \in \mathbf{R} \times [0; T] : x < \varphi(t)\}, \\
D^+ &= \{(x, t) \in \mathbf{R} \times [0; T] : x > \varphi(t)\},
\end{aligned}$$

μ is a positive number.

Taking into account Remark 3.1 we find the representation of the initial values in (4). So, by substituting $\tau = (x - \varphi(t))/\varepsilon$ and putting $t = 0$, we get

$$f_j(x, \varepsilon) := V_j(x, t, \tau) \Big|_{t=0, \tau=\frac{x-\varphi_0}{\varepsilon}} = u_j^-(x, 0) \eta_j \left(0, \frac{x - \varphi_0}{\varepsilon}\right) + \quad (31)$$

$$+\psi_j \left(0, \frac{x - \varphi_0}{\varepsilon}\right) + \rho_j V_{0\tau}(t, \tau) \Big|_{t=0, \tau=\frac{x-\varphi_0}{\varepsilon}}, \quad j = \overline{1, N},$$

where ρ_j , $j = \overline{1, N}$, are real parameters.

The set of values $f_j(x, \varepsilon)$ is denoted by $\mathcal{M}_j(\varepsilon)$ for any $j = \overline{1, N}$.

So, the following theorem is true.

Theorem 3.3 *Let the following propositions be fulfilled:*

- 1⁰. *the functions $a_k(x, t)$, $b_k(x, t)$, $c_k(x, t) \in C^\infty(\mathbf{R} \times [0; T])$, $k = \overline{0, N}$, and the inequality $a_0(x, t)b_0(x, t)c_0(x, t) \neq 0$ holds for all $(x, t) \in \mathbf{R} \times [0; T]$;*
- 2⁰. *the function $f(x, \varepsilon)$ in initial condition (4) can be represented as*

$$f(x, \varepsilon) = \sum_{j=0}^N \varepsilon^j [g_j(x) + f_j(x, \varepsilon)],$$

where $g_j(x) \in C^\infty(\mathbf{R})$ and $f_j(x, \varepsilon) \in \mathcal{M}_j(\varepsilon)$, $j = \overline{0, N}$;

- 3⁰. *equation (8) with the initial condition $u_0(x, 0) = g_0(x)$, $x \in \mathbf{R}$, as well as equation (9) with the initial condition $u_j(x, 0) = g_j(x)$, $x \in \mathbf{R}$, has the solution $u_j(x, t) \in C^\infty(\mathbf{R} \times [0; T])$, $j = \overline{0, N}$;*
- 4⁰. *the function $\mathcal{F}_j(t, \tau) \in G_1^0$, $j = \overline{1, N}$, and the orthogonality condition*

$$\int_{-\infty}^{+\infty} \mathcal{F}_j(t, \tau) v_0(t, \tau) d\tau = 0, \quad j = \overline{1, N}; \quad (32)$$

is satisfied;

- 5⁰. *the function $\mathcal{F}_j(t, \tau)$, $j = \overline{1, N}$, is such that the property*

$$\lim_{\tau \rightarrow -\infty} \Phi_j(t, \tau) = 0, \quad j = \overline{1, N}, \quad (33)$$

takes place;

- 6⁰. *equation (29) has a solution $\varphi(t) \in C^\infty([0; T])$ such that inequality (16) is true and $\varphi(0) = \varphi_0$, $\varphi'(0) = \varphi_0' \neq 0$ hold.*

Then the asymptotic soliton-like solution to the Cauchy problem (1), (4) can be written as

$$Y_N(x, t, \varepsilon) = \sum_{j=0}^N \varepsilon^j [u_j(x, t) + V_j(x, t, \tau)]. \quad (34)$$

It satisfies the Cauchy problem with accuracy $O(\varepsilon^N)$ for all $(x, t) \in \mathbf{R} \times [0; T]$. Moreover, as $\tau \rightarrow \pm\infty$, function (34) satisfies the Cauchy problem (1), (4) with accuracy $O(\varepsilon^{N+1})$, $N \in \mathbf{N}$.

Proof. It is clear that function (34) satisfies initial condition (4). The other part of Theorem 3.3 is proved according to the scheme of proof for Theorem 1 in [21].

Remark 3.2 Condition 5⁰ of Theorem 3.3 provides solution (7), singular part of which belongs to the space C_1^0 . Therefore, we can put $V_j(x, t, \tau) = V_j(x, t, \tau)|_{\Gamma} = v_j(t, \tau)$, $j = \overline{0, N}$.

In the opposite case, the asymptotic soliton-like solution to the Cauchy problem (1), (4) can be written as (30).

Theorem 3.4 Suppose the following propositions are fulfilled:

- 1⁰. conditions 1⁰ – 4⁰, 6⁰ of Theorem 3.3 are true;
- 2⁰. the Cauchy problem (26), (27) has a solution in the domain D^- .

Then the asymptotic soliton-like solution to problem (1), (4) is written as (30) and satisfies the Cauchy problem with accuracy $O(\varepsilon^N)$, $N \in \mathbf{N}$, for all $(x, t) \in \mathbf{R} \times [0; T]$. Moreover, as $\tau \rightarrow \pm\infty$, function (30) satisfies the Cauchy problem (1), (4) with accuracy $O(\varepsilon^{N+1})$, $N \in \mathbf{N}$.

Proof. It is obvious that function (30) satisfies initial condition (4). The last part of Theorem 3.4 is proved according to the scheme of proof for Theorem 2 in [21].

Now let us consider the estimate for the difference between the exact solution and asymptotic soliton-like solution to the Cauchy problem (1), (4).

The following theorem is true.

Theorem 3.5 Suppose the following propositions are satisfied:

- 1⁰. the functions $a(x, t, \varepsilon)$, $b(x, t, \varepsilon)$, $c(x, t, \varepsilon)$ satisfy the assumptions $a(x, t, \varepsilon) = a(x, \varepsilon) \in C^\infty(\mathbf{R})$, $b(x, t, \varepsilon) \in C^\infty(\mathbf{R} \times [0; T])$, $c(x, t, \varepsilon) = c(t, \varepsilon) \in C^\infty([0; T])$;
- 2⁰. the inequalities $r_1 \leq a(x, \varepsilon) \leq r_2$, $|b(x, t, \varepsilon)| < l_1$, $|b_x(x, t, \varepsilon)| < l_2$ take place for all $x \in \mathbf{R}$, $t \in [0; T]$, where r_1 , r_2 , l_1 , l_2 are some positive constants;
- 3⁰. the Cauchy problem (1), (4) has a solution $u(x, t, \varepsilon) \in C^\infty(0, T; S)$;
- 4⁰. the functions $a_k(x) \in C^\infty(\mathbf{R})$, $b_k(x, t) \in C^\infty(\mathbf{R} \times [0; T])$, $c_k(t) \in C^\infty([0; T])$, $k = \overline{0, N}$, are absolutely bounded for all $x \in \mathbf{R}$, $t \in [0; T]$, and the inequality $a_0(x) b_0(x, t) c_0(t) \neq 0$ holds for all $x \in \mathbf{R}$, $t \in [0; T]$;
- 5⁰. the function $f(x, \varepsilon)$ in initial condition (4) can be represented as

$$f(x, \varepsilon) = \sum_{j=0}^N \varepsilon^j [g_j(x) + f_j(x, \varepsilon)],$$

where $g_j(x) \in S(\mathbf{R})$, $f_j(x, \varepsilon) \in \mathcal{M}_j(\varepsilon)$, $j = \overline{0, N}$;

- 6⁰. equation (8) with the initial condition $u_0(x, 0) = g_0(x)$, $x \in \mathbf{R}$, as well as equation (9) with the initial condition $u_j(x, 0) = g_j(x)$, $x \in \mathbf{R}$, $j = \overline{1, N}$, has the solution $u_j(x, t) \in C^\infty(0, T; S)$, $j = \overline{0, N}$;

- 7⁰. the conditions 4⁰ – 6⁰ of Theorem 3.3 are true.

Then for the exact solution $u(x, t, \varepsilon)$ and asymptotic solution (34) to the Cauchy problem (1), (4) the following asymptotic estimate

$$|||u(x, t, \varepsilon) - Y_N(x, t, \varepsilon)||| \leq C\varepsilon^{N+1}, \quad t \in [0; \varepsilon\Theta], \quad (35)$$

is true, where C is a constant not depending on the parameter ε , and Θ is a positive number.

Proof. Similarly to the proof of Theorem 3.2 let us consider the difference $\omega_N(x, t, \varepsilon) = u(x, t, \varepsilon) - Y_N(x, t, \varepsilon)$. As above, we obtain

$$\begin{aligned} -\frac{\varepsilon^2}{2} \frac{d}{dt} \int_{-\infty}^{+\infty} |\omega_{Nx}(x, t, \varepsilon)|^2 dx &= \frac{1}{2} \frac{d}{dt} \int_{-\infty}^{+\infty} a(x, \varepsilon) \omega_N^2(x, t, \varepsilon) dx - \\ -\frac{1}{2} \int_{-\infty}^{+\infty} b_x(x, t, \varepsilon) \omega_N^2(x, t, \varepsilon) dx - \int_{-\infty}^{+\infty} c(t, \varepsilon) Y_N(x, t, \varepsilon) \omega_N(x, t, \varepsilon) \omega_{Nx}(x, t, \varepsilon) dx + \\ + \int_{-\infty}^{+\infty} g_N(x, t, \varepsilon) \omega_N(x, t, \varepsilon) dx, \end{aligned} \quad (36)$$

where

$$\begin{aligned} g_N(x, t, \varepsilon) &= -\varepsilon^2 Y_{Nxt}(x, t, \varepsilon) + a(x, \varepsilon) Y_{Nt}(x, t, \varepsilon) + \\ &+ b(x, t, \varepsilon) Y_{Nx}(x, t, \varepsilon) + c(t, \varepsilon) Y_N(x, t, \varepsilon) Y_{Nx}(x, t, \varepsilon). \end{aligned}$$

According to Theorem 3.3 and the technique of constructing the asymptotic soliton-like solution to problem (1), (4), the function $g_N(x, t, \varepsilon)$ belongs to the space $C^\infty(0, T; S)$. Moreover, it satisfies the asymptotic relation $g_N(x, t, \varepsilon) = O(\varepsilon^N)$ as $\varepsilon \rightarrow 0$.

From (36) we find

$$\frac{1}{2} \frac{d}{dt} E_N^2 \leq p E_N^2 + q E_N, \quad (37)$$

where

$$E_N^2 = |||\omega_N(x, t, \varepsilon)|||^2 = ||\sqrt{a(x, \varepsilon)} \omega_N(x, t, \varepsilon)|||^2 + \varepsilon^2 ||\omega_{Nx}(x, t, \varepsilon)|||^2, \quad (38)$$

$$\begin{aligned} p &= \frac{1}{2} \max_{(x, t) \in \mathbf{R} \times [0; T]} \left| \frac{b_x(x, t, \varepsilon)}{a(x, \varepsilon)} \right| + \max_{(x, t) \in \mathbf{R} \times [0; T]} \left| c(t, \varepsilon) \frac{Y_N(x, t, \varepsilon)}{a(x, \varepsilon)} \right| + \\ &+ \frac{1}{\varepsilon} \max_{(x, t) \in \mathbf{R} \times [0; T]} |c(t, \varepsilon) Y_N(x, t, \varepsilon)|, \end{aligned} \quad (39)$$

$$q = \max_{t \in [0; T]} \left(\int_{-\infty}^{+\infty} \left| \frac{g_N(x, t, \varepsilon)}{\sqrt{a(x, \varepsilon)}} \right|^2 dx \right)^{1/2}. \quad (40)$$

It is easy to see that the values p, q satisfy the asymptotic equalities

$$p = O\left(\frac{1}{\varepsilon}\right), \quad q = O(\varepsilon^N) \quad \text{as } \varepsilon \rightarrow 0.$$

Inequality (37) is equivalent to the relation

$$\frac{dy}{dt} \leq py + q, \quad y(0) = 0, \quad (41)$$

where $y = y(t) = E_N(x, t, \varepsilon)$.

It now follows that

$$y(t) \leq \frac{q}{p} (e^{pt} - 1)$$

providing asymptotic estimate (35).

4 Conclusions

The problem of estimating the difference between the exact solution and asymptotic soliton-like solution to the Cauchy problem for the singularly perturbed BBM equation with variable coefficients is considered. The initial data for the Cauchy problem are defined according to the concept of asymptotic soliton-like solution. In other words, it is taken into account that the asymptotic soliton-like solution is a certain deformation of the soliton solution for the corresponding BBM equation with constant coefficients.

We present asymptotic estimates for the difference between the exact solution to the BBM equation and the N-th approximation for the constructed asymptotic soliton-like solution. Similarly to the singularly perturbed Korteweg-de Vries equation, these estimates are local [27, 28]. Nevertheless, they show that the asymptotic soliton-like solutions constructed through the nonlinear WKB method for the singularly perturbed BBM equation with variable coefficients are sufficiently suitable as the approximate solutions.

Acknowledgment

The second author was supported by the Ministry of Education and Science of Ukraine, and Taras Shevchenko National University of Kyiv, Grant No. 16 BA 038 – 01.

References

- [1] H. Peregrin. Calculations of the development of an undular bore. *J. Fluid Mechanics* **25** (2) (1966) 321–330.
- [2] T. B. Benjamin, J. L. Bona, J. J. Mahony. Model equations for long waves in nonlinear dispersive systems. *Philos. Trans. R. Soc. Lond., Ser. A* **272** (1972) 47–78.
- [3] J. Avrin. Global existence for generalized transport equations. *Mat. Apl. Comput.* **4** (1985) 67–74.
- [4] J. C. Eilbeck, G. R. McGuire. Numerical studies of the regularized long wave equation. I. *J. Comp. Phys.* **19** (1975) 43–57.
- [5] J. C. Eilbeck, G. R. McGuire. Numerical studies of the regularized long wave equation. II. *J. Comp. Phys.* **23** (1977) 63–73.
- [6] B. Wang, W. Yang. Finite-dimensional behaviour for the Benjamin-Bona-Mahony equation. *J. Phys. A, Math. Gen.* **30** (13) (1997) 4877–4885.
- [7] A. M. Wazwaz, M. A. Helal. Nonlinear variants of the BBM equation with compact and noncompact physical structures. *Chaos Solitons Fractals* **26** (3) (2005) 767–776.
- [8] Abdul-Majid Wazwaz. Peakons and Soliton Solutions of Newly Developed Benjamin-Bona-Mahony-Like Equations. *Nonlinear Dynamics and Systems Theory* **15** (2) (2015) 209–220.

- [9] R. Arora, V. Kumar. Nonlinear variants of the BBM equation with compact and noncompact physical structures. *Applied Mathematics* **1** (2011) 59–61.
- [10] A. Seadway, A. Sayed. Travelling Wave Solutions of the Benjamin-Bona-Mahony Wave Equations. *Abstract and Applied Analysis* (2014) <http://doi.org/10.1155/2014/926838>.
- [11] G. El, M. Hoefer, M. Shearer. Expansion shock waves in regularized shallow-water theory. *Proceedings Royal Society. A.* **472** (2189) (2016).
- [12] G. Santarelli. Numerical analysis of the regularized long-wave equation: Anelastic collision of solitary waves. *Nuov Cim B* **46** (1) (1978) 179–188.
- [13] R. K. Dodd, J. C. Eilbeck, J. D. Gibbon, H. C. Morris. *Solitons and Nonlinear Wave Equations*. Academic Press. A Subsidiary of Harcourt Brace Jovanovich, Publishers, London etc., 1982.
- [14] L. Brizhik, A. Eremko, B. Piette, W. Zakrzewski. Solitons in α -helical proteins. *Phys. Rev. E* **70** (2004) DOI: <https://doi.org/10.1103/PhysRevE.70.031914>
- [15] R. B. Djou, E. Tala-Tebue, A. Kenfack-Jiotsa, T. C. Kofane. The Jacobi Elliptic Method and Its Applications to the Generalized Form of the Phi-Four Equation. *Nonlinear Dynamics and Systems Theory* **16** (3) (2016) 260–267.
- [16] V. A. Danylenko, S. I. Skurativskyi. Travelling Wave Solutions of Nonlocal Models for Media with Oscillating Inclusions. *Nonlinear Dynamics and Systems Theory* **12** (4) (2012) 365–374.
- [17] G. Whitham. *Linear and Nonlinear Waves*. John Wiley & Sons, New York, 1974.
- [18] M. H. A. Biswas, M. A. Rahman, T. Das. Optical Soliton in Nonlinear Dynamics and Its Graphical Representation. *Nonlinear Dynamics and Systems Theory* **11** (4) (2011) 383–396.
- [19] M. J. Ablowitz. *Nonlinear Dispersive Waves. Asymptotic Analysis and Solitons*. Cambridge University Press, Cambridge, 2011.
- [20] Monica De Angelis. Asymptotic Estimates Related to an Integro Differential Equation. *Nonlinear Dynamics and Systems Theory* **13** (3) (2013) 217–228.
- [21] V. Samoilenco, Y. Samoilenco. Asymptotic soliton-like solutions to the singularly perturbed Benjamin-Bona-Mahony equation with variable coefficients. *J. Math. Phys.* **60** (1) (2019). <http://doi.org/10.1063/1.5085291>
- [22] R. M. Miura, M. D. Kruskal. Application of a nonlinear WKB method to the Korteweg-deVries equation. *SIAM J. Appl. Math.* **26** (1974) 376–395.
- [23] V. P. Maslov, G. A. Omel'yanov. *Geometric Asymptotics for Nonlinear PDE. I*. American Mathematical Society (AMS), Providence, RI, 2001.
- [24] V. H. Samoilenco, Y. I. Samoilenco. Asymptotic expansions for one-phase soliton-type solutions of the Korteweg-de Vries equation with variable coefficients. *Ukr. Mat. J.* **57** (1) (2005) 132–148.
- [25] V. H. Samoilenco, Y. I. Samoilenco. Asymptotic solutions of the Cauchy problem for the singularly perturbed Korteweg-de Vries equation with variable coefficients. *Ukr. Mat. J.* **59** (1) (2007) 126–139.
- [26] A. H. Nayfeh. *Introduction to Perturbation Techniques*. A Wiley-interscience Publication, New York, Chichester, Brisbane, Toronto, 1981.
- [27] Y. I. Samoilenco. One-phase soliton type solution of the Cauchy problem for a singularly perturbed Korteweg-de Vries equation with variable coefficients (case of special initial data). *Zb. Pr. Inst. Mat. NAN Ukr.* **9** (2) (2012) 327–340. [Ukrainian]
- [28] V. G. Samoilenco, Y. I. Samoilenco. Asymptotic multiphase Σ -solutions to the singularly perturbed korteweg-de vries equation with variable coefficients. *J. Math. Sci.* **200** (3) (2014) 358–373.



Oscillation Criteria for Delay Equations with Several Non-Monotone Arguments

I. P. Stavroulakis ^{*,1,2}, Zh. Kh. Zhunussova ², L. Kh. Zhunussova ³ and K. Dosmagulova ²

¹ Department of Mathematics, University of Ioannina, 451 10 Ioannina, HELLAS (Greece)

² Al-Farabi Kazakh National University, Almaty, 050040 Kazakhstan

³ Abai Kazakh National Pedagogical University, Almaty, 050010, Kazakhstan

Received: May 7, 2019; Revised: January 15, 2020

Abstract: Consider the first-order linear differential equation with several retarded arguments $x'(t) + \sum_{i=1}^m p_i(t)x(\tau_i(t)) = 0$, $t \geq t_0$, where the functions $p_i, \tau_i \in C([t_0, \infty), \mathbb{R}^+)$, for every $i = 1, 2, \dots, m$, $\tau_i(t) \leq t$ for $t \geq t_0$ and $\lim_{t \rightarrow \infty} \tau_i(t) = \infty$. In this paper we review the most interesting sufficient conditions under which all solutions oscillate. An example illustrating the results is given.

Keywords: oscillation; retarded; differential equations; non-monotone arguments.

Mathematics Subject Classification (2010): Primary 34K11, Secondary 34K06.

1 Introduction

Consider the first-order linear differential equation with several non-monotone retarded arguments

$$x'(t) + \sum_{i=1}^m p_i(t)x(\tau_i(t)) = 0, \quad t \geq t_0, \quad (1.1)$$

where the functions $p_i, \tau_i \in C([t_0, \infty), \mathbb{R}^+)$, for every $i = 1, 2, \dots, m$, (here $\mathbb{R}^+ = [0, \infty)$), $\tau_i(t) \leq t$ for $t \geq t_0$ and $\lim_{t \rightarrow \infty} \tau_i(t) = \infty$.

Let $T_0 \in [t_0, +\infty)$, $\tau(t) = \min \{\tau_i(t) : i = 1, \dots, m\}$ and $\tau_{-1}(t) = \sup \{s : \tau(s) \leq t\}$. By a solution of the equation (1.1) we understand a function $x \in C([T_0, +\infty), \mathbb{R})$, continuously differentiable on $[\tau_{-1}(T_0), +\infty]$ and that satisfies (1.1) for $t \geq \tau_{-1}(T_0)$. Such a solution is called *oscillatory* if it has arbitrarily large zeros, and otherwise it is called *non-oscillatory*.

For the general theory the reader is referred to [9, 11, 12, 17].

The oscillatory behavior of functional differential equations has been the subject of many investigations. See, for example, [1–20] and the references cited therein.

* Corresponding author: <mailto:ipstav@uoи.gr>

2 Oscillation Conditions for Eq. (1.1)

Concerning the differential equation (1.1) with several non-monotone arguments the following related oscillation results have been recently published.

Assume that there exist non-decreasing functions $\sigma_i \in C([t_0, \infty), \mathbb{R}^+)$ such that

$$\tau_i(t) \leq \sigma_i(t) \leq t, \quad i = 1, 2, \dots, m. \quad (2.1)$$

In 2015, Infante, Kopladatze and Stavroulakis [14] proved that if

$$\limsup_{t \rightarrow \infty} \prod_{j=1}^m \left[\prod_{i=1}^m \int_{\sigma_j(t)}^t p_i(s) \exp \left(\int_{\tau_i(s)}^{\sigma_i(t)} \sum_{i=1}^m p_i(\xi) \exp \left(\int_{\tau_i(\xi)}^{\xi} \sum_{i=1}^m p_i(u) du \right) d\xi \right) ds \right]^{1/m} > \frac{1}{m^m}, \quad (2.2)$$

then all solutions of Eq. (1.1) oscillate.

Also, in 2015, Kopladatze [15] improved the above condition as follows. Let there exist some $k \in \mathbb{N}$ such that

$$\begin{aligned} \limsup_{t \rightarrow \infty} \prod_{j=1}^m \left[\prod_{i=1}^m \int_{\sigma_j(t)}^t p_i(s) \exp \left(m \int_{\tau_i(s)}^{\sigma_i(t)} \left(\prod_{\ell=1}^m p_\ell(\xi) \right)^{\frac{1}{m}} \psi_k(\xi) d\xi \right) ds \right]^{\frac{1}{m}} \\ > \frac{1}{m^m} \left[1 - \prod_{i=1}^m c_i(\alpha_i) \right], \end{aligned} \quad (2.3)$$

where

$$\psi_1(t) = 0, \quad \psi_i(t) = \exp \left(\sum_{j=1}^m \int_{\tau_j(t)}^t \left(\prod_{\ell=1}^m p_\ell(s) \right)^{\frac{1}{m}} \psi_{i-1}(s) ds \right), \quad i = 2, 3, \dots,$$

$$0 < \alpha_i := \liminf_{t \rightarrow \infty} \int_{\sigma_i(t)}^t p_i(s) ds < \frac{1}{e}, \quad i = 1, 2, \dots, m, \quad (2.4)$$

and

$$c_i(\alpha_i) = \frac{1 - \alpha_i - \sqrt{1 - 2\alpha_i - \alpha_i^2}}{2}, \quad i = 1, 2, \dots, m, \quad (2.5)$$

then all solutions of Eq. (1.1) oscillate.

In 2016, Braverman, Chatzarakis and Stavroulakis [7] obtained the following iterative sufficient oscillation conditions

$$\limsup_{t \rightarrow \infty} \int_{h(t)}^t \sum_{i=1}^m p_i(u) a_r(h(t), \tau_i(u)) du > 1, \quad (2.6)$$

or

$$\limsup_{t \rightarrow \infty} \int_{h(t)}^t \sum_{i=1}^m p_i(u) a_r(h(t), \tau_i(u)) du > 1 - \frac{1 - \alpha - \sqrt{1 - 2\alpha - \alpha^2}}{2}, \quad (2.7)$$

or

$$\liminf_{t \rightarrow \infty} \int_{h(t)}^t \sum_{i=1}^m p_i(u) a_r(h(t), \tau_i(u)) du > \frac{1}{e}, \quad (2.8)$$

where

$$\begin{aligned} h(t) &= \max_{1 \leq i \leq m} h_i(t) \text{ and } h_i(t) = \sup_{t_0 \leq s \leq t} \tau_i(s), \quad i = 1, 2, \dots, m, \\ 0 < \alpha &:= \liminf_{t \rightarrow \infty} \int_{h(t)}^t \sum_{i=1}^m p_i(s) ds \leq \frac{1}{e} \end{aligned} \quad (2.9)$$

$$\text{and } a_1(t, s) = \exp\left(\int_s^t \sum_{i=1}^m p_i(u) du\right), \quad a_{r+1}(t, s) = \exp\left(\int_s^t \sum_{i=1}^m p_i(u) a_r(u, \tau_i(u)) du\right), \quad r \in \mathbb{N}.$$

Also, in 2016, Akca, Chatzarakis and Stavroulakis [1] improved that result replacing condition (2.6) by the iterative condition

$$\limsup_{t \rightarrow \infty} \int_{h(t)}^t \sum_{i=1}^m p_i(u) a_r(h(u), \tau_i(u)) du > \frac{1 + \ln \lambda_0}{\lambda_0}, \quad (2.10)$$

where λ_0 is the smaller root of the equation $\lambda = e^{\alpha\lambda}$, $0 < \alpha := \liminf_{t \rightarrow \infty} \int_{\tau(t)}^t \sum_{i=1}^m p_i(s) ds \leq \frac{1}{e}$ and $\tau(t) = \max_{1 \leq i \leq m} \tau_i(t)$.

In 2018, Attia et al. [3] established the following oscillation conditions.

Assume that $0 < \rho := \liminf_{t \rightarrow \infty} \int_{g(t)}^t \sum_{k=1}^n p_k(s) ds \leq \frac{1}{e}$, and

$$\limsup_{t \rightarrow \infty} \left(\int_{g(t)}^t Q(v) dv + c(\rho) e^{\int_{g(t)}^t \sum_{i=1}^n p_i(s) ds} \right) > 1,$$

where

$$Q(t) = \sum_{k=1}^n \sum_{i=1}^n p_i(t) \int_{\tau_i(t)}^t p_k(s) e^{\int_{g_k(t)}^t \sum_{i=1}^n p_i(s) ds + (\lambda(\rho) - \epsilon) \int_{\tau_k(s)}^{g_k(t)} \sum_{\ell=1}^n p_\ell(u) du} ds,$$

$\epsilon \in (0, \lambda(\rho))$, or

$$\limsup_{t \rightarrow \infty} \left(\int_{g(t)}^t Q_1(v) dv + c(\rho) e^{\int_{g(t)}^t \sum_{i=1}^n p_i(s) ds} \right) > 1,$$

where

$$Q_1(t) = \sum_{k=1}^n \sum_{i=1}^n p_i(t) \int_{\tau_i(t)}^t p_k(s) e^{\int_{g_k(t)}^t \sum_{i=1}^n p_i(s) ds + \int_{\tau_k(s)}^{g_k(t)} \sum_{\ell=1}^n (\lambda(q_\ell) - \epsilon_\ell) p_\ell(u) du} ds,$$

$\epsilon_\ell \in (0, \lambda(q_\ell))$, and $q_\ell = \liminf_{t \rightarrow \infty} \int_{\tau_\ell(t)}^t p_\ell(s) ds$, $\ell = 1, 2, \dots, m$, or

$$\limsup_{t \rightarrow \infty} \left(\prod_{j=1}^n \left(\prod_{k=1}^n \int_{g_j(t)}^t R_k(s) ds \right)^{\frac{1}{n}} + \frac{\prod_{k=1}^n c(\beta_k)}{n^n} e^{\sum_{k=1}^n \int_{g_k(t)}^t \sum_{\ell=1}^n p_\ell(s) ds} \right) > \frac{1}{n^n},$$

where

$$R_k(s) = e^{\int_{g_k(s)}^s \sum_{i=1}^n p_i(u) du} \sum_{i=1}^n p_i(s) \int_{\tau_i(s)}^s p_k(u) e^{(\lambda(\rho) - \epsilon) \int_{\tau_k(u)}^{g_k(s)} \sum_{\ell=1}^n p_\ell(v) dv} du,$$

$\epsilon \in (0, \lambda(\rho))$, and $0 < \beta_k := \liminf_{t \rightarrow \infty} \int_{\sigma_i(t)}^t p_i(s) ds \leq \frac{1}{e}$. Then Eq. (1.1) is oscillatory.

Recently Bereketoglu et al. [4] established the following conditions.

Assume that there exist non-decreasing functions $\sigma_i \in C([t_0, \infty), \mathbb{R}^+)$ such that (2.1) is satisfied and for some $k \in \mathbb{N}$

$$\limsup_{t \rightarrow \infty} \prod_{j=1}^m \left[\prod_{i=1}^m \left(\int_{\sigma_j(t)}^t p_i(s) \exp \left(\int_{\tau_i(s)}^{\sigma_i(t)} P_k(u) du \right) ds \right) \right]^{1/m} > \frac{1}{m^m}, \quad (2.11)$$

or

$$\limsup_{t \rightarrow \infty} \prod_{j=1}^m \left[\prod_{i=1}^m \left(\int_{\sigma_j(t)}^t p_i(s) \exp \left(\int_{\tau_i(s)}^{\sigma_i(t)} P_k(u) du \right) ds \right) \right]^{1/m} > \frac{1}{m^m} \left[1 - \prod_{i=1}^m c_i(\alpha_i) \right], \quad (2.12)$$

where

$$P_k(t) = \sum_{j=1}^m p_j(t) \left\{ 1 + m \left[\prod_{i=1}^m \int_{\sigma_j(t)}^t p_i(s) \exp \left(\int_{\tau_i(s)}^t P_{k-1}(u) du \right) ds \right]^{1/m} \right\},$$

with $P_0(t) = m \left[\prod_{\ell=1}^m p_\ell(t) \right]^{1/m}$, α_i is given by (2.4) and $c_i(\alpha_i)$ by (2.5). Then all solutions of Eq.(1.1) oscillate.

Very recently Moremedi, Jafari and Stavroulakis [19] further improved the above conditions as follows.

Assume that there exist non-decreasing functions $\sigma_i \in C([t_0, \infty), \mathbb{R}^+)$ such that (2.1) is satisfied and for some $k \in \mathbb{N}$

$$\limsup_{t \rightarrow \infty} \prod_{j=1}^m \left[\prod_{i=1}^m \left(\int_{\sigma_j(t)}^t p_i(s) \exp \left(\int_{\tau_i(s)}^{\sigma_i(t)} P_k(u) du \right) ds \right) \right]^{1/m} > \frac{1}{m^m}, \quad (2.13)$$

or

$$\limsup_{t \rightarrow \infty} \prod_{j=1}^m \left[\prod_{i=1}^m \left(\int_{\sigma_j(t)}^t p_i(s) \exp \left(\int_{\tau_i(s)}^{\sigma_i(t)} P_k(u) du \right) ds \right) \right]^{1/m} > \frac{1}{m^m} \left[1 - \prod_{i=1}^m c_i(\alpha_i) \right], \quad (2.14)$$

where

$$P_k(t) = P(t) \left[1 + \int_{\sigma_i(t)}^t P(s) \exp \left(\int_{\tau_i(s)}^t P(u) \exp \left(\int_{\tau_i(u)}^u P_{k-1}(\xi) d\xi \right) du \right) ds \right] \quad (2.15)$$

with $P_0(t) = P(t) = \sum_{i=1}^m p_i(t)$, α_i is given by (2.4) and $c_i(\alpha_i)$ by (2.5). Then all solutions of Eq.(1.1) oscillate.

Remark 2.1 It is clear that the left-hand sides of both conditions (2.11), (2.12) and (2.13), (2.14) are identically the same and also the right-hand side of (2.12) and (2.14) reduces to (2.11) and (2.13) when $c_i(\alpha_i) = 0$. Thus, it seems that the above conditions (2.14) and (2.12) are exactly the same as conditions (2.13) and (2.11), when $c_i(\alpha_i) = 0$. One may notice, however, that the condition (2.4) is required in (2.14) and (2.12) but not in (2.13) and (2.11).

In the case of monotone arguments we have the following.

Let τ_i be non-decreasing functions and for some $k \in \mathbb{N}$

$$\limsup_{t \rightarrow \infty} \prod_{j=1}^m \left[\prod_{i=1}^m \int_{\tau_j(t)}^t \left(p_i(s) \exp \left(\int_{\tau_i(s)}^{\tau_i(t)} P_k(u) du \right) ds \right) \right]^{1/m} > \frac{1}{m^m} \quad (2.16)$$

or

$$\limsup_{t \rightarrow \infty} \prod_{j=1}^m \left[\prod_{i=1}^m \int_{\tau_j(t)}^t \left(p_i(s) \exp \left(\int_{\tau_i(s)}^{\tau_i(t)} P_k(u) du \right) ds \right) \right]^{1/m} > \frac{1}{m^m} \left[1 - \prod_{i=1}^m c_i(\alpha_i) \right], \quad (2.17)$$

where

$$P_k(t) = P(t) \left[1 + \int_{\tau_i(t)}^t P(s) \exp \left(\int_{\tau_i(s)}^t P(u) \exp \left(\int_{\tau_i(u)}^u P_{k-1}(\xi) d\xi \right) du \right) ds \right] \quad (2.18)$$

with $P_0(t) = P(t) = \sum_{j=1}^m p_j(t)$, α_i is given by (2.4), and $c_i(\alpha_i)$ by (2.5). Then all solutions of (1.1) oscillate.

At this point it should be mentioned that in the case of monotone arguments several oscillation conditions involving the \liminf were established.

In 1982, Ladas and Stavroulakis [16] considered the differential equation with several constant delays of the form

$$x'(t) + \sum_{i=1}^m p_i(t)x(t - \tau_i) = 0, \quad (2.19)$$

where τ_i , $i = 1, 2, \dots, m$ are positive constants and $p_i(t)$, $i = 1, 2, \dots, m$ are positive and continuous functions, and established the following oscillation conditions involving \liminf . (See also [1, 2]). Consider the differential equations (2.19) and assume that

$$\liminf_{t \rightarrow \infty} \int_{t-(\tau_i/2)}^t p(s)ds > 0, \quad i = 1, 2, \dots, m. \quad (2.20)$$

Then each one of the following conditions

$$\liminf_{t \rightarrow \infty} \int_{t-\tau_i}^t p_i(s)ds > \frac{1}{e}, \text{ for some } i, \quad i = 1, 2, \dots, m, \quad (2.21)$$

$$\liminf_{t \rightarrow \infty} \int_{t-\tau}^t \sum_{i=1}^m p_i(s)ds > \frac{1}{e}, \text{ where } \tau = \min[\tau_1, \dots, \tau_m], \quad (2.22)$$

$$\left[\prod_{i=1}^m \left(\sum_{j=1}^m \liminf_{t \rightarrow \infty} \int_{t-\tau_j}^t p_i(s)ds \right) \right]^{\frac{1}{n}} > \frac{1}{e} \quad (2.23)$$

or

$$\begin{aligned} & \frac{1}{m} \sum_{i=1}^m \left(\liminf_{t \rightarrow \infty} \int_{t-\tau_i}^t p_i(s)ds \right) + \\ & \frac{2}{m} \sum_{i < j, i, j=1}^m \left[\left(\liminf_{t \rightarrow \infty} \int_{t-\tau_j}^t p_i(s)ds \right) \times \left(\liminf_{t \rightarrow \infty} \int_{t-\tau_i}^t p_j(s)ds \right) \right]^{1/2} > \frac{1}{e} \end{aligned} \quad (2.24)$$

implies that every solution of (2.19) oscillates.

Later in 1996, Li [18] proved that the same conclusion holds if

$$\liminf_{t \rightarrow \infty} \sum_{i=1}^m \int_{t-\tau_i}^t p_i(s)ds > \frac{1}{e}. \quad (2.25)$$

In 1984, Hunt and Yorke [13] considered the differential equation with variable delays of the form

$$x'(t) + \sum_{i=1}^m p_i(t)x(t - \tau_i(t)) = 0, \quad (2.26)$$

where τ_i are continuous and positive valued on $[0, \infty)$ and proved the following. If there is a uniform upper bound τ_0 on the τ_i 's and

$$\liminf_{t \rightarrow \infty} \sum_{i=1}^m p_i(t)\tau_i(t) > \frac{1}{e}, \quad (2.27)$$

then all solutions of Eq. (2.26) oscillate.

In 2003, Grammatikopoulos, Koplatadze and Stavroulakis [10] also studied Eq.(1.1) in the case that $\tau_i(t)$ ($i = 1, 2, \dots, m$) are nondecreasing, and established the following result. Assume that

$$\int_0^\infty |p_i(t) - p_j(t)| dt < \infty \quad (i, j = 1, 2, \dots, m) \quad (2.28)$$

$$\liminf_{t \rightarrow \infty} \int_{\tau_i(t)}^t p_i(s) ds > 0 \quad (i = 1, 2, \dots, m) \quad (2.29)$$

and

$$\sum_{i=1}^m \left(\liminf_{t \rightarrow \infty} \int_{\tau_i(t)}^t p_i(s) ds \right) > \frac{1}{e}. \quad (2.30)$$

Then all solutions of Eq. (1.1) oscillate.

3 Corollaries and Examples

In the case $m = 1$, Eq.(1.1) reduces to the equation

$$x'(t) + p(t)x(\tau(t)) = 0. \quad (3.1)$$

In 2012, Braverman and Karpuz [6] derived the following sufficient oscillation condition for Eq.(3.1):

$$\limsup_{t \rightarrow \infty} \int_{\sigma(t)}^t p(s) \exp \left\{ \int_{\tau(s)}^{\sigma(t)} p(\xi) d\xi \right\} ds > 1, \quad (3.2)$$

while in 2014, Stavroulakis [20] improved the above condition as follows:

$$\limsup_{t \rightarrow \infty} \int_{\sigma(t)}^t p(s) \exp \left\{ \int_{\tau(s)}^{\sigma(t)} p(\xi) d\xi \right\} ds > 1 - \frac{1}{2} \left(1 - \alpha - \sqrt{1 - 2\alpha - \alpha^2} \right), \quad (3.3)$$

where $\sigma(t) := \sup_{s \leq t} \tau(s)$.

From the above conditions (2.13) and (2.14) the following corollary is immediate. It is clear that the conditions in this corollary essentially improve the conditions (3.2) and (3.3).

Corollary 3.1 *Assume that there exists a non-decreasing function $\sigma(t)$ such that $\tau(t) \leq \sigma(t) \leq t$ and for some $k \in \mathbb{N}$*

$$\limsup_{t \rightarrow \infty} \int_{\sigma(t)}^t p(s) \exp \left(\int_{\tau(s)}^{\sigma(t)} P_k(u) du \right) ds > 1 \quad (3.4)$$

or

$$\limsup_{t \rightarrow \infty} \int_{\sigma(t)}^t p(s) \exp \left(\int_{\tau(s)}^{\sigma(t)} P_k(u) du \right) ds > 1 - c(\alpha), \quad (3.5)$$

where

$$P_k(t) = p(t) \left[1 + \int_{\sigma(t)}^t p(s) \exp \left(\int_{\tau(s)}^t p(u) \exp \left(\int_{\tau(u)}^u P_{k-1}(\xi) d\xi \right) du \right) ds \right], \quad P_0(t) = p(t),$$

$$0 < \alpha := \liminf_{t \rightarrow \infty} \int_{\sigma(t)}^t p(s) ds \leq \frac{1}{e}, \quad (3.6)$$

and $c(\alpha) = \frac{1 - \alpha - \sqrt{1 - 2\alpha - \alpha^2}}{2}$. Then all solutions of Eq.(3.1) oscillate.

The following example is given to illustrate the results. Note that in this example (cf. [4, 6, 14, 19]) the interval of the values that p can take is increased.

Example 3.1 Consider the equation

$$x'(t) + px(\tau(t)) = 0, \quad t \geq 0, \quad p > 0, \quad (3.7)$$

with the retarded argument

$$\tau(t) = \begin{cases} t - 1, & t \in [3n, 3n + 1], \\ -3t + (12n + 3), & t \in [3n + 1, 3n + 2], \\ 5t - (12n + 13), & t \in [3n + 2, 3n + 3]. \end{cases}$$

For this equation, as in [6, 14], one may choose the function

$$\sigma(t) = \begin{cases} t - 1, & t \in [3n, 3n + 1], \\ -3n, & t \in [3n + 1, 3n + 2.6], \\ 5t - (12n + 13), & t \in [3n + 2.6, 3n + 3]. \end{cases}$$

If we choose $t_n = 3n + 3$, (cf. [[6], Example 1] and [[14], Example 4.2]), then for $k = 1$, the condition (3.4) of Corollary 1 reduces to

$$\limsup_{t \rightarrow \infty} \int_{\sigma(t)}^t p \exp \left(\int_{\tau(s)}^{\sigma(t)} P_1(u) du \right) ds \geq \lim_{n \rightarrow \infty} \int_{3n+2}^{3n+3} p \exp \left(\int_{5s-(12n+13)}^{3n+2} P_1(u) du \right) ds,$$

where

$$\begin{aligned} P_1(t) &= p \left[1 + \int_{\sigma(t)}^t p \exp \left(\int_{\tau(s)}^t p \exp \left(\int_{\tau(u)}^u pd\xi \right) du \right) ds \right] \\ &\geq p \left[1 + \int_{3n+2}^{3n+3} p \exp \left(\int_{5s-(12n+13)}^{3n+3} p \exp(p) du \right) ds \right] \\ &= p \left[1 + \left(\frac{e^{6pe^p} - e^{pe^p}}{5} \right) e^{-p} \right]. \end{aligned}$$

Therefore

$$\limsup_{t \rightarrow \infty} \int_{\sigma(t)}^t p \exp \left(\int_{\tau(s)}^{\sigma(t)} P_1(u) du \right) ds \geq \frac{p}{5P_1} (e^{5P_1} - 1),$$

where $P_1 = p \left[1 + \left(\frac{e^{6pe^p} - e^{pe^p}}{5} \right) e^{-p} \right]$. For $p = 0.251$, $P_1 \approx 0.4676$, and so $\frac{p}{5P_1} (e^{5P_1} - 1) \approx 1.0052 > 1$. Therefore all solutions of Eq.(3.7) oscillate.

Observe, however, that when we consider the conditions stated in [1, 6, 7, 14, 15, 20] and [4] for the above equation (3.7), we obtain the following.

1. Observe that, for $t_n = 3n + 3$,

$$\int_{\sigma(3n+3)}^{3n+3} p \exp \left\{ \int_{\tau(s)}^{\sigma(3n+3)} p d\xi \right\} ds = \int_{3n+2}^{3n+3} p \exp \left\{ \int_{5s-(12n+13))}^{3n+2} p d\xi \right\} ds = \frac{e^{5p} - 1}{5}$$

and condition (3.2) reduces to $\frac{e^{5p}-1}{5} > 1$. But, for $p = 0.251$, $\frac{e^{5p}-1}{5} \approx 0.50157 < 1$, therefore the condition (3.2) is not satisfied.

2. Similarly, in the condition (3.3), $a = \liminf_{t \rightarrow \infty} \int_{\tau(t)}^t p(s) ds = \lim_{n \rightarrow \infty} \int_{3n+2}^{3n+3} p ds = p$ and $c(a) = c(p) = \frac{1-p-\sqrt{1-2p-p^2}}{2}$. And, as before, (3.3) reduces to $\frac{e^{5p}-1}{5} > 1 - \frac{1-p-\sqrt{1-2p-p^2}}{2}$. Taking $p = 0.251$, the left-hand side of (3.3) is equal to 0.50157, while the right-hand side is 0.95527. Therefore this condition is not satisfied.

3. The condition (2.2) reduces to

$$\limsup_{t \rightarrow +\infty} \int_{\sigma(t)}^t p \exp \left(\int_{\tau(s)}^{\sigma(t)} p \exp \left(\int_{\tau(\xi)}^{\xi} p du \right) d\xi \right) ds > 1, \quad (3.8)$$

and, as in [14], Example 4.2], the choice of $t_n = 3n + 3$ leads to the inequality

$$\frac{(e^{5pe^p} - 1)}{5e^p} > 1. \quad (3.9)$$

Observe, however, that for $p = 0.251$,

$$\frac{(e^{5pe^p} - 1)}{5e^p} \approx 0.62524 < 1.$$

Therefore the condition (3.9) is not satisfied.

4. The condition (2.3), for $k = 2$, reduces to

$$\limsup_{t \rightarrow \infty} \int_{\sigma(t)}^t p \exp \left(\int_{\tau(s)}^{\sigma(t)} p \psi_2(\xi) d\xi \right) ds > 1 - c(\alpha), \quad (3.10)$$

where $\psi_2(\xi) = 1$, and for $t_n = 3n + 3$, as before, it leads to

$$\frac{e^{5p} - 1}{5} > 1 - \frac{1-p-\sqrt{1-2p-p^2}}{2}.$$

For $p = 0.251$, we have

$$\frac{e^{5p} - 1}{5} \approx 0.50157,$$

while the right-hand side

$$1 - c(p) \approx 0.95527.$$

Therefore the condition (3.10) is not satisfied.

5. The condition (2.6) for $r = 1$ reduces to

$$\limsup_{t \rightarrow \infty} \int_{h(t)}^t p a_1(h(t), \tau(s)) ds > 1, \quad (3.11)$$

where

$$h(t) = \sigma(t) \text{ and } a_1(t, s) = \exp \left(\int_s^t p du \right).$$

That is, to the condition

$$\limsup_{t \rightarrow \infty} \int_{\sigma(t)}^t p \exp \left(\int_{\tau(s)}^{\sigma(t)} p d\xi \right) ds > 1, \quad (3.12)$$

and, as before, for $t_n = 3n + 3$ and $p = 0.251$, we have

$$\frac{e^{5p} - 1}{5} \approx 0.50157 < 1. \quad (3.10)$$

Therefore the condition (3.11) is not satisfied.

6. Similarly, condition (2.10) for $r = 1$ reduces to

$$\limsup_{t \rightarrow \infty} \int_{\sigma(t)}^t p \exp \left(\int_{\tau(s)}^{\sigma(t)} p d\xi \right) ds > \frac{1 + \ln \lambda_0}{\lambda_0}, \quad (3.14)$$

where λ_0 is the smaller root of the equation $\lambda = e^{p\lambda}$. As before, for $t_n = 3n + 3$ and $p = 0.251$, we have

$$\frac{e^{5p} - 1}{5} \approx 0.50157,$$

while

$$\frac{1 + \ln \lambda_0}{\lambda_0} \approx 0.94893.$$

Therefore the condition (3.14) is not satisfied.

7. For $k = 1$, condition (2.11) reduces to

$$\limsup_{t \rightarrow \infty} \int_{\sigma(t)}^t p \exp \left(\int_{\tau(s)}^{\sigma(t)} P_1(u) du \right) ds > 1. \quad (3.15)$$

If we choose $t_n = 3n + 3$,

$$\begin{aligned} P_1(t) &= p \left\{ 1 + \int_{\sigma(t)}^t p \exp \left(\int_{\tau(s)}^t pdu \right) ds \right\} = p \left\{ 1 + \int_{3n+2}^{3n+3} p \exp \left(\int_{5s-(12n+13)}^{3n+3} pdu \right) ds \right\} \\ &= p \left(1 + \frac{e^{6p} - e^p}{5} \right). \end{aligned}$$

And, as before, (3.15) reduces to

$$\frac{p}{5P_1} (e^{5P_1} - 1) > 1.$$

For $p = 0.251$ we find $P_1 \approx 0.412812$ and so

$$\frac{p}{5P_1} (e^{5P_1} - 1) \approx 0.836386 < 1.$$

Therefore the condition (3.15) is not satisfied.

We conclude, therefore, that for $p = 0.251$ no one of the conditions (3.2), (3.3), (2.2), (2.3) for $k = 2$, (2.6) and (2.10) for $r = 1$, and (2.11) is satisfied.

It should be also pointed out that not only for this value of $p = 0.251$ but for all values of $p > 0.251$, especially for all values of $p \in [0.251, 0.358]$, (cf. [[14], Example 4.2]),

$$\frac{p}{5P_1} (e^{5P_1} - 1) > 1$$

and therefore all solutions of (3.7) oscillate. Observe, however, that for $p = 0.358$

$$\frac{e^{5p} - 1}{5} \approx 0.99789 < 1,$$

also for $p = 0.3$

$$\begin{aligned} \frac{(e^{5pe^p} - 1)}{5e^p} &\approx 0.974101 < 1, \\ \frac{e^{5p} - 1}{5} &\approx 0.696337 < 0.912993 \approx \frac{1 + \ln \lambda_0}{\lambda_0}, \end{aligned}$$

and for $p = 0.263$, $P_1 \approx 0.44944$ and so

$$\frac{p}{5P_1} (e^{5P_1} - 1) \approx 0.99024 < 1.$$

Therefore for all values of $p \in [0.251, 0.358]$ the conditions of Corollary 1 are satisfied and so all solutions to Eq.(3.7) oscillate, while no one of the above mentioned conditions is satisfied for these values of $p \in [0.251, 0.358]$.

References

- [1] H. Akca, G. E. Chatzarakis, and I. P. Stavroulakis. An oscillation criterion for delay differential equations with several non-monotone arguments. *Appl. Math. Lett.* **59** (1) (2016) 101–108. (arXiv: 1703/04144v1[math.CA]).

- [2] O. Arino, I. Gyori, and A. Jawhari. Oscillation criteria in delay equations. *J. Differential Equations* **53** (1984) 115–123.
- [3] E. R. Attia, V. Benekas, H. A. El-Morshedy and I. P. Stavroulakis. Oscillation of first-order linear differential equations with several non-monotone delays. *Open Math.* **16** (2018) 83–94.
- [4] H. Bereketoglu, F. Karakoc, G. S. Oztepe and I. P. Stavroulakis. Oscillations of first-order differential equations with several non-monotone retarded arguments. *Georgian Math. J.* (2019), doi.org/10.1515/gmj-2019-2055.
- [5] L. Berezansky and A. Domoshnitsky. On stability of a second order integro-differential equation. *Nonlinear Dynamics and Systems Theory* **19** (1-SI) (2019) 117–123.
- [6] E. Braverman, and B. Karpuz. On oscillation of differential and difference equations with non-monotone delays. *Appl. Math. Comput.* **218** (2011) 3880–3887.
- [7] E. Braverman, G. E. Chatzarakis, and I. P. Stavroulakis. Iterative oscillation tests for differential equations with several non-monotone arguments. *Adv. Differential Equations* **2016** (87) (2016) 18 p.
- [8] J. Dzurina, E. Thandapani, B. Baculikova, C. Dharuman and N. Prabaharan. Oscillation of second order nonlinear differential equations with several sub-linear neutral terms *Nonlinear Dynamics and Systems Theory* **19** (1-SI) (2019) 124–132.
- [9] L. H. Erbe, Q. Kong, and B. G. Zhang. *Oscillation Theory for Functional Differential Equations*. Monographs and Textbooks in Pure and Applied Mathematics, 190, Marcel Dekker, Inc., New York, 1995.
- [10] M. K. Grammatikopoulos, R. G. Koplatadze and I. P. Stavroulakis. On the oscillation of solutions of first order differential equations with retarded arguments. *Georgian Math. J.* **10** (2003) 63–76.
- [11] I. Gyori, and G. Ladas. *Oscillation Theory of Delay Differential Equations with Applications*. Oxford Mathematical Monographs, The Clarendon Press, Oxford University Press, N.Y., 1991.
- [12] J. K. Hale. *Theory of Functional Differential Equations*. Second edition, Applied Mathematical Sciences, Vol. 3, Springer-Verlag, New York-Heidelberg, 1977.
- [13] B. R. Hunt and J. A. Yorke. When all solutions of $x' = \sum q_i(t)x(t - T_i(t))$ oscillate. *J. Differential Equations* **53** (1984) 139–145.
- [14] G. Infante, R. Koplatadze, and I. P. Stavroulakis. Oscillation criteria for differential equations with several retarded arguments. *Funkcial. Ekvac.* **58** (2015) 347–364.
- [15] R. G. Koplatadze. Specific properties of solutions of first order differential equations with several delay arguments. *J. Contemp. Math. Anal.* **50** (2015) 229–235.
- [16] G. Ladas, and I. P. Stavroulakis. Oscillations caused by several retarded and advanced arguments. *J. Differential Equations* **44** (1982) 134–152.
- [17] G. S. Ladde, V. Lakshmikantham, and B. G. Zhang. *Oscillation Theory of Differential Equations with Deviating Arguments*. Monographs and Textbooks in Pure and Applied Mathematics, 110, Marcel Dekker, Inc., New York, 1987.
- [18] B. Li. Oscillations of first order delay differential equations. *Proc. Amer. Math. Soc.* **124** (1996) 3729–3737.
- [19] G. M. Moremed, H. Jafari and I. P. Stavroulakis. Oscillation Criteria for differential equations with several monotone or non-monotone argument. *J. Comput. Anal. Appl.* **28** (2020) 136–151.
- [20] I. P. Stavroulakis. Oscillation criteria for delay and difference equations with non-monotone arguments. *Appl. Math. Comput.* **226** (2014) 661–672.